

A Nonconvex Framework for Structured Dynamic Covariance Recovery

Katherine Tsai¹, Mladen Kolar², and Oluwasanmi Koyejo³

¹Department of Electrical and Computer Engineering, University of Illinois at Urbana-Champaign

²Booth School of Business, The University of Chicago

³Department of Computer Science, Beckman Institute for Advanced Science and Technology, and Statistics, University of Illinois at Urbana-Champaign

Abstract

We propose a flexible yet interpretable model for high-dimensional data with time-varying second-order statistics, motivated and applied to functional neuroimaging data. Our approach implements the neuroscientific hypothesis of discrete cognitive processes by factorizing the covariances into sparse spatial and smooth temporal components. While this factorization results in parsimony and domain interpretability, the resulting estimation problem is nonconvex. We design a two-stage optimization scheme with a tailored spectral initialization, combined with iteratively refined alternating projected gradient descent. We prove a linear convergence rate up to a nontrivial statistical error for the proposed descent scheme and establish sample complexity guarantees for the estimator. Empirical results using simulated data and brain imaging data illustrate that our approach outperforms existing baselines.

Keywords: Dynamic covariance; Structured factor model; Alternating projected gradient descent; Time-series data; Functional connectivity.

1 Introduction

The manuscript proposes and evaluates a model for dynamic functional brain network connectivity, defined as the time-varying covariance of associations between brain regions (Fox & Raichle, 2007). Understanding the variation of brain connectivity between individuals is believed to be a crucial step towards uncovering the mechanisms of neural information processing (Sakoğlu et al., 2010; Chang et al., 2016), with potentially transformative applications to understanding and treating neurological and neuropsychiatric disorders (Calhoun et al., 2014).

In the neuroscience literature, estimators for time-varying covariances range from sliding window methods to hidden Markov models. The commonly used sliding window sample covariance estimator is computationally efficient (Preti et al., 2017). However, this estimate is sensitive to the selected window length, and spurious correlations may occur when the underlying window length is misspecified (Leonardi & Van De Ville, 2015). Discrete-state hidden Markov models construct

interpretable estimates of brain connectivity in terms of recurring connectivity patterns (Vidaurre et al., 2017), yet they fail to capture the smooth nature of brain dynamics (Shine et al., 2016a,b). These shortcomings motivate a new approach. Specifically, our proposed approach implements the neuroscientific hypothesis that brain functions are interactions between cognitive processes (Posner et al., 1988a), which we model as weighted combinations of low-rank components (Andersen et al., 2018). Beyond the neuroscientific underpinnings, high-dimensional data often has a low dimensional representation (Udell & Townsend, 2019), and low rank can help prevent overfitting (Udell et al., 2016). Specifically, we propose a smooth, structured low-rank time-varying covariance model inspired by the observed sparsity of brain factors (Eavani et al., 2012), and temporal dynamics of brain activity (Shine et al., 2016a,b). Hence, we constrain the temporal components to be smoothly varying via projection to a temporal kernel and restrict the sparsity of the spatial components via hard-thresholding, respectively.

We estimate parameters of the resulting model using a first-order optimization scheme that is analogous to a Burer-Monteiro factorization (Burer & Monteiro, 2003, 2005). While the first-order approach reduces the computational complexity as compared to semidefinite programming, the resulting optimization program is nonconvex, and special care is needed to design and analyze an optimization scheme that avoids converging to bad local optima. To this end, we build on the growing literature studying matrix estimation problems (Candes et al., 2015; Chi et al., 2019) using a two-stage algorithm. First, spectral initialization is used to find an initial point lying within a local region, where the objective satisfies local regularity conditions. Next, projected gradient descent is used to refine the estimate and find a stationary point of the objective.

In summary, our contributions include a novel dynamic covariance model motivated by neuroscientific models of functional brain connectivity networks. We provide an efficient procedure for estimation, along with the convergence analysis and sample complexity. Specifically, under the assumption that spatial components are shared across time, we develop a structured spectral initialization method, which effectively uses the available samples and provides a better spatial estimate than separate initialization per individual. We prove linear convergence of the factored gradient method to an estimate with a nontrivial statistical error and provide a non-asymptotic bound on the statistical error when data are Gaussian. Experiments show that the model successfully recovers temporal smoothness and detects temporal changes induced by task activation.

2 Background

2.1 Notation

The inner product of two matrices is denoted as $\langle X, Y \rangle = \text{tr}(X^T Y)$. For a matrix X , $\sigma_k(X)$ denotes the k th largest singular value, $\|X\|_F^2 = \text{tr}(X^T X)$ denotes the Frobenius norm, $\|X\|_2 = \sigma_1(X)$ denotes the spectral norm, and $\|X\|_\infty = \max_{i,j} |X_{i,j}|$ denotes the max norm. For two symmetric matrices X and Y , $X \leq Y$ denotes $Y - X$ is positive semi-definite. The pseudoinverse of X is denoted X^\dagger . The set of $K \times K$ rotation matrices is denoted as $\mathcal{O}(K)$. We use $\kappa(\cdot, \cdot)$ to denote a positive-definite kernel function. The function $\text{diag} : \mathbb{R}^K \rightarrow \mathbb{R}^{K \times K}$ converts a K -dimensional vector to a $K \times K$ diagonal matrix. For scalars a and b , $a \vee b$ denotes $\max(a, b)$ and $a \wedge b$ denotes $\min(a, b)$. We use $a \gtrsim b$ ($a \lesssim b$) to denote that there exists a constant $C > 0$ such that $a \geq Cb$ ($a \leq Cb$).

($a \leq Cb$). We use $a \asymp b$ to denote $a \gtrsim b$ and $a \lesssim b$. We use $[J]$ to denote the index set $\{1, \dots, J\}$.

2.2 Problem Statement

Given samples from N subjects recorded at J time points, denoted $x_j^{(n)} \in \mathbb{R}^P$, $n \in [N]$, $j \in [J]$, let $S_{N,j} = N^{-1} \sum_{n=1}^N x_j^{(n)} x_j^{(n)T}$ be the sample covariance across subjects at time j . We assume the population covariance takes a factorized form as

$$E(S_{N,j}) = \Sigma_j^* + E_j = V^* \text{diag}(a_j^*) V^{*T} + E_j, \quad j \in [J], \quad (2.1)$$

where Σ_j^* is at most rank K and E_j is a noise matrix such that the largest singular value of E_j is strictly smaller than the smallest nonzero singular value of Σ_j^* . This factorization employs time-invariant and columnwise orthonormal spatial components $V^* = (v_1^*, \dots, v_K^*) \in \mathbb{R}^{P \times K}$ that are the top- K eigenvectors of $\{E(S_{N,j})\}_{j \in [J]}$. Analogously, $A^* = (a_1^*, \dots, a_J^*) \in \mathbb{R}^{K \times J}$ represents the temporal components. To facilitate estimation in a high-dimensional setting, we further assume that the columns of V^* are sparse and belong to $\mathcal{C}_V(s^*) = \{v \in \mathbb{R}^P : \|v\|_0 \leq s^*, \|v\|_2 = 1\}$. The rows of A^* , denoted as A_k^* , $k \in [K]$, are smooth, bounded, and belong to $\mathcal{C}_A(c^*, \gamma^*) = \{\alpha = Qu \in \mathbb{R}^J : 0 \leq \alpha_j \leq c^*, u^T \Lambda u \leq \gamma^*\}$, where $G = (G_{x,y} = \kappa(x, y))_{x,y \in [J]} \in \mathbb{R}^{J \times J}$ is a positive semi-definite kernel matrix, the kernel κ is known a priori, and $G^\dagger = Q \Lambda Q^T$ is the eigendecomposition of G^\dagger . The kernel κ is used to model temporal smoothness of the rows of A^* and the box constraint ensures that $\alpha_j \geq 0$, so the covariance model is positive semi-definite, and is upper bounded by a positive constant for $j \in [J]$.

Eigenvalues of the kernel matrix G may decay quickly, which may result in numerically unstable algorithms when projecting onto the set \mathcal{C}_A . For example, eigenvalues of a kernel matrix corresponding to the Sobolev kernel decay at a polynomial rate, while for the Gaussian kernel they decay at an exponential-polynomial rate (Schölkopf et al., 2002). Instead of working with the kernel matrix G , we are going to construct a low-rank approximation, \tilde{G} , of G by truncating small eigenvalues. Write $Q = (\tilde{Q}, Q_1)$, where the columns of \tilde{Q} are eigenvectors of G corresponding to eigenvalues greater or equal to δ_A , and $\tilde{\Lambda}^{-1} = \text{diag}(\Lambda_{jj}^{-1} \geq \delta_A \mid j \in [J])$. Then $\tilde{G}^\dagger = \tilde{Q} \tilde{\Lambda} \tilde{Q}^T$. We define $\tilde{\mathcal{C}}_A(c, \gamma) = \{\alpha = \tilde{Q}u : 0 \leq \alpha_j \leq c, u^T \tilde{\Lambda} u \leq \gamma\}$ and the rank of \tilde{G} is denoted as $r(\tilde{G})$.

Under the model (2.1), we estimate the parameters $Z^* = (V^{*T}, A^*)^T$ by minimizing the following objective

$$\min_Z f_N(Z) = \min_{\substack{v_k \in \mathcal{C}_V(s), k \in [K] \\ A_k \in \tilde{\mathcal{C}}_A(c, \gamma), k \in [K]}} \frac{1}{J} \sum_{j=1}^J \frac{1}{2} \|S_{N,j} - V \text{diag}(a_j) V^T\|_F^2, \quad (2.2)$$

where A_k is the k th row of A . Although f_N is nonconvex with respect to $Z = (V^T, A)^T$, the corresponding covariance loss $\ell_{N,j}(\Sigma_j) = \frac{1}{2} \|S_{N,j} - \Sigma_j\|_F^2$ is m -strongly convex and L -smooth with $m = L = 1$ (Nesterov, 2013). We use alternating projected gradient descent to update V and A . The selection of tuning parameters of \mathcal{C}_V and $\tilde{\mathcal{C}}_A$ is discussed in Section 3.2.

2.3 Related work

Dynamic covariance models are common for analyzing time-series data in applications ranging from computational finance and economics (Engle et al., 2019) to epidemiology (Fox & Dunson,

2015) and neuroscience (Foti & Fox, 2019). Factor models are among the most popular analysis approaches, some of which encode temporal structure using latent kernel regularization (Paciorek, 2003; Kastner et al., 2017). For instance, Andersen et al. (2018) encoded smooth temporal dynamics by introducing a latent Gaussian process prior. Li (2019) also used piecewise Gaussian process factors to capture the combinations of gradual and abrupt changes. For spatial structure in factor models, Kolar et al. (2010) and Danaher et al. (2014) implemented variants of group lasso and fused lasso to impose sparsity. Along similar lines, our approach implements temporal and spatial structure through projection onto suitable constraint sets.

Our work is also related to dictionary learning (Olshausen & Field, 1997; Mairal et al., 2010), which can be viewed as a type of factorization where the signal is decomposed into atoms and coefficients. In such a factorization, sparsity is controlled through a sparse penalty on the coefficients. Mishne & Charles (2019) extended this approach to encode temporal data by constructing time-trace atoms with spatial coefficients. In comparison, our model has shared spatial structure and individual temporal structure.

Autoregressive models have also been applied to model dynamic connectivity in fMRI (Qiu et al., 2016; Liégeois et al., 2019). Although autoregressive models employ different modeling assumptions from ours, they can capture smooth temporal dynamics of signals. However, the forecasts of autoregressive models can become unreliable in high-dimensional settings (Bańbura et al., 2010). To this end, various implementations of structured transition matrices (Davis et al., 2016; Ahelegbey et al., 2016; Skripnikov & Michailidis, 2019) have been proposed and shown to improve computational efficiency and prediction accuracy.

The optimization problem in (2.2) is nonconvex and is optimized by alternating minimization. Recent literature has established a linear convergence rate to global optima (Jain et al., 2013; Hardt, 2014; Gu et al., 2016). In particular, our work builds on Bhojanapalli et al. (2016), who showed linear convergence in V when the underlying objective function is strongly convex with respect to $X = VV^T$. Subsequently Park et al. (2018) and Yu et al. (2020) proved a linear convergence rate for non-symmetric matrices. Unlike previous work, our factorization scheme $V\text{diag}(a_j)V^T$ imposes additional structure on the eigenvalues, thus having potential applications in regularizing graph-structured models (Kumar et al., 2020).

In nonconvex optimization, finding a good initialization in a local region is often useful to avoid convergence to bad local optima (e.g., $Z = 0$ is a trivial stationary point in our model). Spectral methods are typically employed for this task as they have good consistency properties (Chen & Candes, 2015). We employ a problem-specific spectral approach to develop a novel initialization method. Post-initialization, a first-order gradient descent method is sufficient to ensure convergence to desired optima (Candes et al., 2015). Combining with the structured constraints, Chen & Wainwright (2015) provided a theoretical framework for projected gradient descent method onto convex constraint sets. In our work, we are projecting onto a nonconvex set, which might increase the distance $\|V - V^*R\|_F^2$. Therefore, we need a problem-specific analysis to quantify the expansion coefficient.

3 Methodology

3.1 Two-stage algorithm

We develop a two-stage algorithm for solving the optimization problem in (2.2). As the objective is nonconvex, a local iterative procedure may converge to bad local optima or saddle points. In the first stage of the algorithm, spectral decomposition is used to find an initialization point. In the second stage, projected gradient descent is used to locally refine the initial estimate and find a stationary point that is within the statistical error of the population parameters. Algorithm 1 summarizes our initialization procedure. Here, the eigendecomposition of $\{S_{N,j}\}_{j \in [J]}$ is performed to obtain initial estimates of V^* and A^* . Specifically, the initialization uses the shared spatial structure of $\{\Sigma_j^*\}_{j \in [J]}$ to increase the effective sample size, i.e., the initial estimate V^0 is obtained from the eigenvectors corresponding to the largest K eigenvalues of the covariance matrix pooled across time, $M_N = J^{-1} \sum_{j=1}^J S_{N,j}$. The initial estimate of the temporal coefficients, A^0 , is obtained by projecting $\{S_{N,j}\}_{j \in [J]}$ onto V^0 .

Algorithm 1 Spectral initialization

Set $M_N = (NJ)^{-1} \sum_{j=1}^J \sum_{n=1}^N x_j^{(n)} x_j^{(n)T}$
Set $V^0 = (v_1^0, v_2^0, \dots, v_k^0) \leftarrow$ top K eigenvectors of M_N
For $j = 1$ to $j = J$ and $k = 1$ to $k = K$
 $a_{k,j}^0 \leftarrow v_k^{0T} S_{N,j} v_k^0$
Set $A^0 = (a_{k,j}^0)_{k \in [K], j \in [J]}$
Output V^0, A^0

After initialization, we iteratively refine estimates of V and A via alternating projected gradient descent. In each iteration, the iterates V and A are updated using the gradient of f_N , where η denotes the step size. Note that we scale down the step size for the V update by J to balance the magnitude of the gradient. After a gradient update, we project the iterates onto the constraint sets \mathcal{C}_V and $\tilde{\mathcal{C}}_A$ to enforce sparsity on V and smoothness on A . Details are given in Algorithm 2.

Algorithm 2 Dynamic covariance estimation

Set $V^0, A^0 =$ Spectral initialization($\{x_j^{(n)}\}_{n \in [N], j \in [J]}$)
While $|f_N(Z^{i-1}) - f_N(Z^{i-2})| > \varepsilon$
 $\hat{A}^i \leftarrow A^{i-1} - \eta \nabla_A f_N(Z^{i-1})$
 $A^i \leftarrow$ Project rows of \hat{A}^i to $\tilde{\mathcal{C}}_A$
 $\hat{V}^i \leftarrow V^{i-1} - \frac{\eta}{J} \nabla_V f_N(Z^{i-1})$
 $V^i \leftarrow$ Project columns of \hat{V}^i to \mathcal{C}_V
Output V, A

Although \mathcal{C}_V is a nonconvex set, projection onto this set can be computed efficiently by picking

the top- s largest entries in magnitude and then projecting the constructed vector to the unit sphere. Despite projecting onto a nonconvex set, we are able to show that the gradient and projection step jointly result in a contraction (see Supplementary Material). On the other hand, the projection onto the convex set $\tilde{\mathcal{C}}_A$ can be computed efficiently via convex programming: we project onto $\tilde{\mathcal{C}}_A$ by iteratively projecting onto $\{\alpha \in \mathbb{R}^J : 0 \leq \alpha_j \leq c, j \in [J]\}$ and $\{\alpha = \tilde{Q}u : u^T \tilde{\Lambda}u \leq \gamma\}$, which gives us a point in the intersection of the sets by von-Neumann’s theorem (Escalante & Raydan, 2011).

3.2 Selection of tuning parameters

The parameters of the proposed model include the sparsity level s , the rank K , the kernel length scale l , the smoothness coefficient γ , the truncation level δ_A , and the limits of the projected upper bound of the box c . For some kernels (e.g., Gaussian kernel, Matérn five-half kernel, and other radial basis function kernels), one must also select the length scale parameter l , which captures the smoothness of the curves (i.e., $\{A_k^*\}_{k \in [K]}$); For example, a Gaussian kernel function is $\kappa_l(x, y) = \sigma^2 \exp\{-(x - y)^2 / (2l^2)\}$, where l affects the slope of the eigenvalues decay. We denote such kernel functions as κ_l rather than κ . Our theory suggests that δ_A should be upper bounded by the magnitude of $\min_{j \in [J]} \sigma_K^2(\Sigma_j^*)$ to obtain good statistical error. Further, δ_A is selected for numerical stability. In experiments, we find that $\delta_A = 10^{-5}$ is a good empirical choice, and satisfies the sufficient conditions. In principle, we do not want to cut off any important signals, so we choose c as a value greater than $\max_{j \in [J]} \|S_{N,j}\|_2$ and $c^* = \max_{j \in [J]} \|\Sigma_j^*\|_2$. In terms of the estimation performance, we observe that the selection of sparsity and rank have a larger effect than the selection of γ and l . While under-selection of s and K leads to poor evaluation scores, improper selection of l and γ have relatively minor influence. Hence, we adopt a two-stage approach to selecting parameters. In the first stage, we perform grid search on s, K, γ, l and find the configuration that minimizes the Bayesian information criterion $\text{BIC} = \log N \sum_{k=1}^K \|v_k\|_0 - 2\hat{L}_N$, where \hat{L}_N is the maximized Gaussian log-likelihood function. However, varying γ and l have subtle influence on BIC. Consequently, in the second stage, we fix s, K with values selected in the first stage and select γ and l using 5-fold cross-validation with the Gaussian log-likelihood, which is motivated by prior work on nonparametric dynamic covariances (Yin et al., 2010; Zhang & Li, 2019). Empirically, we find that tuning the length scale parameter l is more effective than tuning γ in producing globally smooth temporal structures (see Supplementary Material).

4 Theory

4.1 Preliminaries

Before presenting our main theoretical results, we introduce two tools that will help us establish the results.

First, we discuss orthogonalization. The spatial component V produced by Algorithm 2 is not necessarily orthonormal. However, V^* is full rank and if $\min_{Y \in \mathcal{O}(K)} \|V - V^*Y\|_2^2 < 1$ is guaranteed at each iteration, then V is full rank as well. As a result, the subspace spanned by columns of V is equal to the subspace spanned by columns of the orthogonalized version of it. To simplify the analysis of Algorithm 2, we add a QR decomposition step that orthogonalizes V after the projection

onto \mathcal{C}_V . That is, in each iteration we compute

$$V_{ortho}^i \leftarrow V^i (L^i)^{-1} \quad (\text{QR decomposition}),$$

where L^i is the upper triangular matrix, with diagonal entries less or equal to 1. Note that orthogonalization of V in each iteration of Algorithm 2 is not needed in practice and is only used in establishing theoretical properties. Such an approach is commonly used in the literature (Jain et al., 2013; Zhao et al., 2015). We further note that an addition of the QR decomposition only increases the distance of the iterate V^i to V^*R by a mild constant (Stewart, 1977; Zhao et al., 2015) (see Supplementary Material). Furthermore, QR decomposition increases the number of nonzero elements of the iterate V to at most Ks . As we consider the rank K to be fixed and $P \gtrsim s$, the effect of the QR decomposition is mild. Our experiments further demonstrate that optimization with and without the QR decomposition step result in comparable performance.

Next we introduce the notion of the statistical error, which allows us to quantify the distance of the population parameters from the stationary point to which the optimization algorithm converges. Note that the notion of statistical error has been previously adopted in M-estimation (Loh & Wainwright, 2015). Let $\mathcal{B}_t = \{v \in \mathbb{R}^P \mid \|v\|_0 \leq t, \|v\|_2 \leq 1\}$ and

$$\Upsilon(r, t, h, \delta_A) = \{\{\Delta_j = V \text{diag}(a_j) W^T\}_{j \in [J]} \mid v_k \in \mathcal{B}_t, w_k \in \mathcal{B}_t, A_k^T \tilde{G}^\dagger A_k \leq h, k \in [r]\},$$

where \tilde{G} is the truncation of G at the level of δ_A . We define the statistical error as

$$\varepsilon_{stat} = \varepsilon_{stat}(2K, 2s + s^*, 2\gamma, \delta_A) = \max_{\{\Delta_j\}_{j \in [J]} \in \Upsilon(2K, 2s + s^*, 2\gamma, \delta_A)} \frac{\sum_{j=1}^J \langle \nabla \ell_{N,j}(\Sigma_j^*), \Delta_j \rangle}{\left(\sum_{j=1}^J \|\Delta_j\|_F^2\right)^{1/2}}.$$

The statistical error describes the geometric landscape around the optimum—it quantifies the magnitude of gradient of the empirical loss function evaluated at the population parameter in the directions constrained to the set Υ .

4.2 Assumptions and Main Results

We begin by stating the assumptions needed to establish the main results. Note that V in this section is used to denote an iterate in after the QR factorization step.

An upper bound on the step size is required for convergence of Algorithm 2. Let $Z_j^0 = (V^{0T}, \text{diag}(a_j^0))^T$, $j \in [J]$, denote the output of Algorithm 1.

Assumption 4.1. *The step size satisfies $\eta \leq \min_{j \in [J]} J^{1/2} / (64 \|Z_j^0\|_2^2)$.*

Note that the step size depends on the initial estimate, but remains constant throughout the iterations. Let $\beta = 1 - \eta / (4J\xi^2) < 1$, $\chi = 4\beta^{1/2} (1 - 2I_0 / \sqrt{J})^{-2} (1 + 32 \|A^*\|_\infty^2)$, and $\tau = J^{-1} \{9/2 + (1/2 \vee K/8)\}$, where

$$I_0^2 = \left\{ \frac{1}{16\xi^2} \frac{1}{(1 + \|A^*\|_\infty^2 J^{-1})} \wedge \frac{J}{4} \right\}, \quad \xi^2 = \max_{j \in [J]} \left\{ \frac{16}{\sigma_K^2(\Sigma_j^*)} + \left(1 + \frac{8c}{\sigma_K(\Sigma_j^*)}\right)^2 \right\}. \quad (4.1)$$

We also require the tuning parameters to be selected appropriately.

Assumption 4.2. We have $c \geq c^*$, $\gamma \geq \gamma^*$, $s \geq [\{4(1/\chi - 1)^{-2} + 1\} \vee 2]s^*$. The matrix \tilde{G} is obtained with the truncation level $\delta_A \leq (16\gamma^*)^{-1} \min_{j \in [J]} \sigma_K^2(\Sigma_j^*)$.

Note that the condition on δ_A is mild. It guarantees that we do not truncate too much of the signal. Finally, we require an assumption on the statistical error.

Assumption 4.3. We have $\varepsilon_{stat}^2 \leq JI_0^2\{(\beta^{1/2} - \beta)/(\tau\eta) \wedge \min_{j \in [J]} 3\|Z_j^*\|_2^2\}$.

Assumption 4.3 is essentially a requirement on the sample size N , since for a large enough N the assumption will be satisfied with high probability. Notice that as the sample size increases, the statistical error gets smaller, while the radius of the local region of convergence, I_0 , stays constant. Furthermore, if Assumption 4.3 is not satisfied, this implies that the initialization point is already close enough to the population parameters and the subsequent refinement by Algorithm 2 is not needed.

With these assumptions, we are ready to state the main result, which tells us how far are the estimates obtained by Algorithm 1 and 2 from the population parameters. Let $\Sigma_j^I = V^I \text{diag}(a_j^I)(V^I)^T$, $j \in [J]$, denote the estimate of the covariance at the I th iteration.

Theorem 4.4. Suppose Assumption 4.1–4.3 are satisfied and $J \geq 4$. Furthermore, for a sufficiently large constant C_0 , suppose that we are given $N = C_0KP \log(PJ/\delta_0)$ independent samples such that $\|x_j^{(n)}\|_2^2 \leq P\|A^*\|_\infty$ almost surely, $j \in [j]$, with zero mean and covariance as in (2.1). Then, with probability at least $1 - \delta_0$, the estimate obtained by Algorithm 1 and Algorithm 2 satisfies

$$\sum_{j=1}^J \|\Sigma_j^I - \Sigma_j^*\|_F^2 \leq \beta^{I/2}(4\mu^2\xi^2) \sum_{j=1}^J \|\Sigma_j^0 - \Sigma_j^*\|_F^2 + \frac{2\tau\mu^2\eta}{\beta^{1/2} - \beta} \varepsilon_{stat}^2 + 2K\gamma^*\delta_A, \quad (4.2)$$

where $\mu = \max_{j \in [J]} (17/8)\|Z_j^*\|_2$.

The first term on the right hand side of (4.2) corresponds to the optimization error and we observe a linear rate of convergence. The second and third term of (4.2) correspond to the statistical error and approximation error due to the truncation of the kernel matrix, respectively. From the bound, we observe a trade-off between ε_{stat} and the truncation error δ_A : if δ_A is decreased, ε_{stat} increases.

The proof of Theorem 4.4 is given in two steps. First, we establish the convergence rate of iterates obtained by Algorithm 2 by first assuming that V^0 and A^0 lie in a neighborhood around V^* and A^* (see §4.3). Subsequently, we show in Theorem 4.7 that Algorithm 1 provides suitable V^0 and A^0 with high probability (see §4.5).

To give an example of Theorem 4.4, we consider the case where data are generated from a multivariate Gaussian distribution and for a Gaussian kernel.

Proposition 4.5. Let $x_j^{(n)} \in \mathbb{R}^P$ be independent Gaussian samples with mean zero and covariance as in (2.1) with $J \geq 4$ and $N \gtrsim K(P + \log J/\delta_0)$. Suppose G is a Gaussian kernel matrix whose eigenvalue decays at the rate $\exp(-l^2j^2)$ for some length-scale $l > 0$. Let $\delta_A \asymp (\gamma^*lN)^{-1}\{\log(\gamma^*lN)\}^{1/2}$. Suppose that Assumption 4.1–4.2 hold, $s^* \log(P/s^*) < PJ$ and $\max_{j \in [J]} \|E_j\|_2 \lesssim I_0$. Then after $I \gtrsim \log(1/\delta_1)$ iterations of Algorithm 2, with probability at least $1 - \delta_0$, we have

$$\sum_{j=1}^J \|\Sigma_j^I - \Sigma_j^*\|_F^2 \lesssim \delta_1 + \frac{1}{N} \left[K \left\{ \frac{1}{l} (\log \gamma^*lN)^{1/2} + s^* \log \frac{P}{s^*} \right\} + \log \delta_0^{-1} \right] + J \max_{j \in [J]} \|E_j\|_2^2.$$

The condition $s^* \log(P/s^*) < PJ$ is mild, since $s^* \lesssim P$, while the condition $\max_{j \in [J]} \|E_j\|_2 \lesssim I_0$ is mild, since $\|E_j\|_2 < \sigma_K(\Sigma_j^*)$, $j \in [J]$. Under the Gaussian distribution, the sample complexity is improved to $N \gtrsim K(P + \log J)$ from $N \gtrsim KP(\log P + \log J)$ in Theorem 4.4. Proposition 4.5 provides an explicit bound on the estimator that can be obtained under an assumption on the eigenvalue decay. The statistical error is comprised of two terms that correspond to errors when estimating smooth temporal components and sparse spatial components. In our choice of δ_A , the truncation error is at the same order as the statistical error induced by the smooth temporal components.

4.3 Linear Convergence

We establish the linear rate of convergence of Algorithm 2 when it is appropriately initialized. Recall that rows of A^* belong to $\mathcal{C}_A(c^*, \gamma^*) \subseteq \mathcal{C}_A(c, \gamma)$, while the projected gradient descent is implemented on the set $\tilde{\mathcal{C}}_A(c, \gamma) \subset \mathcal{C}_A(c, \gamma)$. Let

$$\tilde{A}^* = \operatorname{argmin}_{B_{k \in \tilde{\mathcal{C}}_A(c, \gamma), k \in [K]}} \|B - A^*\|_F^2,$$

be the best approximation of A^* in $\tilde{\mathcal{C}}_A(c, \gamma)$. See Supplementary Material for details on the construction of \tilde{A}^* . We define $\tilde{\Sigma}_j^* = V^* \operatorname{diag}(\tilde{a}_j^*) V^{*T}$, $j \in [J]$, and $\tilde{Z}^{*T} = (V^{*T}, \tilde{A}^*)$. With these definitions, we establish the linear rate of convergence of the iterates to $\tilde{\Sigma}_j^*$ and \tilde{Z}^* . The convergence rate in Theorem 4.4 will then follow by combining the results with the truncation error.

Observe that the covariance factorization is not unique, since, for any $R \in \mathcal{O}(K)$, we have $\Sigma_j = V \operatorname{diag}(a_j) V^T = V R_j R_j^T \operatorname{diag}(a_j) R_j R_j^T V^T$, $j \in [J]$. By triangle inequality, we have

$$\sum_{j=1}^J \|\Sigma_j - \tilde{\Sigma}_j^*\|_F^2 \leq \sum_{j=1}^J \alpha_{V,j} \|V - V^* R\|_F^2 + \alpha_A \|\operatorname{diag}(a_j) - R^T \operatorname{diag}(\tilde{a}_j^*) R\|_F^2, \quad (4.3)$$

where $\alpha_{V,j} = 3\{\|V \operatorname{diag}(a_j)\|_2^2 + \|V^* \operatorname{diag}(\tilde{a}_j^*)\|_2^2\}$, $j \in [J]$, and $\alpha_A = 3\|V^*\|_2^2 \|V\|_2^2$. This implies that if $\|V - V^* R\|_F^2 + \|\operatorname{diag}(a_j) - R^T \operatorname{diag}(\tilde{a}_j^*) R\|_F^2$ is small for some rotation matrix R and every $j \in [J]$, then the left hand side will also be small. To this end, our goal is to show that the following distance metric contracts at each iterate of Algorithm 2. Let

$$\begin{aligned} R = \operatorname{argmin}_{Y \in \mathcal{O}(K)} \|V - V^* Y\|_F^2, \quad \operatorname{dist}^2(Z, \tilde{Z}^*) &= \sum_{j=1}^J d^2(Z_j, \tilde{Z}_j^*); \\ d^2(Z_j, \tilde{Z}_j^*) &= \|V - V^* R\|_F^2 + \|\operatorname{diag}(a_j) - R^T \operatorname{diag}(\tilde{a}_j^*) R\|_F^2, \end{aligned} \quad (4.4)$$

where $Z_j^T = (V^T, \operatorname{diag}(a_j))$ and $\tilde{Z}_j^{*T} = (V^{*T}, \operatorname{diag}(\tilde{a}_j^*))$. The metric first finds the rotation matrix that aligns two subspaces and then computes the transformation of $\operatorname{diag}(\tilde{a}_j^*)$ along the rotation R . This metric is similar to the distance metric commonly used in matrix factorization problems (Anderson & Rubin, 1956; Ten Berge, 1977), but in our model the choice of R only depends on V .

To show the convergence of $\operatorname{dist}^2(Z, \tilde{Z}^*)$, we need following assumptions.

Assumption 4.6. *Suppose that Z_j^0 satisfies $d^2(Z_j^0, Z_j^*) \leq I_0^2$, for $j \in [J]$, where I_0 is defined in (4.1). Assume that $\|V^0 - V^* R\|_F^2 \leq I_0^2/J$ and $\|\operatorname{diag}(a_j^0) - R^T \operatorname{diag}(a_j^*) R\|_F^2 \leq (J-1)I_0^2/J$.*

Since $d^2(Z_j^0, \tilde{Z}_j^*) \leq d^2(Z_j^0, Z_j^*)$ for $j \in [J]$, Assumption 4.6 ensures that the distance of initial estimates and the population parameters are bounded within the ball of radius I_0 . In addition, $I_0^2 \leq J$ ensures that $\|V - V^*R\|_2 \leq 1$, so that V is full-rank. Intuitively, we assume the squared distance for V is $1/(J-1)$ times smaller than the squared distance for A , because we have J times more samples to estimate V compared to A .

Theorem 4.7. *Assume that Assumption 4.1–4.6 hold. After I iterations of Algorithm 2, we have*

$$\text{dist}^2(Z^I, \tilde{Z}^*) \leq \beta^{I/2} \text{dist}^2(Z^0, \tilde{Z}^*) + \frac{\tau\eta\varepsilon_{stat}^2}{\beta^{1/2} - \beta}. \quad (4.5)$$

The above result obtains a linear rate of convergence in $\text{dist}^2(Z, \tilde{Z}^*)$. The second term on the left hand side denotes the constant multiple of the statistical error, which depends on the distribution of the data and the sample size. Combining with (4.3) yields a linear rate of convergence in $\sum_{j=1}^J \|\Sigma_j - \tilde{\Sigma}_j^*\|_F^2$.

4.4 Statistical Error

Theorem 4.7 shows linear convergence of the algorithm to a region around population parameters characterized by the statistical error. One may wonder how large the statistical error can be? While Assumption 4.3 provides a condition under which convergence is guaranteed, this bound is loose as it does not depend on the sample size. We establish a tighter bound under the Gaussian distribution.

Proposition 4.8 (Statistical Error of Gaussian Distributed Data). *Suppose that samples $x_j^{(n)} \in \mathbb{R}^P$ are Gaussian with mean zero and covariance as in (2.1). Then, with probability at least $1 - \delta$,*

$$\varepsilon_{stat}(2K, (2m+1)s^*, 2m'\gamma^*, \delta_A) \leq (\nu \vee \nu^2) + \sqrt{J} \max_{j \in [J]} \|E_j\|_2,$$

where

$$\nu = \frac{\|A^*\|_\infty}{e_0} \left[\frac{1}{N} \left\{ \log \frac{1}{\delta} + Kr(\tilde{G}) + Ks^* \log \frac{P}{s^*} \right\} \right]^{\frac{1}{2}},$$

m, m' are positive integers, e_0 is an absolute constant depending on m and m' , and $r(\tilde{G})$ is the rank of the δ_A -truncated kernel matrix \tilde{G} .

To interpret ε_{stat} , the first term corresponds to the error in estimating the low-rank matrix, while the second term corresponds to the essential error incurred from approximating the covariance matrix by a low-rank matrix. The low-rank matrix can be estimated with the rate that converges to zero as $[K\{r(\tilde{G}) + s^* \log P\}/N]^{-1/2}$, which corresponds to the rate of convergence of temporal and spatial components. We also highlight that truncation of G simplifies the statistical analysis because we can view the projection to \tilde{C}_A as restricting rows of A to a subset of a $r(\tilde{G})$ -dimensional smooth subspace with $r(\tilde{G})$ much smaller than J , the original dimension.

4.5 Sample Complexity of Spectral Initialization

We discuss the sample complexity required to satisfy Assumption 4.6. That is, we characterize the sample size needed for Algorithm 1 to give a good initial estimate, so that Algorithm 2 outputs a solution characterized in Theorem 4.7. We consider a general case of a bounded distribution.

Theorem 4.9 (Sample Complexity of Spectral Initialization). *Let $x_j^{(n)} \in \mathbb{R}^P$ be independent zero mean samples with $\|x_j^{(n)}\|_2^2 \leq P\|A^*\|_\infty$ almost surely, $n \in [N]$, $j \in [J]$, $J \geq 4$. Let $M^* = J^{-1} \sum_{j=1}^J E(S_{N,j})$ and $g = \sigma_K(M^*) - \sigma_{K+1}(M^*) > 0$ be the eigengap. Then, with probability at least $1 - \delta$,*

$$\begin{aligned} \text{dist}^2(Z^0, Z^*) &\leq \phi(g, A^*) \left\{ \frac{KJP^2}{N^2} \left(\log \frac{4JP}{\delta} \right)^2 + \frac{KJP}{N} \log \frac{4JP}{\delta} \right\}; \\ \phi(g, A^*) &= 4\|A^*\|_\infty^2 \left\{ \frac{5(1 + 16\varphi^2\|A^*\|_\infty^2)}{g^2J} \vee 8\varphi^2 \right\}, \end{aligned} \quad (4.6)$$

where $\varphi^2 = \max_{j \in [J]} \{1 + 4\sqrt{2}\|A^*\|_\infty/\sigma_K(\Sigma_j^*)\}$.

From (4.6) we note that if $N \gtrsim P \log(PJ/\delta)$, then Assumption 4.6 will be satisfied with high probability. The eigengap g must be greater than 0 for the bound in (4.6) to be nontrivial. Moreover, since $g \leq \|A^*\|_\infty$, the first term of $\phi(g, A^*)$ dominates when J is small. Combining results from (4.3), Theorem 4.7 and Theorem 4.9, we can establish Theorem 4.4.

5 Simulations

We use the metric (4.4) to evaluate recovery. We also compare results to other methods using the average log-Euclidean metric (Arsigny et al., 2006). Unless stated otherwise, we use the Matérn five-half kernel (Minasny & McBratney, 2005) as the smoothing kernel for all the simulations. We evaluate the algorithm with a variety of temporal dynamics and compare with methods stated in Table 1. As for the data generation process, we create synthetic samples from the Gaussian distribution: $x_j^{(n)} \sim \mathcal{N}(0, \Sigma_j^* + \sigma I)$, $n \in [N]$, $j \in [J]$, where $\Sigma_j^* = \sum_{k=1}^K a_{k,j}^* v_k^* v_k^{*T}$ and σI is the additive noise.

Table 1: Competing methods

Abbr.	Model	low-rank	smooth A	sparse V
M1	Sliding window principal component analysis	✓	✓	✗
M2	Hidden Markov model	✗	✗	✗
M3	Autoregressive hidden Markov model (Poritz, 1982)	✗	✓	✗
M4	Sparse dictionary learning (Mairal et al., 2010)	✓	✗	✓
M5	Bayesian structured learning (Andersen et al., 2018)	✓	✓	✓
M6	Sliding window shrunk covariance (Ledoit & Wolf, 2004)	✗	✓	✗
M*	Spectral initialization (Algorithm 1)	✓	✗	✗
M**	Proposed model (Algorithm 2)	✓	✓	✓
MQ**	Proposed model (Algorithm 2) with QR decomposition step	✓	✓	✓

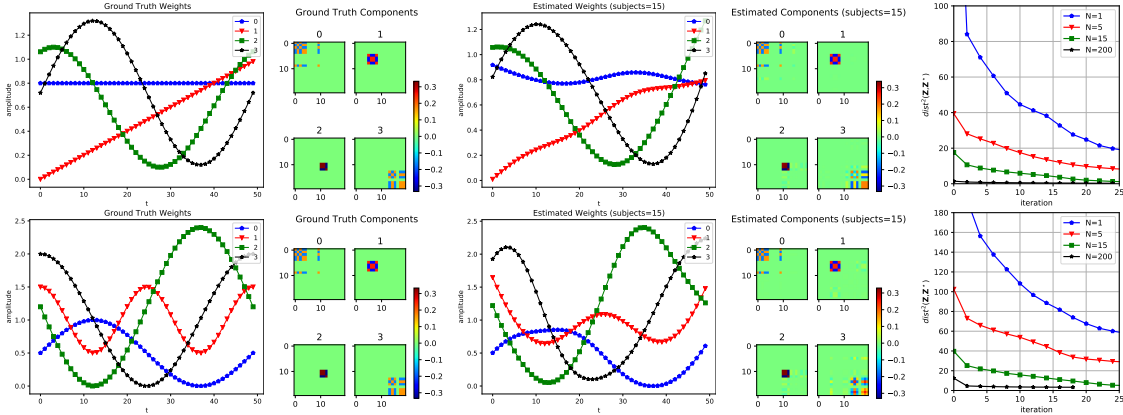


Figure 1: Covariance recovery of $K = 4, P = 20, J = 50$. The left two columns show the simulation ground truth, the center two columns show the recovery of $N = 15$, and the rightmost column shows the convergence rate under different number of subjects. The results indicate good spatial and temporal recovery and demonstrate linear rate of convergence.

5.1 Simulation of different temporal dynamics

Ground truth recovery and linear convergence: We demonstrate the algorithm in the noiseless setting and evaluate the recovery using the distance metric $\text{dist}^2(Z, Z^*)$. The objective of this experiment is to evaluate the algorithm under different smooth temporal structures. All the tuning parameters are selected based on Section 3.2. The ground truth and results are shown in Figure 1. The top row shows the first setting of mixing temporal weights, where we have sine functions, a constant function, and a ramp function. The bottom row shows the second setting of different sine functions. On the right side of Figure 1, we plot the distance metric $\text{dist}^2(Z, Z^*)$ with different number of subjects $N = \{1, 5, 15, 200\}$. For each trial, we see the linear convergence of the distance metric up to some statistical error, and the error decreases with the increase of sample size, as predicted by Theorem 4.7. Moreover, the statistical error is consistent with the number of subjects. More simulation results for different temporal structures are presented in the Supplementary Material.

5.2 Simulations in high dimension

We increase both the data dimension P and the number of components K to demonstrate the effectiveness of the proposed algorithm. The data generation process is described in the Supplementary Material. Note that the spatial components are non-overlapping in the previous simulation, whereas we generate spatial components that are partially overlapping in the high-dimensional setting, making the task more challenging.

To compare with other methods, we use the average log-Euclidean metric (Arsigny et al., 2006): $J^{-1} \sum_{j=1}^J \|\log(\Sigma_j) - \log(\Sigma_j^*)\|_F$, where $\log(\Sigma_j) = U_j \log(\Lambda_j) U_j^T$ and U is the eigenvector matrix, and Λ is the diagonal eigenvalue matrix of Σ_j . In practice, we truncate the eigenvalues whose magnitude is smaller than 10^{-5} to maintain stability of the evaluation.

Dimension v.s. rank: We first test the proposed algorithm with following experimental settings

Table 2: Average log-Euclidean metric of high dimensional low-rank simulated data

	$P = 50$	$P = 100$	$P = 150$	$P = 200$	$P = 300$
$K = 10$	0.35 ± 0.01	0.35 ± 0.02	0.41 ± 0.02	0.35 ± 0.01	0.34 ± 0.03
$K = 20$	0.66 ± 0.02	0.66 ± 0.02	0.69 ± 0.02	0.66 ± 0.03	0.66 ± 0.01
$K = 30$	0.82 ± 0.01	0.82 ± 0.01	0.82 ± 0.02	0.80 ± 0.01	0.79 ± 0.01
$K = 40$	0.97 ± 0.01	0.93 ± 0.01	0.93 ± 0.01	0.88 ± 0.01	0.87 ± 0.01
$K = 50$	1.11 ± 0.01	1.10 ± 0.01	1.04 ± 0.01	0.99 ± 0.01	0.99 ± 0.01

$N = 100$, $P = \{50, 100, 150, 200, 300\}$, $J = 100$, $K = \{10, 20, 30, 40, 50\}$. The result of different configurations are shown in Table 2. The results indicate that with fixed N , the distance increases with the increment of rank, which can be expected as there are more parameters to estimate. Moreover, we also find the dimension P has a small influence on the performance.

Competing methods: To compare with other methods, we select relatively small $P = 100$ as some methods are not scalable to high dimensions. The settings are $J = 100$, $K = 10$, and noise level $\sigma = 0.5$. Moreover, to make fair comparisons, we set the number of components for all methods to be 10. We run 20 trials for each method. For the Bayesian model (M5), we draw 30 samples from the posterior distribution and compute the estimated covariance.

From Table 3, we see that the proposed model performs the best compared to competing methods and the log-Euclidean distance decreases as the number of samples increases for M^{**} . This observation matches the result of Theorem 4.4 and Proposition 4.8. When comparing M^* and M^{**} , we see the decrease of the log-Euclidean distance resulting from Algorithm 2. Comparing M^{**} and MQ^{**} , we see that their scores are very close, implying that estimation with and without QR decomposition does not change much, supporting the theory that V and V_{ortho} span the same subspace. Notably, our model yields comparable performance with M5. We can expect this because the model structure of M5 and the proposed model are similar, though M5 takes the Bayesian framework and uses variational inference (Blei et al., 2017). Moreover, we compare the running time of different methods. From Table 4, we see that the running time of the proposed method remains relatively stable as the number of subjects increases. On the other side, the running time of other methods, M2-M4, increases as N increases. While our method remains efficient in high dimension settings, many other methods become slow as the dimension increases. Finally, even though M5 has comparable performance to ours, our method is more computationally efficient than the counterparts.

Table 3: Average log-Euclidean metric of high dimensional low-rank data ($\sigma = 0.5$)

Methods	Number of training subjects				
	10	20	30	40	50
M1 $W = 20$	0.49 ± 0.01	0.46 ± 0.01	0.45 ± 0.01	0.45 ± 0.01	0.442 ± 0.01
M2	1.22 ± 0.01	1.04 ± 0.01	1.00 ± 0.01	0.98 ± 0.01	0.97 ± 0.01
M3	71.50 ± 6.46	1.90 ± 0.26	1.12 ± 0.01	1.14 ± 0.01	1.12 ± 0.01
M4	0.94 ± 0.03	0.46 ± 0.01	0.41 ± 0.01	0.39 ± 0.01	0.38 ± 0.01
M5	0.51 ± 0.01	0.46 ± 0.01	0.43 ± 0.01	0.42 ± 0.01	0.41 ± 0.01
M^*	0.43 ± 0.01	0.40 ± 0.01	0.40 ± 0.01	0.39 ± 0.01	0.39 ± 0.01
M^{**}	0.42 ± 0.03	0.35 ± 0.05	0.36 ± 0.04	0.33 ± 0.04	0.32 ± 0.02
MQ^{**}	0.40 ± 0.04	0.40 ± 0.01	0.35 ± 0.04	0.32 ± 0.03	0.32 ± 0.02

Table 4: Running time (*seconds*) of high dimensional low-rank data ($\sigma = 0.5$)

Methods	Number of training subjects				
	10	20	30	40	50
M1 $W = 20$	0.8 ± 0.4	0.5 ± 0.3	1.2 ± 0.6	1.5 ± 0.5	1.8 ± 0.5
M2	151.9 ± 17.9	222.6 ± 51.0	376.7 ± 53.6	498.8 ± 40.0	635.5 ± 58.2
M3	422.0 ± 33.3	729.7 ± 161.6	1154.4 ± 53.6	1427.4 ± 64.4	1751.7 ± 52.0
M4	267.0 ± 112.1	378.4 ± 148.5	846.2 ± 358.8	872.0 ± 440.8	1841.5 ± 697.2
M5	2243.8 ± 33.3	2263.3 ± 38.4	2273.7 ± 36.0	2259.8 ± 34.2	2278.9 ± 35.1
M*	0.1 ± 0.0	0.1 ± 0.1	0.2 ± 0.1	0.2 ± 0.1	0.2 ± 0.1
M**	1.2 ± 0.6	1.3 ± 0.7	2.9 ± 1.4	3.9 ± 0.8	3.6 ± 0.7
MQ**	2.2 ± 1.3	1.4 ± 0.7	2.5 ± 1.0	3.8 ± 0.7	3.5 ± 0.6

6 Experiment on neuroimaging data

To investigate the proposed model on real data, we focus on (i) the interpretability of the model and (ii) the out-of-sample prediction. We use the motor task data from the Human Connectome Project functional magnetic resonance imaging (fMRI) data (Van Essen et al., 2013). The data is preprocessed using the existing pipeline (Van Essen et al., 2013), and an additional high-pass filter with a cutoff frequency $0.015Hz$ to remove the physiological noise as recommended by Smith et al. (1999). The data consists of five motor tasks: right hand tapping, left foot tapping, tongue wagging, right foot tapping, and left hand tapping.

For the model interpretation experiment, we select $N = 20$ subjects. Preprocessed time series $J = 284$ for each subject were extracted from $P = 375$ cortical and subcortical parcels, following (Shine et al., 2019). The regions include 333 cortical parcels (161 and 162 regions from the left and right hemispheres, respectively) using the Gordon atlas (Gordon et al., 2016), 14 subcortical regions from the Harvard–Oxford subcortical atlas (bilateral thalamus, caudate, putamen, ventral striatum, globus pallidus, amygdala, and hippocampus), and 28 cerebellar regions from the SUIT atlas 54 (Diedrichsen et al., 2009).

During the session, each task is activated twice (see the activation sequence in Supplementary Material). The goal is to analyze the corresponding dynamic connectivity. To investigate the temporal and spatial components, we compute the correlation of each weight A_k for every $k \in [K]$ with the onset task activation, and select the component that has the highest correlation shown in Figure 2. Our results show that the temporal fluctuations of the top components coincide with the task activation.

Following the hypothesis that the neural activity are the consequence of multiple components rather than single components (Posner et al., 1988b), for each task, we select three components with the highest correlations and plot the connectivity patterns in Figure 3. The spatial hubs in the connectivity matrices closely match with the expected motor regions as defined in the cortical homunculus (Marieb & Hoehn, 2007). Thus, the results indicate that the proposed algorithm can separate and identify the components of each task, and each task has a unique connectivity pattern.

As the ground truth is unknown, and motivated by the hypothesis that each task has a separate activation pattern, we design a classification task as a surrogate experiment to evaluate the algorithm. Prior observations (Zalesky et al., 2012; Calhoun et al., 2014) also indicate that task fMRI data share similar connectivity patterns across test subjects. Thus, if we can recover the functional connectivity patterns of the training subjects, then similar patterns exist in testing subjects. We partition the Human Connectome Project motor task dataset (Van Es-

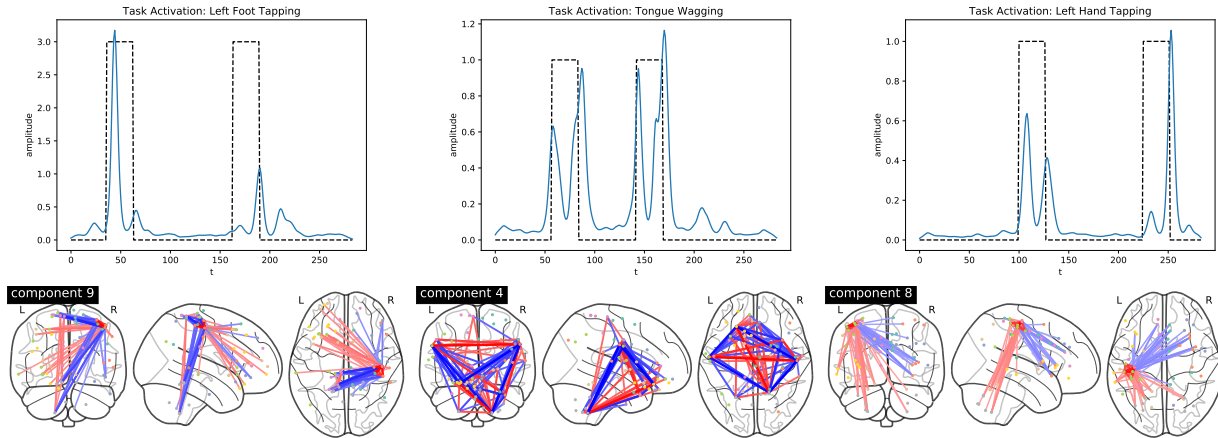


Figure 2: The top row shows the temporal components (blue solid lines) whose correlations are the largest with respect to the task activation (black dotted lines). The bottom row shows the corresponding brain connectivity patterns (spatial components) of the tasks above. The red lines denote positive connectivity and the blue lines denote negative connectivity.

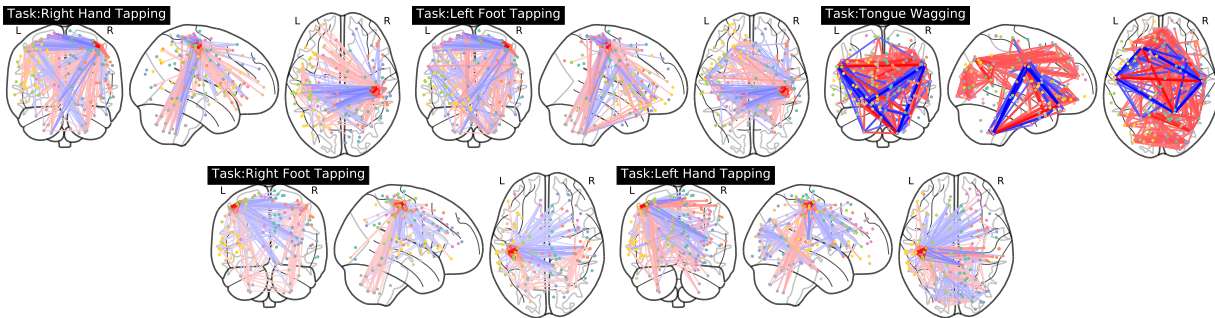


Figure 3: Each connectome is the superposition of top three spatial components. The spatial hubs in the connectivity matrices closely match with the expected motor regions (hands, feet, tongue) as defined in the cortical homunculus (Marieb & Hoehn, 2007).

Table 5: The test classification accuracy of using covariance parameters to predict tasks in the Human Connectome Project motor dataset (%)

Methods	Number of training subjects				
	10	20	30	40	50
M1 ($W = 10, K = 15$)	49.6 ± 6.4	70.8 ± 3.4	77.3 ± 3.2	79.7 ± 2.8	80.8 ± 1.7
M1 ($W = 50, K = 15$)	26.5 ± 4.7	34.9 ± 3.3	36.5 ± 3.5	38.4 ± 2.0	39.6 ± 2.4
M2 ($K = 15$)	27.7 ± 3.5	27.1 ± 4.3	25.1 ± 2.0	24.3 ± 4.4	24.8 ± 2.0
M2 ($K = 60$)	37.6 ± 5.3	44.5 ± 4.7	40.9 ± 5.8	38.2 ± 3.9	44.1 ± 6.7
M4 ($K = 15$)	52.6 ± 8.3	77.4 ± 6.8	85.0 ± 3.5	89.0 ± 3.0	90.5 ± 2.5
M6 ($W = 10$)	70.9 ± 2.7	78.3 ± 3.3	81.0 ± 1.6	79.8 ± 3.0	81.2 ± 2.6
M** ($K = 15$)	61.5 ± 7.4	81.5 ± 5.4	87.4 ± 2.5	90.0 ± 1.7	90.5 ± 2.5

sen et al., 2013), which contains 103 subjects, into a training set and testing set. The length of each task is identical, 27 time points for each activation, and 2 activations in each session. Since each task partially overlaps with others (see the activation map in Supplementary Material), we predict the task based on the activation blocks rather than single time points. We group the estimated covariances $\{\Sigma_j\}_{j \in [J]}$ and the testing data based on the task activation map and perform a nearest neighbor search. The clustered covariance is denoted as $\Sigma_{task,i}$, where $task \in \{\text{right hand tapping, left foot tapping, tongue wagging, right foot tapping, left hand tapping}\}$ and $i \in [54]$. The task score of each block of testing data is defined as

$$score_{task}(\{x_i\}_{i \in [54]}) = \sum_{i=1}^{54} \|x_i x_i^T - \Sigma_{task,i}\|_F^2.$$

where $\{x_i\}_{i \in [54]}$ is a block of testing data. We predict the task of the block data by choosing the task with the minimum score. We repeat the experiment 10 times and the result is shown in Table 5. Note that the Markov model (M2) performs the worst even if we increase the number of states to 60. The dictionary learning model (M4) has comparable performance to our model when the sample size is large, and yet our model performs better with small sample sizes.

7 Discussion

Several directions are worthy of further investigation. We plan to explore more flexible spatial structure. Prior work (Gibberd & Nelson, 2017; Hallac et al., 2017) applied fused graphical lasso and group graphical lasso to encourage similar sparse structures for time-varying graphical models. These approaches did not restrict the spatial components to be identical, but only similar, and thus are more flexible compared to the proposed model. To this end, one idea is to build factor models that encourage similar, but not identical spatial structures, while retaining low-rank. Finally, while our work has focused on fixed sampling intervals, another direction is to explore models with samples obtained at irregular time intervals (Tank et al., 2019; Qiao et al., 2020), as this setting is common in multimodal data.

Acknowledgement

We thank James M. Shine for help with data pre-processing and helpful modeling discussions. The research project is partially funded by the U.S.A. National Institutes of Health 1R01MH116226-

01A, National Science Foundation Graduate Research Fellowships Program, and Strategic Research Initiatives Grainger College of Engineering, the University of Illinois at Urbana-Champaign. Data were provided by the Human Connectome Project, WU-Minn Consortium (Principal Investigators: David Van Essen and Kamil Ugurbil; 1U54MH091657) funded by the 16 NIH Institutes and Centers that support the NIH Blueprint for Neuroscience Research; and by the McDonnell Center for Systems Neuroscience at Washington University.

Supplementary material

The supplementary material contains technical proofs and additional experimental results.

References

- AHELEGBEY, D. F., BILLIO, M. & CASARIN, R. (2016). Bayesian graphical models for structural vector autoregressive processes. *Journal of Applied Econometrics* **31**, 357–386.
- ANDERSEN, M. R., WINTHER, O., HANSEN, L. K., POLDRACK, R. & KOYEJO, O. (2018). Bayesian structure learning for dynamic brain connectivity. In *21st International Conference on Artificial Intelligence and Statistics, AISTATS 2018*.
- ANDERSON, T. W. & RUBIN, H. (1956). Statistical inference in factor analysis. In *Proceedings of the Third Berkeley Symposium on Mathematical Statistics and Probability, Volume 5: Contributions to Econometrics, Industrial Research, and Psychometry*. Berkeley, Calif.: University of California Press.
- ARSIGNY, V., FILLARD, P., PENNEC, X. & AYACHE, N. (2006). Log-Euclidean metrics for fast and simple calculus on diffusion tensors. *Magnetic Resonance in Medicine: An Official Journal of the International Society for Magnetic Resonance in Medicine* **56**, 411–421.
- BAÑBURA, M., GIANNONE, D. & REICHLIN, L. (2010). Large bayesian vector auto regressions. *Journal of applied Econometrics* **25**, 71–92.
- BHOJANAPALLI, S., KYRILLIDIS, A. & SANGHAVI, S. (2016). Dropping convexity for faster semi-definite optimization. In *Conference on Learning Theory*.
- BLEI, D. M., KUCUKELBIR, A. & MCAULIFFE, J. D. (2017). Variational inference: A review for statisticians. *Journal of the American Statistical Association* **112**, 859–877.
- BURER, S. & MONTEIRO, R. D. (2003). A nonlinear programming algorithm for solving semidefinite programs via low-rank factorization. *Mathematical Programming* **95**, 329–357.
- BURER, S. & MONTEIRO, R. D. (2005). Local minima and convergence in low-rank semidefinite programming. *Mathematical Programming* **103**, 427–444.
- CALHOUN, V. D., MILLER, R., PEARLSON, G. & ADALI, T. (2014). The chronnectome: Time-varying connectivity networks as the next frontier in fmri data discovery. *Neuron* **84**, 262–274.
- CANDES, E. J., LI, X. & SOLTANOLKOTABI, M. (2015). Phase retrieval via Wirtinger flow: Theory and algorithms. *IEEE Transactions on Information Theory* **61**, 1985–2007.
- CHANG, C., LEOPOLD, D. A., SCHÖLVINCK, M. L., MANDELKOW, H., PICCHIONI, D., LIU, X., FRANK, Q. Y., TURCHI, J. N. & DUYN, J. H. (2016). Tracking brain arousal fluctuations with fmri. *Proceedings of the National Academy of Sciences* , 201520613.
- CHEN, Y. & CANDES, E. (2015). Solving random quadratic systems of equations is nearly as easy as solving linear systems. In *Advances in Neural Information Processing Systems*.
- CHEN, Y. & WAINWRIGHT, M. J. (2015). Fast low-rank estimation by projected gradient descent: General statistical and algorithmic guarantees. *arXiv preprint arXiv:1509.03025* .

- CHI, Y., LU, Y. M. & CHEN, Y. (2019). Nonconvex optimization meets low-rank matrix factorization: An overview. *IEEE Transactions on Signal Processing* **67**.
- DANAHER, P., WANG, P. & WITTEN, D. M. (2014). The joint graphical lasso for inverse covariance estimation across multiple classes. *Journal of the Royal Statistical Society: Series B (Statistical Methodology)* **76**, 373–397.
- DAVIS, R. A., ZANG, P. & ZHENG, T. (2016). Sparse vector autoregressive modeling. *Journal of Computational and Graphical Statistics* **25**, 1077–1096.
- DIEDRICHSSEN, J., BALSTERS, J. H., FLAVELL, J., CUSSANS, E. & RAMNANI, N. (2009). A probabilistic mr atlas of the human cerebellum. *Neuroimage* **46**, 39–46.
- EAVANI, H., FILIPOVYCH, R., DAVATZIKOS, C., SATTERTHWAITE, T. D., GUR, R. E. & GUR, R. C. (2012). Sparse dictionary learning of resting state fmri networks. In *2012 Second International Workshop on Pattern Recognition in NeuroImaging*. IEEE.
- ENGLE, R. F., LEDOIT, O. & WOLF, M. (2019). Large dynamic covariance matrices. *Journal of Business & Economic Statistics* **37**, 363–375.
- ESCALANTE, R. & RAYDAN, M. (2011). *Alternating Projection Methods*, vol. 8. SIAM.
- FOTI, N. J. & FOX, E. B. (2019). Statistical model-based approaches for functional connectivity analysis of neuroimaging data. *Current opinion in neurobiology* **55**, 48–54.
- FOX, E. B. & DUNSON, D. B. (2015). Bayesian nonparametric covariance regression. *The Journal of Machine Learning Research* **16**, 2501–2542.
- FOX, M. D. & RAICHLE, M. E. (2007). Spontaneous fluctuations in brain activity observed with functional magnetic resonance imaging. *Nature Reviews Neuroscience* **8**, 700–711.
- GIBBERD, A. J. & NELSON, J. D. (2017). Regularized estimation of piecewise constant gaussian graphical models: The group-fused graphical lasso. *Journal of Computational and Graphical Statistics* **26**, 623–634.
- GORDON, E. M., LAUMANN, T. O., ADEYEMO, B., HUCKINS, J. F., KELLEY, W. M. & PETERSEN, S. E. (2016). Generation and evaluation of a cortical area parcellation from resting-state correlations. *Cerebral cortex* **26**, 288–303.
- GU, Q., WANG, Z. W. & LIU, H. (2016). Low-rank and sparse structure pursuit via alternating minimization. In *Proceedings of Machine Learning Research*, A. Gretton & C. C. Robert, eds., vol. 51. PMLR.
- HALLAC, D., PARK, Y., BOYD, S. & LESKOVEC, J. (2017). Network inference via the time-varying graphical lasso. In *Proceedings of the 23rd ACM SIGKDD International Conference on Knowledge Discovery and Data Mining*.
- HARDT, M. (2014). Understanding alternating minimization for matrix completion. In *2014 IEEE 55th Annual Symposium on Foundations of Computer Science*. IEEE.

- JAIN, P., NETRAPALLI, P. & SANGHAVI, S. (2013). Low-rank matrix completion using alternating minimization. In *Proceedings of the Forty-Fifth Annual ACM Symposium on Theory of Computing*.
- KASTNER, G., FRÜHWIRTH-SCHNATTER, S. & LOPES, H. F. (2017). Efficient Bayesian inference for multivariate factor stochastic volatility models. *Journal of Computational and Graphical Statistics* **26**, 905–917.
- KOLAR, M., SONG, L., AHMED, A. & XING, E. P. (2010). Estimating time-varying networks. *The Annals of Applied Statistics* **4**, 94–123.
- KUMAR, S., YING, J., DE MIRANDA CARDOSO, J. V. & PALOMAR, D. P. (2020). A unified framework for structured graph learning via spectral constraints. *Journal of Machine Learning Research* **21**, 1–60.
- LEDOIT, O. & WOLF, M. (2004). A well-conditioned estimator for large-dimensional covariance matrices. *Journal of multivariate analysis* **88**, 365–411.
- LEONARDI, N. & VAN DE VILLE, D. (2015). On spurious and real fluctuations of dynamic functional connectivity during rest. *Neuroimage* **104**, 430–436.
- LI, R. (2019). Multivariate sparse coding of nonstationary covariances with Gaussian processes. In *Advances in Neural Information Processing Systems*.
- LI, X., ZHAO, T., ARORA, R., LIU, H. & HAUPT, J. (2016). Stochastic variance reduced optimization for nonconvex sparse learning. In *International Conference on Machine Learning*.
- LIÉGEOIS, R., LI, J., KONG, R., ORBAN, C., VAN DE VILLE, D., GE, T., SABUNCU, M. R. & YEO, B. T. (2019). Resting brain dynamics at different timescales capture distinct aspects of human behavior. *Nature communications* **10**, 1–9.
- LOH, P.-L. & WAINWRIGHT, M. J. (2015). Regularized m-estimators with nonconvexity: Statistical and algorithmic theory for local optima. *The Journal of Machine Learning Research* **16**, 559–616.
- MAIRAL, J., BACH, F., PONCE, J. & SAPIRO, G. (2010). Online learning for matrix factorization and sparse coding. *Journal of Machine Learning Research* **11**, 19–60.
- MARIEB, E. N. & HOEHN, K. (2007). *Human anatomy & physiology*. Pearson education.
- MINASNY, B. & MCBRATNEY, A. B. (2005). The matérn function as a general model for soil variograms. *Geoderma* **128**, 192–207.
- MISHNE, G. & CHARLES, A. S. (2019). Learning spatially-correlated temporal dictionaries for calcium imaging. In *ICASSP 2019-2019 IEEE International Conference on Acoustics, Speech and Signal Processing (ICASSP)*. IEEE.
- NESTEROV, Y. (2013). *Introductory Lectures on Convex Optimization: A Basic Course*, vol. 87. Springer Science & Business Media.

- OLSHAUSEN, B. A. & FIELD, D. J. (1997). Sparse coding with an overcomplete basis set: A strategy employed by v1? *Vision research* **37**, 3311–3325.
- PACIOREK, C. J. (2003). *Nonstationary Gaussian processes for regression and spatial modelling*. Ph.D. thesis, Citeseer.
- PARK, D., KYRILLIDIS, A., CARAMANIS, C. & SANGHAVI, S. (2018). Finding low-rank solutions via nonconvex matrix factorization, efficiently and provably. *SIAM Journal on Imaging Sciences* **11**, 2165–2204.
- PORITZ, A. (1982). Linear predictive hidden markov models and the speech signal. In *ICASSP'82. IEEE International Conference on Acoustics, Speech, and Signal Processing*, vol. 7. IEEE.
- POSNER, M. I., PETERSEN, S. E., FOX, P. T. & RAICHLE, M. E. (1988a). Localization of cognitive operations in the human brain. *Science* **240**, 1627–1631.
- POSNER, M. I., PETERSEN, S. E., FOX, P. T. & RAICHLE, M. E. (1988b). Localization of cognitive operations in the human brain. *Science* **240**, 1627–1631.
- PRETI, M. G., BOLTON, T. A. & VAN DE VILLE, D. (2017). The dynamic functional connectome: State-of-the-art and perspectives. *Neuroimage* **160**, 41–54.
- QIAO, X., QIAN, C., JAMES, G. M. & GUO, S. (2020). Doubly functional graphical models in high dimensions. *Biometrika* **107**, 415–431.
- QIU, H., HAN, F., LIU, H. & CAFFO, B. (2016). Joint estimation of multiple graphical models from high dimensional time series. *Journal of the Royal Statistical Society: Series B (Statistical Methodology)* **78**, 487–504.
- SAKOĞLU, Ü., PEARLSON, G. D., KIEHL, K. A., WANG, Y. M., MICHAEL, A. M. & CALHOUN, V. D. (2010). A method for evaluating dynamic functional network connectivity and task-modulation: application to schizophrenia. *Magnetic Resonance Materials in Physics, Biology and Medicine* **23**, 351–366.
- SCHÖLKOPF, B., SMOLA, A. J., BACH, F. et al. (2002). *Learning with kernels: support vector machines, regularization, optimization, and beyond*. MIT press.
- SHINE, J. M., BISSETT, P. G., BELL, P. T., KOYEJO, O., BALSTERS, J. H., GORGOLEWSKI, K. J., MOODIE, C. A. & POLDRACK, R. A. (2016a). The dynamics of functional brain networks: Integrated network states during cognitive task performance. *Neuron* **92**, 544–554.
- SHINE, J. M., BREAKSPEAR, M., BELL, P. T., MARTENS, K. A. E., SHINE, R., KOYEJO, O., SPORNS, O. & POLDRACK, R. A. (2019). Human cognition involves the dynamic integration of neural activity and neuromodulatory systems. *Nature neuroscience* **22**, 289–296.
- SHINE, J. M., KOYEJO, O. & POLDRACK, R. A. (2016b). Temporal metastates are associated with differential patterns of time-resolved connectivity, network topology, and attention. *Proceedings of the National Academy of Sciences* **113**, 9888–9891.

- SKRIPNIKOV, A. & MICHAILIDIS, G. (2019). Regularized joint estimation of related vector autoregressive models. *Computational Statistics & Data Analysis* **139**, 164 – 177.
- SMITH, A. M., LEWIS, B. K., RUTTIMANN, U. E., FRANK, Q. Y., SINNWELL, T. M., YANG, Y., DUYN, J. H. & FRANK, J. A. (1999). Investigation of low frequency drift in fmri signal. *Neuroimage* **9**, 526–533.
- STEWART, G. (1977). Perturbation bounds for the qr factorization of a matrix. *SIAM Journal on Numerical Analysis* **14**, 509–518.
- TANK, A., FOX, E. B. & SHOJAIE, A. (2019). Identifiability and estimation of structural vector autoregressive models for subsampled and mixed-frequency time series. *Biometrika* **106**, 433–452.
- TEN BERGE, J. M. (1977). Orthogonal procrustes rotation for two or more matrices. *Psychometrika* **42**, 267–276.
- TROPP, J. A. (2015). An introduction to matrix concentration inequalities. *Foundations and Trends® in Machine Learning* **8**, 1–230.
- UDELL, M., HORN, C., ZADEH, R., BOYD, S. et al. (2016). Generalized low rank models. *Foundations and Trends® in Machine Learning* **9**, 1–118.
- UDELL, M. & TOWNSEND, A. (2019). Why are big data matrices approximately low rank? *SIAM Journal on Mathematics of Data Science* **1**, 144–160.
- VAN ESSEN, D. C., SMITH, S. M., BARCH, D. M., BEHRENS, T. E., YACOUB, E., UGURBIL, K., CONSORTIUM, W.-M. H. et al. (2013). The WU-Minn human connectome project: An overview. *Neuroimage* **80**, 62–79.
- VERSHYNIN, R. (2010). Introduction to the non-asymptotic analysis of random matrices. *arXiv preprint arXiv:1011.3027* .
- VIDAURRE, D., SMITH, S. M. & WOOLRICH, M. W. (2017). Brain network dynamics are hierarchically organized in time. *Proceedings of the National Academy of Sciences* **114**, 12827–12832.
- YIN, J., GENG, Z., LI, R. & WANG, H. (2010). Nonparametric covariance model. *Statistica Sinica* **20**, 469.
- YU, M., GUPTA, V. & KOLAR, M. (2020). Recovery of simultaneous low rank and two-way sparse coefficient matrices, a nonconvex approach. *Electronic Journal of Statistics* **14**, 413–457.
- ZALESKY, A., FORNITO, A. & BULLMORE, E. (2012). On the use of correlation as a measure of network connectivity. *Neuroimage* **60**, 2096–2106.
- ZHANG, J. & LI, J. (2019). Factorized estimation of high-dimensional nonparametric covariance models. *Annals of Statistics* .
- ZHAO, T., WANG, Z. & LIU, H. (2015). A nonconvex optimization framework for low rank matrix estimation. *Advances in Neural Information Processing Systems* **28**, 559.

Supplementary material for A Nonconvex Framework for Structured Dynamic Covariance Recovery

We propose a nonconvex framework to estimate structured covariance matrices. In the present setting, the dynamic covariance matrices are decomposed into low-rank sparse spatial components and smooth temporal components. We employ a two-stage approach to minimize the proposed nonconvex objective function: we design a spectral initialization method to obtain a good initial guess followed by iterative refinements via projected gradient descent. This approach converges linearly to a statistically useful solution, which can be quantified by the statistical error rate. In this supplementary material, we provide technical proofs and additional experimental results.

A Projection to constraint sets

We describe the algorithms used to project iterates to the constraints \mathcal{C}_V , $\tilde{\mathcal{C}}_V$, and $\tilde{\mathcal{C}}_A$. Next, we characterize the expansion coefficient induced by projecting to nonconvex sets.

A.1 Projections to \mathcal{C}_V and $\tilde{\mathcal{C}}_V$

Recall that $\mathcal{C}_V(s) = \{v \in \mathbb{R}^P : \|v\|_0 \leq s, \|v\|_2 = 1\}$. To project a vector v onto $\mathcal{C}_V(s)$, we want to solve the following problem

$$\arg \min_{x \in \mathcal{C}_V} \|v - x\|_2^2. \quad (\text{A.1})$$

Let $\mathcal{S}(x) = \{i : x_i \neq 0\}$ be the support of x . Given a support $E \subset [P]$, let $[x]_E \in \mathbb{R}^P$ be a vector whose i th entry is equal to x_i if $i \in E$ and 0 otherwise. Let

$$d(E) = \min_x \|v - x\|_2^2 \quad \text{subject to} \quad \mathcal{S}(x) \subseteq E, \|x\|_2 = 1,$$

and observe that

$$\begin{aligned} d(E) &= \min_x \|v\|_2^2 + \|x\|_2^2 - 2\langle x, v \rangle \\ &= \|v\|_2^2 + 1 - 2 \max_x \langle x, v \rangle \\ &= \|v\|_2^2 + 1 - 2\|[v]_E\|_2. \end{aligned}$$

Then we can conclude that

$$\hat{E} = \arg \min_{E: |E| \leq s} d(E) = \arg \max_{E: |E| \leq s} \|[v]_E\|_2, \quad (\text{A.2})$$

which can be solved by finding the top- s entries of v in magnitude. This can be done with computational complexity $O(P \log P)$. After finding the support in (A.2), we can obtain (A.1) by projecting $[x]_{\hat{E}}$ to the unit sphere. Algorithm 3 summarizes the procedure.

Next, we discuss the projection procedure when we additionally orthogonalize the estimate via QR decomposition. Let $\hat{V} = \Pi_{\mathcal{C}_V}(V)$ and $\hat{V} = BL$ be the QR decomposition of \hat{V} , where B has orthonormal columns and L is upper triangular matrix. We define

$$\Pi_{\tilde{\mathcal{C}}_V}(V) = B. \quad (\text{A.3})$$

Algorithm 3 Projection to $\mathcal{C}_V(s)$

Input: $v \in \mathbb{R}^P$
 $v_S \leftarrow$ Pick the top- s entries of v in magnitude and set the rest of entries to 0
 $\hat{v} \leftarrow$ Project v_S to the unit sphere S^{P-1}
Output \hat{v}

A.2 Projection to $\tilde{\mathcal{C}}_A$

Recall that $\tilde{\mathcal{C}}_A(c, \gamma) = \{\alpha = \tilde{Q}u : 0 \leq \alpha_j \leq c, u^T \tilde{\Lambda}u \leq \gamma\}$, where $\tilde{G}^\dagger = \tilde{Q}\tilde{\Lambda}\tilde{Q}^T$ is the eigendecomposition of \tilde{G}^\dagger and λ_j denotes the j th diagonal entry of $\tilde{\Lambda}$. To project to the convex set $\tilde{\mathcal{C}}_A$, we use an alternating projection method. While the convergence rate of the alternating projection method is not our focus, in the experiments, we observe that often one iteration of the alternating projection results in an iterate that satisfies both constraints. Algorithm 4 summarizes the alternating projection procedure.

Algorithm 4 Projection to $\tilde{\mathcal{C}}_A(c, \gamma)$

Input: $\alpha \in \mathbb{R}^J$
While $\alpha \notin \tilde{\mathcal{C}}_A(c, \gamma)$
 $\hat{\alpha} \leftarrow$ Project α to the hypercube $[0, c]^J$
 $\alpha \leftarrow$ Project $\hat{\alpha}$ to the set $\{\alpha = \tilde{Q}u : u^T \tilde{\Lambda}u \leq \gamma\}$ using Algorithm 5
Output α

Next, we provide an algorithm for projecting to the ellipsoid $\{\alpha = \tilde{Q}u : u^T \tilde{\Lambda}u \leq \gamma\}$, which is one of the steps in Algorithm 4. It is easy to see that a vector y belonging to $\{\alpha = \tilde{Q}u : u^T \tilde{\Lambda}u \leq \gamma\}$ lies in the range space of \tilde{Q} , which has dimension $r(\tilde{G})$. Let Q_1 be the matrix whose orthonormal columns form the subspace orthogonal to columns of \tilde{Q} , which has dimension $J - r(\tilde{G})$. In this case, we have $Q_1^T y = 0$.

Projection of $\hat{\alpha}$ to the ellipsoid $\{\alpha = \tilde{Q}u : u^T \tilde{\Lambda}u \leq \gamma\}$ is conducted by solving the following constrained optimization problem

$$\arg \min_y \|\hat{\alpha} - y\|_2^2, \quad \text{subject to } y^T \tilde{G}^\dagger y \leq \gamma, y \in \mathcal{R}(\tilde{Q}), \quad (\text{A.4})$$

where $\mathcal{R}(\tilde{Q})$ denote the range space of \tilde{Q} . We can find the solution by finding the Karush-Kuhn-Tucker condition of the Lagrangian function. The following proposition characterizes the solution, which justifies Algorithm 5.

Proposition A.1. *The solution to (A.4) is*

$$\begin{cases} \tilde{Q}\tilde{Q}^T\hat{\alpha}, & \text{if } \hat{\alpha}^T \tilde{G}^\dagger \hat{\alpha} \leq \gamma; \\ \tilde{Q}\tilde{\Lambda}^{-1}(\hat{x}I + \tilde{\Lambda}^{-1})^{-1}\tilde{Q}^T\hat{\alpha}, & \text{otherwise,} \end{cases}$$

Algorithm 5 Projection to $\{\alpha = \tilde{Q}u : u^T \tilde{\Lambda}u \leq \gamma\}$

Input: $\hat{\alpha} \in \mathbb{R}^J$
 If $\hat{\alpha}^T \tilde{G}^\dagger \hat{\alpha} \leq \gamma$
 $a \leftarrow \tilde{Q} \tilde{Q}^T \hat{\alpha}$
 Else
 $u \leftarrow \tilde{Q}^T \hat{\alpha}$
 $D \leftarrow$ Find the roots of $x: 3x^2 \sum_{j=1}^{r(\tilde{G})} \lambda_j^3 u_j^2 - 2x \sum_{j=1}^{r(\tilde{G})} \lambda_j^2 u_j^2 + \sum_{j=1}^{r(\tilde{G})} \lambda_j u_j^2 - \gamma = 0$
 $\hat{x} \leftarrow$ Pick the largest nonnegative value in the set D
 $a \leftarrow \tilde{Q} \tilde{\Lambda}^{-1} (\hat{x}I + \tilde{\Lambda}^{-1})^{-1} \tilde{Q}^T \hat{\alpha}$
 Output a

where $\tilde{G}^\dagger = \tilde{Q} \tilde{\Lambda} \tilde{Q}^T$ is the eigendecomposition of \tilde{G}^\dagger and λ_j denotes the j th diagonal entry of $\tilde{\Lambda}$, \hat{x} is the largest nonnegative solution to

$$3x^2 \sum_{j=1}^{r(\tilde{G})} \lambda_j^3 u_j^2 - 2x \sum_{j=1}^{r(\tilde{G})} \lambda_j^2 u_j^2 + \sum_{j=1}^{r(\tilde{G})} \lambda_j u_j^2 - \gamma = 0,$$

and $u = \tilde{Q}^T \hat{\alpha}$.

Proof. Let (\tilde{Q}, Q_1) be a unitary matrix with $\tilde{Q}^T Q_1 = 0$. Let $\hat{u} = (\tilde{Q}, Q_1)^T \hat{\alpha}$, and $\hat{z} = (\tilde{Q}, Q_1)^T y$. Since (\tilde{Q}, Q_1) is unitary, we have

$$\|\hat{\alpha} - y\|_2^2 = \|(\tilde{Q} \ Q_1)^T (\hat{\alpha} - y)\|_2^2 = \|\hat{u} - \hat{z}\|_2^2.$$

Let $u = \tilde{Q}^T \hat{\alpha}$ and $z = \tilde{Q}^T y$. Since $Q_1^T \tilde{Q} = 0$ and we must have $Q_1^T y = 0$, the problem (A.4) is equivalent to the following

$$\arg \min_z \|u - z\|_2^2, \quad \text{subject to } z^T \tilde{\Lambda} z \leq \gamma. \quad (\text{A.5})$$

Letting $w = \tilde{\Lambda}^{1/2} z$, we can rewrite the objective function (A.5) as follows

$$\arg \min_w \|u - \tilde{\Lambda}^{-1/2} w\|_2^2, \quad \text{subject to } w^T w \leq \gamma.$$

Let the corresponding Lagrangian function be

$$\mathcal{L}(w, x) = \|u - \tilde{\Lambda}^{-1/2} w\|_2^2 + x(w^T w - \gamma).$$

The condition $\nabla_w \mathcal{L} = 0$ implies that

$$w = (xI + \tilde{\Lambda}^{-1})^{-1} \tilde{\Lambda}^{-1/2} u.$$

By the Karush–Kuhn–Tucker condition, if $w^T w < \gamma$, then $y^* = \tilde{Q}\tilde{Q}^T \hat{\alpha}$. Otherwise, $w^T w = \gamma$. This implies that

$$\sum_{j=1}^{r(\tilde{G})} \frac{(u_j^2 \lambda_j)}{(1 + x \lambda_j)^2} = \gamma. \quad (\text{A.6})$$

Using the second order Taylor expansion, we write (A.6) as

$$3x^2 \sum_{j=1}^{r(\tilde{G})} \lambda_j^3 u_j^2 - 2x \sum_{j=1}^{r(\tilde{G})} \lambda_j^2 u_j^2 + \sum_{j=1}^{r(\tilde{G})} \lambda_j u_j^2 - \gamma = 0. \quad (\text{A.7})$$

Then, finding x is equivalent as finding the roots of the above polynomial function. Finally, we plug \hat{x} , the largest nonnegative solution to (A.7), into $y^* = \tilde{Q}\tilde{\Lambda}^{-1}(\hat{x}I + \tilde{\Lambda}^{-1})^{-1}\tilde{Q}^T \hat{\alpha}$ and complete the proof. \square

A.3 Expansion Coefficients of Projections to \mathcal{C}_V and $\tilde{\mathcal{C}}_V$

Let v be a column of V , v^* be a column of V^* , and let \hat{v} denote projection of v to \mathcal{C}_V . Since \mathcal{C}_V is a nonconvex set, \hat{v} may be further away from v^* compared to v . We denote $\Pi_{\mathcal{C}_V}(V)$ as the projection operator that projects columns of V to \mathcal{C}_V . We characterize ρ such that

$$\|\Pi_{\mathcal{C}_V}(V) - V^*R\|_F^2 \leq \rho \|V - V^*R\|_F^2.$$

Lemma A.4 characterizes ρ by combining results from Lemma A.2 and Lemma A.3. Lemma A.6 provides a bound on ρ when an additional step to orthogonalize V via QR decomposition is performed.

The following lemma shows the expansion coefficient of the hard thresholding operator, which corresponds to the first step in Algorithm 3.

Lemma A.2 (Lemma 4.1 in Li et al. (2016)). *Suppose that $u \in \mathbb{R}^P$ is a sparse vector such that $\|u\|_0 \leq s^*$. Let $\Pi_s(\cdot) : \mathbb{R}^P \rightarrow \mathbb{R}^P$ be the hard thresholding operator, which outputs a vector by selecting the top- s entries of the input vector in absolute value and setting the rest of the entries to 0. Given $s > s^*$, for any vector $v \in \mathbb{R}^P$, we have*

$$\|\Pi_s(v) - u\|_2^2 \leq \left\{ 1 + \frac{2\sqrt{s^*}}{\sqrt{(s - s^*)}} \right\} \|v - u\|_2^2.$$

The following results characterizes the expansion coefficient for the second step in Algorithm 3.

Lemma A.3. *Assume that $v^T u \geq 0$, $\|u\|_2 = 1$, and $\|v\|_2 \leq 1$. Then*

$$2\|v - u\|_2^2 \geq \left\| \frac{v}{\|v\|_2} - u \right\|_2^2.$$

of Lemma A.3. Showing $2\|v - u\|_2^2 \geq \|v/\|v\|_2 - u\|_2^2$ is equivalent to showing

$$2\|v\|_2^2 + 2v^T u \left(\frac{1}{\|v\|_2} - 2 \right) \geq 0.$$

Let $\cos \theta = (v^T u) / (\|v\|_2 \|u\|_2)$. Then we need to show that

$$2\|v\|_2^2 + 2\cos \theta - 4\|v\|_2 \cos \theta \geq 0. \quad (\text{A.8})$$

Since $(a + b) \geq 2\sqrt{ab}$, for $a \geq 0$ and $b \geq 0$, and $\cos^{1/2} \theta \geq \cos \theta$ for $\cos \theta \geq 0$, we have established (A.8). \square

Combining Lemma A.2 and Lemma A.3, we obtain the following result.

Lemma A.4. *Consider two matrices $U, V \in \mathbb{R}^{P \times K}$, and assume that $v_k^T u_k \geq 0$ and $\|u_k\|_0 \leq s^*$ for $k \in [K]$. Assume that $s > s^*$. Let $\Pi_{\mathcal{C}_V} : \mathbb{R}^{P \times K} \rightarrow \mathbb{R}^{P \times K}$ be the projection operator that projects columns of the matrix onto the set \mathcal{C}_V , defined in Section A.1. Then*

$$\|\Pi_{\mathcal{C}_V}(V) - U\|_F^2 \leq 2 \left\{ 1 + \frac{2\sqrt{s^*}}{\sqrt{(s - s^*)}} \right\} \|V - U\|_F^2. \quad (\text{A.9})$$

of Lemma A.4. Lemma A.2 states the expansion coefficient of the first projection in Algorithm 3. Similarly, Lemma A.3 states the expansion coefficient of the second projection in Algorithm 3 when the vector before projection has norm smaller than 1. If the vector before projection has norm greater or equal to 1, then the projection to the unit sphere is equivalent as the projection to the unit ball, which is a convex set. Then, the resulting projection is a contraction. By multiplying the results of two lemmas, we can obtain the expansion coefficient of projection to \mathcal{C}_V for each column vector. Stacking all the column vectors together, we obtain the result (A.9). \square

The following lemmas characterize the expansion coefficient ρ when an additional QR decomposition step is used. We first state a result from the perturbation theory of QR decomposition (Stewart, 1977).

Lemma A.5 (Adapter from Theorem 1 in (Stewart, 1977)). *Let A^\dagger be the pseudo inverse of a rank K matrix $A \in \mathbb{R}^{P \times K}$. Suppose that $E \in \mathbb{R}^{P \times K}$ and $\|E\|_2 \|A^\dagger\|_2 < 1$. Then, given a QR decomposition of $(A + E) = BL$, there exists a decomposition of $A = B^* L^*$, such that B^* has orthonormal columns and L^* is a nonsingular upper triangular matrix and*

$$\|B - B^*\|_F \leq \frac{\sqrt{2} \|A^\dagger\|_2 \|E\|_F}{1 - \|E\|_2 \|A^\dagger\|_2}. \quad (\text{A.10})$$

Next, we apply Lemma A.5 to our setting and establish the following lemma.

Lemma A.6. *Let U be a matrix with orthonormal columns. Let $V \in \mathbb{R}^{P \times K}$ be a rank K matrix with unit norm columns, and $\|V - U\|_2 \leq r' < 1$. Let $V = BL$ be the QR decomposition of V , where $B \in \mathbb{R}^{P \times K}$ has orthonormal columns and $L \in \mathbb{R}^{K \times K}$ is an upper triangular matrix. Then*

$$\|B - B^*\|_F^2 \leq \frac{2}{(1 - r')^2} \|V - U\|_F^2.$$

Proof. Let $E = V - U$ and $A = U$. We have $\|E\|_2 \leq r'$, $\|A^\dagger\|_2 = 1$. The result then follows from Lemma A.5 as

$$\|B - B^*\|_F \leq \frac{\sqrt{2} \|V - U\|_F}{1 - r'}.$$

\square

B Linear Convergence and Statistical Error

B.1 Upper bound for the distance metric

We establish an upper bound on $\text{dist}^2(Z, \tilde{Z}^*)$ in terms of $\{\|\Sigma_j - \tilde{\Sigma}_j^*\|_F^2\}_{j \in [J]}$, which serves as an important ingredient in the analysis of linear convergence.

Lemma B.1. *For two matrices $V, V^* \in \mathbb{R}^{P \times K}$ with orthonormal columns, let*

$$R = \underset{Y \in \mathcal{O}(K)}{\text{argmin}} \|V - V^*Y\|_F^2.$$

Let $\Sigma_j = V \text{diag}(a_j) V^T$, $\tilde{\Sigma}_j^* = V^* \text{diag}(\tilde{a}_j^*) V^{*T}$, $\Sigma_j^* = V^* \text{diag}(a_j^*) V^{*T}$ and c be a positive constant such that $\|\text{diag}(a_j)\|_2 \leq c$ for $j \in [J]$. Suppose that $\sigma_K(\Sigma_j^* - \tilde{\Sigma}_j^*) \leq 1/4 \sigma_K(\Sigma_j^*)$ for $j \in [J]$, then

$$\sum_{j=1}^J \|V - V^*R\|_F^2 + \|\text{diag}(a_j) - R^T \text{diag}(\tilde{a}_j^*) R\|_F^2 \leq \xi^2 \sum_{j=1}^J \|\Sigma_j - \tilde{\Sigma}_j^*\|_F^2,$$

where

$$\xi^2 = \max_{j \in [J]} \left\{ \frac{16}{\sigma_K^2(\Sigma_j^*)} + \left(1 + \frac{8c}{\sigma_K(\Sigma_j^*)} \right)^2 \right\}.$$

of Lemma B.1. We establish the result for a single $j \in [J]$. The bound can easily be extended to the sum of all $j \in [J]$.

Since $\tilde{\Sigma}_j^*$ is rank K , we have $\sigma_{K+1}(\tilde{\Sigma}_j^*) = 0$ for $j \in [J]$. Consequently,

$$\sigma_K(\tilde{\Sigma}_j^*) - \sigma_{K+1}(\tilde{\Sigma}_j^*) = \sigma_K(\tilde{\Sigma}_j^*) > 0,$$

for $j \in [J]$ and we can use Lemma G.2 to obtain

$$\|V - V^*R\|_F^2 \leq \frac{8}{\sigma_K^2(\tilde{\Sigma}_j^*)} \|\Sigma_j - \tilde{\Sigma}_j^*\|_F^2. \quad (\text{B.1})$$

Moreover, since

$$\sigma_K(\tilde{\Sigma}_j^*) \geq \sigma_K(\Sigma_j^*) - \sigma_K(\Sigma_j^* - \tilde{\Sigma}_j^*) \geq \frac{3}{4} \sigma_K(\Sigma_j^*),$$

we have

$$\|V - V^*R\|_F^2 \leq \frac{16}{\sigma_K^2(\Sigma_j^*)} \|\Sigma_j - \tilde{\Sigma}_j^*\|_F^2.$$

Next, by the triangular inequality, we have

$$\begin{aligned} \|\Sigma_j - \tilde{\Sigma}_j^*\|_F &= \|V \text{diag}(a_j) V^T - V^* R R^T \text{diag}(\tilde{a}_j^*) R R^T V^{*T}\|_F \\ &\geq \|V^* R \{\text{diag}(a_j) - R^T \text{diag}(\tilde{a}_j^*) R\} R^T V^{*T}\|_F \\ &\quad - \|(V - V^*R) \text{diag}(a_j) V^T\|_F - \|V^* R \text{diag}(a_j) (V - V^*R)^T\|_F. \end{aligned}$$

Since

$$\|V^*R\{\text{diag}(a_j) - R^T \text{diag}(\tilde{a}_j^*)R\}R^T V^{*T}\|_F = \|\text{diag}(a_j) - R^T \text{diag}(\tilde{a}_j^*)R\|_F$$

and

$$\|V\|_2 + \|V^*R\|_2 = 2, \tag{B.2}$$

we further have

$$\begin{aligned} \|\Sigma_j - \tilde{\Sigma}_j^*\|_F &\geq \|\text{diag}(a_j) - R^T \text{diag}(\tilde{a}_j^*)R\|_F \\ &\quad - \|(V - V^*R)\|_F \{ \|\text{diag}(a_j)V^T\|_2 + \|V^*R\text{diag}(a_j)\|_2 \} \\ &\geq \|\text{diag}(a_j) - R^T \text{diag}(\tilde{a}_j^*)R\|_F - 2\|\text{diag}(a_j)\|_2 \|V - V^*R\|_F. \end{aligned}$$

Therefore,

$$\|\text{diag}(a_j) - R^T \text{diag}(\tilde{a}_j^*)R\|_F \leq \|\Sigma_j - \tilde{\Sigma}_j^*\|_F + 2\|\text{diag}(a_j)\|_2 \|V - V^*R\|_F.$$

Combining (B.1) and $\|\text{diag}(a_j)\|_2 \leq c$, we have

$$\|\text{diag}(a_j) - R^T \text{diag}(\tilde{a}_j^*)R\|_F \leq \left(1 + \frac{8c}{\sigma_K(\Sigma_j^*)}\right) \|\Sigma_j - \tilde{\Sigma}_j^*\|_F. \tag{B.3}$$

The proof is complete by combining (B.1) and (B.3). \square

B.2 Proof of Theorem 4.7

We prove Theorem 4.7 in several steps. First, we show that given a current iterate Z , which satisfies suitable assumptions, the subsequent iterate Z^+ obtained by Algorithm 2 with a suitable step size satisfies

$$\text{dist}^2(Z^+, \tilde{Z}^*) \leq \beta^{1/2} \text{dist}^2(Z, \tilde{Z}^*) + C_1 \varepsilon_{stat}^2,$$

with $0 < \beta^{1/2} < 1$ and some constant C_1 . Second, we show that the step size can be chosen in a way that does not depend on the specific iterate. Finally, the lemma follows by applying the first step of the proof I times starting from Z^0 .

We start by introducing some additional notation for simplicity of presentation. We define

$$Z = \begin{pmatrix} V \\ A^T \end{pmatrix}, \quad Z^+ = \begin{pmatrix} V^+ \\ A^{+T} \end{pmatrix}, \quad \tilde{Z}^* = \begin{pmatrix} V^* \\ \tilde{A}^{*T} \end{pmatrix},$$

where Z is the current iterate, Z^+ is the iterate obtained by one step of Algorithm 2 starting from Z , and \tilde{Z}^* is the truncated version of the ground truth parameter Z^* . Furthermore, let

$$R = \underset{Y \in \mathcal{O}(K)}{\text{argmin}} \|V - V^*Y\|_F^2, \quad R^+ = \underset{Y \in \mathcal{O}(K)}{\text{argmin}} \|V^+ - V^*Y\|_F^2.$$

be the optimal rotation matrices in the current and subsequent step.

Let $\Pi_{\tilde{\mathcal{C}}_V}(X)$ be the projection operator defined in (A.3). Let $\Pi_{\tilde{\mathcal{C}}_A}(Y)$ be the projection operator that projects rows of Y to $\tilde{\mathcal{C}}_A$, given in Algorithm 4. One update of Algorithm 2 can be written as

$$V^+ = \Pi_{\tilde{\mathcal{C}}_V}(V - \eta_V \nabla_V f_N), \quad A^+ = \Pi_{\tilde{\mathcal{C}}_A}(A - \eta_A \nabla_A f_N), \quad (\text{B.4})$$

where

$$\nabla_V f_N(Z) = \frac{2}{J} \sum_{j=1}^J \nabla \ell_{N,j}(\Sigma_j) V \text{diag}(a_j), \quad \nabla_A f_N(Z) = \frac{1}{J} W(V), \quad (\text{B.5})$$

with

$$W(V) = [w_{kj}(v_k)] \in \mathbb{R}^{K \times J}, \quad w_{kj}(v_k) = v_k^T \nabla \ell_{N,j}(\Sigma_j) v_k, \quad \nabla \ell_{N,j}(\Sigma_j) = \Sigma_j - S_{N,j}.$$

Similarly, we define

$$W^*(V) = [w_{kj}^*(v_k)] \in \mathbb{R}^{K \times J}, \quad w_{kj}^*(v_k) = v_k^T \nabla \ell_{N,j}(\Sigma_j^*) v_k.$$

Let $\mathcal{S}_U = \mathcal{S}(V) \cup \mathcal{S}(V^+) \cup \mathcal{S}(V^*)$ and note that $|\mathcal{S}_U| \leq 2s + s^*$. Given the index set \mathcal{S}_U , we write $[X]_{\mathcal{S}_U}$ to denote the projection of X to the support \mathcal{S}_U

$$[X]_{\mathcal{S}_U} = \begin{cases} X_{ij} & (i, j) \in \mathcal{S}_U \\ 0 & (i, j) \notin \mathcal{S}_U \end{cases}.$$

With some abuse of notation, given a matrix Y with the factored form $Y = XX^T$, we write

$$[Y]_{\mathcal{S}_U, \mathcal{S}_U} = [X]_{\mathcal{S}_U} [X]_{\mathcal{S}_U}^T.$$

With this notation, we have

$$V^+ = \Pi_{\tilde{\mathcal{C}}_V}(V - \eta_V \nabla_V f_N) = \Pi_{\tilde{\mathcal{C}}_V}(V - \eta_V [\nabla_V f_N]_{\mathcal{S}_U}). \quad (\text{B.6})$$

Furthermore, recall that \tilde{Q} is the matrix whose columns are eigenvectors of \tilde{G} . Then $\tilde{Q}\tilde{Q}^T$ is the projection operator to the subspace spanned by the columns of \tilde{Q} . Since the output of Algorithm 5 is in the range space of \tilde{Q} , we have that $A\tilde{Q}\tilde{Q}^T = A$ and

$$A^+ = \Pi_{\tilde{\mathcal{C}}_A}(A - \eta_A \nabla_A f_N) = \Pi_{\tilde{\mathcal{C}}_A}\{(A - \eta_A \nabla_A f_N)\tilde{Q}\tilde{Q}^T\} = \Pi_{\tilde{\mathcal{C}}_A}\{A - \eta_A(\nabla_A f_N \tilde{Q}\tilde{Q}^T)\}. \quad (\text{B.7})$$

For later convenience, we also note that for a rotation matrix $R \in \mathcal{O}(K)$, we have

$$\langle \nabla_V f_N(Z), V - V^* R \rangle = \frac{2}{J} \sum_{j=1}^J \langle \nabla \ell_{N,j}(\Sigma_j), V \text{diag}(a_j) V^T - V^* R \text{diag}(a_j) V^T \rangle \quad (\text{B.8})$$

and

$$\begin{aligned} & \langle \text{diag}\{(\nabla_A f_N)_j\}, \text{diag}(a_j) - R^T \text{diag}(\tilde{a}_j^*) R \rangle \\ &= \frac{1}{J} \langle \nabla \ell_{N,j}(\Sigma_j), V \text{diag}(a_j) V^T - V R^T \text{diag}(\tilde{a}_j^*) R V^T \rangle. \end{aligned} \quad (\text{B.9})$$

With this notation, we are ready to state the result of the first step of the proof.

Lemma B.2. *Suppose that Z satisfies*

$$d^2(Z_j, Z_j^*) \leq I_0^2, \quad \|V - V^*R\|_F \leq I_0^2/J, \quad \|\text{diag}(a_j) - R^T \text{diag}(a_j^*)R\|_F^2 \leq (J-1)I_0^2/J, \quad (\text{B.10})$$

where I_0^2 is given in (4.1). Furthermore, suppose Assumption 4.1, 4.2, and 4.3 hold. Then

$$\text{dist}^2(Z^+, \tilde{Z}^*) \leq \beta^{1/2} \text{dist}^2(Z, \tilde{Z}^*) + \tau \beta^{-1/2} \eta \varepsilon_{stat}^2,$$

where Z^+ is obtained with one iteration of Algorithm 2 starting from Z and $\tau = J^{-1}\{9/2 + (1/2 \vee K/8)\}$.

Note that $d^2(Z_j \tilde{Z}_j^*) \leq d^2(Z_j, Z_j^*)$ for $j \in [J]$ and δ_A quantifies how close Z^* is to \tilde{Z}^* . Therefore we do not need additional assumptions for \tilde{Z}^* .

Starting from Z^0 , which satisfies Assumption 4.6 (that is also restated in (B.10)), we show that Z^1 also satisfies (B.10). Therefore, we can apply Lemma B.2 over I iterations to obtain Theorem 4.7.

of Theorem 4.7. When we apply one iteration of Algorithm 2, Lemma B.2 gives us

$$\text{dist}^2(Z^+, \tilde{Z}^*) \leq \beta^{1/2} \text{dist}^2(Z, \tilde{Z}^*) + \tau \beta^{-1/2} \eta \varepsilon_{stat}^2. \quad (\text{B.11})$$

Under Assumption 4.3, the right hand side of (B.11) is bounded by $J I_0^2$. This implies that the new estimate is still in a good region where we can apply Lemma B.2. That is, Z^+ satisfies (B.10). Consequently, since Z^0 satisfies Assumption 4.6 and, therefore, equation (B.10), we can apply the result of Lemma B.2 for I iterations to obtain

$$\text{dist}^2(Z^I, \tilde{Z}^*) \leq \beta^{I/2} \text{dist}^2(Z^0, \tilde{Z}^*) + \frac{\tau \eta \varepsilon_{stat}^2}{\beta^{1/2} - \beta}.$$

□

B.3 Proof of Lemma B.2

of Lemma B.2. Recall that

$$\text{dist}^2(Z^+, \tilde{Z}^*) = \sum_{j=1}^J \|V^+ - V^*R^+\|_F^2 + \|\text{diag}(a_j^+) - R^{+T} \text{diag}(\tilde{a}_j^*)R^+\|_F^2. \quad (\text{B.12})$$

We bound the two terms on the right hand side of (B.12) separately. From the triangle inequality, we have

$$\begin{aligned} \|\text{diag}(a_j^+) - R^{+T} \text{diag}(\tilde{a}_j^*)R^+\|_F^2 &\leq 2\|\text{diag}(a_j^+) - R^T \text{diag}(\tilde{a}_j^*)R\|_F^2 \\ &\quad + 2\|R^T \text{diag}(\tilde{a}_j^*)R - R^{+T} \text{diag}(\tilde{a}_j^*)R^+\|_F^2. \end{aligned}$$

By Lemma B.6, $\|R^T \text{diag}(\tilde{a}_j^*)R - R^{+T} \text{diag}(\tilde{a}_j^*)R^+\|_F \leq 4\|\text{diag}(\tilde{a}_j^*)\|_2 \|V^+ - V^*R\|_F$ and

$$\begin{aligned} &\sum_{j=1}^J \|\text{diag}(a_j^+) - R^{+T} \text{diag}(\tilde{a}_j^*)R^+\|_F^2 \\ &\leq 32J \|\tilde{A}^*\|_\infty^2 \|V^+ - V^*R\|_F^2 + 2 \sum_{j=1}^J \|\text{diag}(a_j^+) - R^T \text{diag}(\tilde{a}_j^*)R\|_F^2. \quad (\text{B.13}) \end{aligned}$$

Combining (B.13) with (B.12) and recalling the definition of V^+ and A^+ from (B.6) and (B.7) we have

$$\begin{aligned} \text{dist}^2(Z^+, \tilde{Z}^*) &\leq J\kappa \|\Pi_{\tilde{\mathcal{C}}_V}(V - \eta_V[\nabla_V f_N]_{S_U}) - V^*R\|_F^2 \\ &\quad + 2 \sum_{j=1}^J \left\| \text{diag} \left[\Pi_{\tilde{\mathcal{C}}_A} \{A - \eta_A(\nabla_A f_N \tilde{Q} \tilde{Q}^T)\}_j \right] - R^T \text{diag}(\tilde{a}_j^*) R \right\|_F^2. \end{aligned} \quad (\text{B.14})$$

where $\kappa = (1 + 32\|\tilde{A}^*\|_\infty^2)$. Next, we define

$$\tilde{V}^+ = \Pi_{\mathcal{C}_V}(V - \eta_V[\nabla_V f_N]_{S_U}),$$

where we recall that $\Pi_{\tilde{\mathcal{C}}_V}(\cdot)$ is the projection operator by first applying $\Pi_{\mathcal{C}_V}(\cdot)$ followed by a QR decomposition step. By Lemma B.8, we have $\|\tilde{V}^+ - V^*R\|_2 \leq 2I_0/J^{1/2}$. Therefore, we can apply Lemma A.6 with $U = V^*R = B^*L^*$, where $B^* = V^*R$ and a nonsingular matrix $L^* = I$. Then,

$$\begin{aligned} \|\Pi_{\tilde{\mathcal{C}}_V}(V - \eta_V[\nabla_V f_N]_{S_U}) - V^*R\|_F^2 &\leq \frac{2}{(1 - \frac{2I_0}{J^{1/2}})^2} \|\tilde{V}^+ - V^*R\|_F^2 \\ &= \frac{2}{(1 - \frac{2I_0}{J^{1/2}})^2} \|\Pi_{\mathcal{C}_V}(V - \eta_V[\nabla_V f_N]_{S_U}) - V^*R\|_F^2. \end{aligned}$$

By the fact $\|V - V^*R\|_F \leq I_0/J^{1/2}$ and Lemma B.7, we have

$$\|V - \eta_V[\nabla_V f_N]_{S_U} - V^*R\|_F \leq \|V - V^*R\|_F + \|\eta_V[\nabla_V f_N]_{S_U}\|_F \leq \frac{7I_0}{6J^{1/2}} < 1. \quad (\text{B.15})$$

Since columns of V^*R are unit norm, the result in (B.15) implies that the inner product of the k th column of $V - \eta_V[\nabla_V f_N]_{S_U}$ and the k th column of V^*R is nonnegative for every $k \in [K]$. Therefore, we can apply Lemma A.4 and the further bound $\|\Pi_{\tilde{\mathcal{C}}_V}(V - \eta_V[\nabla_V f_N]_{S_U}) - V^*R\|_F^2$ as

$$\|\Pi_{\tilde{\mathcal{C}}_V}(V - \eta_V[\nabla_V f_N]_{S_U}) - V^*R\|_F^2 \leq \rho \|V - \eta_V[\nabla_V f_N]_{S_U} - V^*R\|_F^2,$$

where $\rho = 4(1 - r')^{-2} \{1 + 2\sqrt{s^*}/\sqrt{(s - s^*)}\}$ and $r' = 2I_0/J^{1/2}$. By the contraction property of projection to convex sets, we have

$$\begin{aligned} \sum_{j=1}^J \left\| \text{diag} \left[\Pi_{\tilde{\mathcal{C}}_A} \{A - \eta_A(\nabla_A f_N \tilde{Q} \tilde{Q}^T)\}_j \right] - R^T \text{diag}(\tilde{a}_j^*) R \right\|_F^2 \\ \leq \sum_{j=1}^J \left\| \text{diag}(a_j) - \eta_A \text{diag}\{(\nabla_A f_N \tilde{Q} \tilde{Q}^T)_j\} - R^T \text{diag}(\tilde{a}_j^*) R \right\|_F^2, \end{aligned}$$

where $(\nabla_A f_N \tilde{Q} \tilde{Q}^T)_j$ denotes the j th column of $\nabla_A f_N \tilde{Q} \tilde{Q}^T \in \mathbb{R}^{K \times J}$. Combining the last two displays and noting that $\rho' = \rho\kappa > 2$, we have

$$\begin{aligned} \text{dist}^2(Z^+, \tilde{Z}^*) &\leq \rho' \left[J \|V - \eta_V[\nabla_V f_N]_{S_U} - V^*R\|_F^2 \right. \\ &\quad \left. + \sum_{j=1}^J \left\| \text{diag}(a_j) - \eta_A \text{diag}\{(\nabla_A f_N \tilde{Q} \tilde{Q}^T)_j\} - R^T \text{diag}(\tilde{a}_j^*) R \right\|_F^2 \right]. \end{aligned} \quad (\text{B.16})$$

Recall that $\eta_V = \eta/J$ and $\eta_A = \eta$. Therefore

$$\text{dist}^2(Z^+, \tilde{Z}^*) \leq \rho' \text{dist}^2(Z, \tilde{Z}^*) + \eta^2 \rho' (B1 + B2) - \eta \rho' (A1 + A2), \quad (\text{B.17})$$

where

$$\begin{aligned} A1 &= 2 \langle [\nabla_V f_N]_{S_U}, V - V^* R \rangle, \\ A2 &= 2 \sum_{j=1}^J \langle \text{diag}\{(\nabla_A f_N \tilde{Q} \tilde{Q}^T)_j\}, \text{diag}(a_j) - R^T \text{diag}(\tilde{a}_j^*) R \rangle, \\ B1 &= J^{-1} \|[\nabla_V f_N]_{S_U}\|_F^2, \\ B2 &= \sum_{j=1}^J \|\text{diag}\{(\nabla_A f_N \tilde{Q} \tilde{Q}^T)_j\}\|_F^2. \end{aligned}$$

Next, we upper bound $B = B1 + B2$ and lower bound $A = A1 + A2$ in Lemma B.3 and Lemma B.4, respectively. With these bounds, we will be able to show contraction $\text{dist}^2(Z^+, \tilde{Z}^*)$ with respect to $\text{dist}^2(Z, \tilde{Z}^*)$.

Lemma B.3. *Under same conditions of Lemma B.2, we have*

$$A \geq \frac{1}{J} \left\{ \frac{3}{4} \sum_{j=1}^J \|\Sigma_j - \tilde{\Sigma}_j^*\|_F^2 - \frac{9}{2} \varepsilon_{stat}^2 + \frac{1}{2} \sum_{j=1}^J \left\| [\nabla \ell_{N,j}(\Sigma_j) - \nabla \ell_{N,j}(\Sigma_j^*)]_{S_U, S_U} \right\|_F^2 - 8 \left(1 + \frac{\|A^*\|_\infty^2}{J} \right) I_0^2 \text{dist}^2(Z, \tilde{Z}^*) \right\}.$$

Lemma B.4. *Under same conditions of B.2, we have*

$$B \leq \frac{16}{J^2} \sum_{j=1}^J \left\{ \|\nabla \ell_{N,j}(\Sigma_j) - \nabla \ell_{N,j}(\Sigma_j^*)\|_F^2 \right\} \|Z_j\|_2^2 + \frac{4(4 \vee K)}{J^2} \varepsilon_{stat}^2 \max_{j \in [J]} \|Z_j\|_2^2.$$

Using Lemma B.3 and Lemma B.4, we have

$$\begin{aligned} \eta \rho' A - \eta^2 \rho' B &\geq \underbrace{\frac{\rho' \eta}{J} \left\{ \frac{3}{4} \sum_{j=1}^J \|\Sigma_j - \tilde{\Sigma}_j^*\|_F^2 - 8 \left(1 + \frac{\|A^*\|_\infty^2}{J} \right) I_0^2 \text{dist}^2(Z, \tilde{Z}^*) \right\}}_{C1} \\ &\quad - \underbrace{\rho' \eta \varepsilon_{stat}^2 \left(\frac{9}{2J} + \frac{4(4 \vee K) \eta}{J^2} \max_{j \in [J]} \|Z_j\|_2^2 \right)}_{C2} \\ &\quad + \underbrace{\frac{\eta \rho'}{J} \left(\frac{1}{2} - 16 \frac{\eta}{J} \max_{j \in [j]} \|Z_j\|_2^2 \right)}_{C3} \sum_{j=1}^J \|\nabla \ell_{N,j}(\Sigma_j) - \nabla \ell_{N,j}(\Sigma_j^*)\|_F^2. \end{aligned}$$

Under the assumption that $\delta_A \leq (16\gamma^*)^{-1} \min_{j \in [J]} \sigma_K^2(\Sigma_j^*)$ and the inequality in (E.2), we have

$$\begin{aligned} \sigma_K(\Sigma_j^* - \tilde{\Sigma}_j^*) &= \sigma_K(V^* \text{diag}(a_j^* - \tilde{a}_j^*) V^{*T}) = \min_{k \in [K]} |a_{jk}^* - \tilde{a}_{jk}^*| \\ &\leq \max_{k \in [K]} \|\tilde{A}_{k\cdot}^* - A_{k\cdot}^*\|_2 \leq (\delta_A \gamma^*)^{1/2} \leq \frac{1}{4} \sigma_K(\Sigma_j^*) \end{aligned}$$

for $j \in [J]$. Therefore, using Lemma B.1, we have

$$\sum_{j=1}^J \|\Sigma_j - \tilde{\Sigma}_j\|_F^2 \geq \frac{1}{\xi^2} \text{dist}^2(Z, \tilde{Z}^*).$$

Furthermore, from the definition of I_0^2 in Assumption 4.6, we have that

$$8I_0^2 \left(1 + \frac{\|A^*\|_\infty^2}{J}\right) \leq \frac{1}{2\xi^2}.$$

Therefore, combining the last two displays, we arrive at

$$C1 \geq \frac{1}{4\xi^2} \text{dist}^2(Z, \tilde{Z}^*).$$

In fact, we can verify that $C3$ is nonnegative because the step size η that satisfies Assumption 4.1 is small enough such that the following inequality holds.

Lemma B.5. *Under the conditions of Lemma B.2 we have $\|Z_j\|_2^2 \leq 2\|Z_j^0\|_2^2$.*

Therefore,

$$\eta \leq \min_{j \in [J]} \frac{J}{32\|Z_j\|_2^2}$$

and $C3 \geq 0$ can be omitted, while $C2 \leq \tau$. Then

$$\eta \rho' A - \eta^2 \rho' B \geq \frac{\rho' \eta}{J} \frac{1}{4\xi^2} \text{dist}^2(Z, \tilde{Z}^*) - \varepsilon_{stat}^2 \tau \rho' \eta.$$

Under Assumption 4.2, it is easy to verify that $\rho' \leq \beta^{-1/2}$, where $\beta = 1 - \eta/(4J\xi^2)$. Plugging into (B.17), we have

$$\text{dist}^2(Z^+, \tilde{Z}^*) \leq \beta^{1/2} \text{dist}^2(Z, \tilde{Z}^*) + \tau \beta^{-1/2} \eta \varepsilon_{stat}^2,$$

which completes the proof. □

B.4 Proofs of Lemma B.3–B.5

of Lemma B.3. Using (B.8) and $\langle [\nabla \ell_{N,j}(\Sigma_j) V \text{diag}(a_j)]_{S_U^c}, [V - V^* R]_{S_U} \rangle = 0$, we have

$$\begin{aligned}
A1 &= \frac{4}{J} \sum_{j=1}^J \langle [\nabla \ell_{N,j}(\Sigma_j) V \text{diag}(a_j)]_{S_U}, [V - V^* R]_{S_U} \rangle \\
&= \frac{4}{J} \sum_{j=1}^J \langle [\nabla \ell_{N,j}(\Sigma_j) V \text{diag}(a_j)]_{S_U} + [\nabla \ell_{N,j}(\Sigma_j) V \text{diag}(a_j)]_{S_U^c}, [V - V^* R]_{S_U} \rangle \\
&= \frac{4}{J} \sum_{j=1}^J \langle \nabla \ell_{N,j}(\Sigma_j) V \text{diag}(a_j), [V - V^* R]_{S_U} \rangle \\
&= \frac{4}{J} \sum_{j=1}^J \langle \nabla \ell_{N,j}(\Sigma_j), [V - V^* R]_{S_U} \text{diag}(a_j) V^T \rangle \\
&= \frac{4}{J} \sum_{j=1}^J \langle \nabla \ell_{N,j}(\Sigma_j), [V - V^* R]_{S_U} [\text{diag}(a_j) V^T]_{S_U} \rangle \\
&= \frac{4}{J} \sum_{j=1}^J \langle \nabla \ell_{N,j}(\Sigma_j), [V \text{diag}(a_j) V^T - V^* R \text{diag}(a_j) V^T]_{S_U, S_U} \rangle.
\end{aligned}$$

Furthermore, we can write A1 as

$$\begin{aligned}
A1 &= A13 + \frac{4}{J} \sum_{j=1}^J \langle \nabla \ell_{N,j}(\Sigma_j), \overbrace{[(V - V^* R) R^T \text{diag}(\tilde{a}_j^*) R V^T]}^{\Delta V} \rangle_{S_U, S_U}; \tag{B.18} \\
A13 &= \frac{4}{J} \sum_{j=1}^J \langle \nabla \ell_{N,j}(\Sigma_j), \overbrace{[(V - V^* R) \{\text{diag}(a_j) - R^T \text{diag}(\tilde{a}_j^*) R\} V^T]}^{\Delta a_j} \rangle_{S_U, S_U}.
\end{aligned}$$

We also write A2 in a suitable way. Note that $\text{diag}\{R^T \text{diag}(\tilde{a}_j^*) R\} = \text{diag}(H a_j^*)$, where $H = (h_{ij})_{i \in [K], j \in [K]}$ with $h_{ij} = r_{ij}^2$ and r_{ij} is the ij th entry of R . Then

$$\begin{aligned}
A2 &= 2 \sum_{j=1}^J \langle \text{diag}\{(\nabla_A f_N \tilde{Q} \tilde{Q}^T)_j\}, \text{diag}(a_j) - R^T \text{diag}(\tilde{a}_j^*) R \rangle \\
&= 2 \langle \nabla_A f_N \tilde{Q} \tilde{Q}^T, A - H \tilde{A}^* \rangle \\
&= 2 \langle \nabla_A f_N, A - H \tilde{A}^* \rangle \\
&= 2 \sum_{j=1}^J \langle \text{diag}\{(\nabla_A f_N)_j\}, \text{diag}(a_j) - R^T \text{diag}(\tilde{a}_j^*) R \rangle,
\end{aligned}$$

since rows of A and \tilde{A}^* belong to the subspace spanned by eigenvectors of \tilde{G} and $A\tilde{Q}\tilde{Q}^T = A$ and $\tilde{A}^*\tilde{Q}\tilde{Q}^T = \tilde{A}^*$. Finally, using (B.9), we have

$$\begin{aligned} A2 &= \frac{2}{J} \sum_{j=1}^J \langle \nabla \ell_{N,j}(\Sigma_j), [V \text{diag}(a_j) V^T - V R^T \text{diag}(\tilde{a}_j^*) R V^T]_{\mathcal{S}_U, \mathcal{S}_U} \rangle \\ &= A11 + A12 + \frac{2}{J} \sum_{j=1}^J \langle \nabla \ell_{N,j}(\Sigma_j), [\tilde{\Sigma}_j^* - V R^T \text{diag}(\tilde{a}_j^*) R V^T]_{\mathcal{S}_U, \mathcal{S}_U} \rangle \end{aligned} \quad (\text{B.19})$$

$$A11 = \frac{2}{J} \sum_{j=1}^J \langle \nabla \ell_{N,j}(\Sigma_j) - \nabla \ell_{N,j}(\Sigma_j^*), [\Sigma_j - \tilde{\Sigma}_j^*]_{\mathcal{S}_U, \mathcal{S}_U} \rangle;$$

$$A12 = \frac{2}{J} \sum_{j=1}^J \langle \nabla \ell_{N,j}(\Sigma_j^*), [\Sigma_j - \tilde{\Sigma}_j^*]_{\mathcal{S}_U, \mathcal{S}_U} \rangle.$$

Combining (B.18) and (B.19), we obtain

$$A = A11 + A12 + A13 + A14;$$

$$A14 = \frac{2}{J} \sum_{j=1}^J \langle \nabla \ell_{N,j}(\Sigma_j), [\overbrace{(V - V^* R)}^{\Delta V} R^T \text{diag}(\tilde{a}_j^*) R \overbrace{(V - V^* R)^T}^{\Delta V^T}]_{\mathcal{S}_U, \mathcal{S}_U} \rangle,$$

where we have used that

$$\begin{aligned} &\frac{4}{J} \sum_{j=1}^J \langle \nabla \ell_{N,j}(\Sigma_j), [\Delta V R^T \text{diag}(\tilde{a}_j^*) R V^T]_{\mathcal{S}_U, \mathcal{S}_U} \rangle \\ &= \frac{2}{J} \sum_{j=1}^J \langle \nabla \ell_{N,j}(\Sigma_j), [\Delta V R^T \text{diag}(\tilde{a}_j^*) R V^T]_{\mathcal{S}_U, \mathcal{S}_U} \rangle \\ &\quad + \frac{2}{J} \sum_{j=1}^J \langle \nabla \ell_{N,j}(\Sigma_j), [V R^T \text{diag}(\tilde{a}_j^*) R \Delta V^T]_{\mathcal{S}_U, \mathcal{S}_U} \rangle, \end{aligned}$$

since $\nabla \ell_{N,j}(\Sigma_j)$ for $j \in [J]$ is symmetric. Next, we lower bound $A11$, $A12$, $A13$, and $A14$ separately.

Recall that $\Sigma_j = V \text{diag}(a_j) V^T$ and $\tilde{\Sigma}_j^* = V^* \text{diag}(\tilde{a}_j^*) V^{*T}$. Additionally, since $[V]_{\mathcal{S}_U^c} = [V^*]_{\mathcal{S}_U^c} = 0$,

$$[\Sigma_j - \tilde{\Sigma}_j^*]_{\mathcal{S}_U, \mathcal{S}_U^c} = [\Sigma_j - \tilde{\Sigma}_j^*]_{\mathcal{S}_U, \mathcal{S}_U^c} = [\Sigma_j - \tilde{\Sigma}_j^*]_{\mathcal{S}_U^c, \mathcal{S}_U^c} = 0,$$

for every $j \in [J]$, and therefore $[\Sigma_j - \tilde{\Sigma}_j^*]_{\mathcal{S}_U, \mathcal{S}_U} = \Sigma_j - \tilde{\Sigma}_j^*$. Then

$$\begin{aligned} A11 &= \frac{2}{J} \sum_{j=1}^J \langle \nabla \ell_{N,j}(\Sigma_j) - \nabla \ell_{N,j}(\Sigma_j^*), \Sigma_j - \tilde{\Sigma}_j^* \rangle \\ &\geq \frac{1}{J} \sum_{j=1}^J \left\{ \|\Sigma_j - \tilde{\Sigma}_j^*\|_F^2 + \|\nabla \ell_{N,j}(\Sigma_j) - \nabla \ell_{N,j}(\Sigma_j^*)\|_F^2 \right\}, \end{aligned}$$

where we applied Lemma G.1 with $m = L = 1$. For A12, we have

$$A12 \geq -\frac{2}{J} \left| \sum_{j=1}^J \langle \nabla \ell_{N,j}(\Sigma_j^*), [\Sigma_j - \tilde{\Sigma}_j^*]_{\mathcal{S}_U, \mathcal{S}_U} \rangle \right|.$$

Since $\{[\Sigma_j - \tilde{\Sigma}_j^*]_{\mathcal{S}_U, \mathcal{S}_U}\}_{j \in [J]} \in \Upsilon(2K, 2s + s^*, 2\gamma, \delta_A)$, we have

$$A12 \geq -\frac{2}{J} \varepsilon_{stat} \left(\sum_{j=1}^J \|\Sigma_j - \tilde{\Sigma}_j^*\|_{\mathcal{S}_U, \mathcal{S}_U}^2 \right)^{1/2} \geq -\frac{2}{J} \left(\frac{\varepsilon_{stat}^2}{2e_1} + \frac{e_1}{2} \sum_{j=1}^J \|\Sigma_j - \tilde{\Sigma}_j^*\|_F^2 \right),$$

where the last inequality follows by Young's inequality $ab \leq a^2/(2\varepsilon) + (\varepsilon b^2)/2$ for every $\varepsilon > 0$. We will use this bound with $e_1 = 1/4$. For A13, we have

$$\begin{aligned} A13 \geq & -\frac{4}{J} \left| \sum_{j=1}^J \langle \nabla \ell_{N,j}(\Sigma_j^*), [\Delta V \Delta a_j V^T]_{\mathcal{S}_U, \mathcal{S}_U} \rangle \right| \\ & - \frac{4}{J} \sum_{j=1}^J |\langle \nabla \ell_{N,j}(\Sigma_j) - \nabla \ell_{N,j}(\Sigma_j^*), [\Delta V \Delta a_j V^T]_{\mathcal{S}_U, \mathcal{S}_U} \rangle|. \end{aligned} \quad (\text{B.20})$$

We first bound the second term on the right hand side of (B.20). Applying the Cauchy-Schwarz inequality and using $\|V\|_2 = 1$, we have

$$\begin{aligned} & -\frac{4}{J} \sum_{j=1}^J |\langle \nabla \ell_{N,j}(\Sigma_j) - \nabla \ell_{N,j}(\Sigma_j^*), [\Delta V \Delta a_j V^T]_{\mathcal{S}_U, \mathcal{S}_U} \rangle| \\ & \geq -\frac{4}{J} \sum_{j=1}^J \|\nabla \ell_{N,j}(\Sigma_j) - \nabla \ell_{N,j}(\Sigma_j^*)\|_F \|\Delta a_j\|_F \|\Delta V\|_F. \end{aligned}$$

Using the fact that $\|\Delta V\|_F \|\Delta a_j\|_F \leq \frac{1}{2} d^2(Z_j, \tilde{Z}_j^*)$, the above display can be further lower bounded as

$$\geq -\frac{2}{J} \sum_{j=1}^J \|\nabla \ell_{N,j}(\Sigma_j) - \nabla \ell_{N,j}(\Sigma_j^*)\|_F d^2(Z_j, \tilde{Z}_j^*). \quad (\text{B.21})$$

Since $\{[\Delta V \Delta a_j V^T]_{\mathcal{S}_U, \mathcal{S}_U}\}_{j \in [J]} \in \Upsilon(2K, 2s + s^*, 2\gamma, \delta_A)$, we can bound the first term of (B.20) as

$$\begin{aligned} & -\frac{4}{J} \left| \sum_{j=1}^J \langle \nabla \ell_{N,j}(\Sigma_j^*), [\Delta V \Delta a_j V^T]_{\mathcal{S}_U, \mathcal{S}_U} \rangle \right| \geq -\frac{4}{J} \varepsilon_{stat} \left(\sum_{j=1}^J \|V\|_2^2 \|\Delta a_j\|_F^2 \|\Delta V\|_F^2 \right)^{1/2} \\ & = -\frac{4}{J} \varepsilon_{stat} \left(\sum_{j=1}^J \|\Delta a_j\|_F^2 \|\Delta V\|_F^2 \right)^{1/2} \\ & \geq -\frac{4}{J} \varepsilon_{stat} \left(\frac{1}{4} \sum_{j=1}^J d^4(Z_j, \tilde{Z}_j^*) \right)^{1/2}, \end{aligned} \quad (\text{B.22})$$

where the last inequality uses that $\|\Delta V\|_F \|\Delta a_j\|_F \leq \frac{1}{2} d^2(Z_j, \tilde{Z}_j^*)$. Combining (B.21) and (B.22), we have

$$A13 \geq -\frac{2}{J} \sum_{j=1}^J \|\nabla \ell_{N,j}(\Sigma_j) - \nabla \ell_{N,j}(\Sigma_j^*)\|_F \cdot d^2(Z_j, \tilde{Z}_j^*) - \frac{4}{J} \varepsilon_{stat} \left(\frac{1}{4} \sum_{j=1}^J d^4(Z_j, \tilde{Z}_j^*) \right)^{1/2}.$$

Applying Young's inequality with $e_2 = 4$, the above display can be bounded as

$$\begin{aligned} A13 &\geq -\frac{1}{J} \sum_{j=1}^J \left\{ \frac{1}{e_2} \|\nabla \ell_{N,j}(\Sigma_j) - \nabla \ell_{N,j}(\Sigma_j^*)\|_F^2 + e_2 d^4(Z_j, \tilde{Z}_j^*) \right\} \\ &\quad - \frac{1}{J} \left\{ \frac{1}{e_2} \varepsilon_{stat}^2 + e_2 \sum_{j=1}^J d^4(Z_j, \tilde{Z}_j^*) \right\} \\ &\geq -\frac{1}{e_2 J} \left\{ \varepsilon_{stat}^2 + \sum_{j=1}^J \|\nabla \ell_{N,j}(\Sigma_j) - \nabla \ell_{N,j}(\Sigma_j^*)\|_F^2 \right\} - \frac{2e_2}{J} \sum_{j=1}^J I_0^2 d^2(Z_j, \tilde{Z}_j^*), \end{aligned}$$

where the last inequality follows by $d^2(Z_j, \tilde{Z}_j^*) \leq d^2(Z_j, Z_j^*) \leq I_0^2$.

A lower bound for A14 can be obtained in a similar way to the one for A13. We have

$$\begin{aligned} A14 &\geq -\frac{2}{J} \sum_{j=1}^J \|\nabla \ell_{N,j}(\Sigma_j) - \nabla \ell_{N,j}(\Sigma_j^*)\|_F \|\Delta V\|_F^2 \|\text{diag}(\tilde{a}_j^*)\|_F \\ &\quad - \frac{2}{J} \varepsilon_{stat} \left(\sum_{j=1}^J \|\Delta V\|_F^4 \|\text{diag}(\tilde{a}_j^*)\|_2^2 \right)^{1/2}. \end{aligned}$$

Applying Young's inequality with $e_3 = 4 > 0$, the above display can be bounded as

$$\begin{aligned} A14 &\geq -\frac{1}{e_3 J} \left\{ \varepsilon_{stat}^2 + \sum_{j=1}^J \|\nabla \ell_{N,j}(\Sigma_j) - \nabla \ell_{N,j}(\Sigma_j^*)\|_F^2 \right\} - \frac{2e_3}{J} \sum_{j=1}^J \|\Delta V\|_F^4 \|\text{diag}(\tilde{a}_j^*)\|_2^2 \\ &\geq -\frac{1}{e_3 J} \left\{ \varepsilon_{stat}^2 + \sum_{j=1}^J \|\nabla \ell_{N,j}(\Sigma_j) - \nabla \ell_{N,j}(\Sigma_j^*)\|_F^2 \right\} - \frac{2e_3}{J^2} \sum_{j=1}^J \|A^*\|_\infty^2 I_0^2 d^2(Z_j, \tilde{Z}_j^*), \end{aligned}$$

where the last inequality is followed by $\|\text{diag}(a_j^*)\|_2 \leq \|A^*\|_\infty$ and $\|\Delta V\|_F^4 \leq J^{-1} I_0^2 d^2(Z_j, \tilde{Z}_j^*)$.

Putting everything together, we have

$$\begin{aligned} A &\geq \frac{1}{J} \left\{ \frac{3}{4} \sum_{j=1}^J \|\Sigma_j - \tilde{\Sigma}_j^*\|_F^2 - \frac{9}{2} \varepsilon_{stat}^2 + \frac{1}{2} \sum_{j=1}^J \|\nabla \ell_{N,j}(\Sigma_j) - \nabla \ell_{N,j}(\Sigma_j^*)\|_F^2 \right. \\ &\quad \left. - 8 \left(1 + \frac{\|A^*\|_\infty^2}{J} \right) I_0^2 \text{dist}^2(Z, \tilde{Z}^*) \right\}. \quad (\text{B.23}) \end{aligned}$$

□

of Lemma B.4. We separately bound B1 and B2. Since $\Sigma_j = V \text{diag}(a_j) V^T$, recalling (B.5), we have

$$\begin{aligned} B1 &= \frac{1}{J} \left\| \frac{2}{J} \sum_{j=1}^J [\nabla \ell_{N,j}(\Sigma_j) V \text{diag}(a_j)]_{\mathcal{S}_U} \right\|_F^2 \\ &= \frac{4}{J^3} \left\| \sum_{j=1}^J [\nabla \ell_{N,j}(\Sigma_j^*) V \text{diag}(a_j)]_{\mathcal{S}_U} + [\{\nabla \ell_{N,j}(\Sigma_j) - \nabla \ell_{N,j}(\Sigma_j^*)\} V \text{diag}(a_j)]_{\mathcal{S}_U} \right\|_F^2. \end{aligned}$$

Using the Cauchy–Schwarz inequality and along with the fact that $(a+b)^2 \leq 2(a^2 + b^2)$, the above display can be bounded as

$$\begin{aligned} &\leq \frac{8}{J^2} \sum_{j=1}^J \left\| [\{\nabla \ell_{N,j}(\Sigma_j) - \nabla \ell_{N,j}(\Sigma_j^*)\} V \text{diag}(a_j)]_{\mathcal{S}_U} \right\|_F^2 \\ &\quad + \frac{8}{J^3} \left\| \sum_{j=1}^J [\nabla \ell_{N,j}(\Sigma_j^*) V \text{diag}(a_j)]_{\mathcal{S}_U} \right\|_F^2. \end{aligned} \tag{B.24}$$

For any $X_{\mathcal{S}_U}$ with $\|X_{\mathcal{S}_U}\|_F = 1$, we have $\{[V \text{diag}(a_j) X^T]_{\mathcal{S}_U, \mathcal{S}_U}\}_{j \in [J]} \in \Upsilon(2K, 2s + s^*, 2\gamma, \delta_A)$. We can bound the second term in (B.24) as

$$\begin{aligned} \left\| \sum_{j=1}^J [\nabla \ell_{N,j}(\Sigma_j^*) V \text{diag}(a_j)]_{\mathcal{S}_U} \right\|_F &= \sup_{\|X_{\mathcal{S}_U}\|_F=1} \sum_{j=1}^J \text{tr}([\nabla \ell_{N,j}(\Sigma_j^*) V \text{diag}(a_j)]_{\mathcal{S}_U} X_{\mathcal{S}_U}^T) \\ &= \sup_{\|X_{\mathcal{S}_U}\|_F=1} \sum_{j=1}^J \langle \nabla \ell_{N,j}(\Sigma_j^*), [V \text{diag}(a_j)]_{\mathcal{S}_U} X_{\mathcal{S}_U}^T \rangle \\ &\leq \varepsilon_{stat} \cdot \sup_{\|X_{\mathcal{S}_U}\|_F=1} \left(\sum_{j=1}^J \|[V \text{diag}(a_j) X^T]_{\mathcal{S}_U, \mathcal{S}_U}\|_F^2 \right)^{1/2} \\ &\leq \varepsilon_{stat} J^{1/2} \|V\|_2^2 \|A\|_\infty. \end{aligned} \tag{B.25}$$

Plugging (B.25) back into (B.24), we arrive at

$$\begin{aligned} B1 &\leq \frac{8}{J^2} \sum_{j=1}^J \|\nabla \ell_{N,j}(\Sigma_j) - \nabla \ell_{N,j}(\Sigma_j^*)\|_F^2 \|V\|_2^2 \|\text{diag}(a_j)\|_2^2 + \frac{8}{J^2} \varepsilon_{stat}^2 \|V\|_2^4 \|A\|_\infty^2 \\ &\leq \frac{8}{J^2} \sum_{j=1}^J \|\nabla \ell_{N,j}(\Sigma_j) - \nabla \ell_{N,j}(\Sigma_j^*)\|_F^2 \|\text{diag}(a_j)\|_2^2 + \frac{8}{J^2} \varepsilon_{stat}^2 \|A\|_\infty^2, \end{aligned}$$

where the last inequality follows since $\|V\|_2 = 1$.

For B2, we have

$$\begin{aligned} B2 &= \frac{1}{J^2} \|W(V) \tilde{Q} \tilde{Q}^T\|_F^2 = \frac{1}{J^2} \|\{W(V) - W^*(V) + W^*(V)\} \tilde{Q} \tilde{Q}^T\|_F^2 \\ &\leq \frac{2}{J^2} \|\{W(V) - W^*(V)\} \tilde{Q} \tilde{Q}^T\|_F^2 + \frac{2}{J^2} \|W^*(V) \tilde{Q} \tilde{Q}^T\|_F^2. \end{aligned}$$

Since $\tilde{Q}\tilde{Q}^T$ is an orthogonal projection operator, we have $\|X\tilde{Q}\tilde{Q}^T\|_F \leq \|X\|_F$ for a matrix X . Then

$$\begin{aligned} \|\{W(V) - W^*(V)\}\tilde{Q}\tilde{Q}^T\|_F^2 &\leq \|W(V) - W^*(V)\|_F^2 \leq \sum_{j=1}^J \|V^T \{\nabla \ell_{N,j}(\Sigma_j) - \nabla \ell_{N,j}(\Sigma_j^*)\} V\|_F^2 \\ &\leq \left\{ \sum_{j=1}^J \|\nabla \ell_{N,j}(\Sigma_j) - \nabla \ell_{N,j}(\Sigma_j^*)\|_F^2 \right\}, \end{aligned} \quad (\text{B.26})$$

since $\|V\|_2 = 1$. Furthermore, we have

$$\begin{aligned} \|W^*(V)\tilde{Q}\tilde{Q}^T\|_F^2 &= \sum_{k=1}^K \|\tilde{Q}\tilde{Q}^T W_k^*(v_k)\|_2^2 \leq \left\{ \sum_{k=1}^K \|\tilde{Q}\tilde{Q}^T W_k^*(v_k)\|_2 \right\}^2 \\ &= \left\{ \sum_{k=1}^K \sup_{\|x_k\|_2 \leq 1} \langle x_k, \tilde{Q}\tilde{Q}^T W_k^*(v_k) \rangle \right\}^2 \\ &\leq \left\{ \sum_{k=1}^K \sup_{\|\tilde{Q}\tilde{Q}^T x_k\|_2 \leq 1} \langle \tilde{Q}\tilde{Q}^T x_k, W_k^*(v_k) \rangle \right\}^2 \\ &\leq \left\{ \sum_{k=1}^K \left(\frac{1}{2\delta_A \gamma} \right)^{1/2} \sup_{\|\tilde{Q}\tilde{Q}^T x'_k\|_2 \leq 2\delta_A \gamma} \langle \tilde{Q}\tilde{Q}^T x'_k, W_k^*(v_k) \rangle \right\}^2. \end{aligned}$$

Let $y_k = \tilde{Q}\tilde{Q}^T x'_k$ for $k \in [K]$. Since a ball of radius $(2\delta_A \gamma)^{1/2}$ is contained in the truncated ellipsoid $\{\alpha = \tilde{Q}u : u^T \tilde{\Lambda} u \leq 2\gamma\}$, y_k , for $k \in [K]$, lies in the ellipsoid. Therefore, $\{\sum_{k=1}^K y_{kj} v_k v_k^T\}_{j \in [J]}$ is in $\Upsilon(2K, 2s + s^*, 2\gamma, \delta_A)$ and we can bound the above display as

$$\begin{aligned} &\leq \varepsilon_{stat}^2 \cdot \frac{1}{2\delta_A \gamma} \left(\sum_{k=1}^K \sup_{\|\tilde{Q}\tilde{Q}^T x'_k\|_2 \leq 2\delta_A \gamma} \|\tilde{Q}\tilde{Q}^T x'_k\|_2^2 \right) \\ &= \varepsilon_{stat}^2 K. \end{aligned} \quad (\text{B.27})$$

Combining (B.26)–(B.27) and noting that $\|V\|_2 = 1$, we have

$$B2 \leq \frac{2}{J^2} \left\{ \sum_{j=1}^J \|\nabla \ell_{N,j}(\Sigma_j) - \nabla \ell_{N,j}(\Sigma_j^*)\|_F^2 \right\} \|V\|_2^2 + \frac{2}{J^2} K \varepsilon_{stat}^2 \|V\|_2^2.$$

Finally, combining B1 and B2 we arrive at the following

$$\begin{aligned} B &\leq \frac{8}{J^2} \sum_{j=1}^J \left\{ \|\nabla \ell_{N,j}(\Sigma_j) - \nabla \ell_{N,j}(\Sigma_j^*)\|_F^2 (\|\text{diag}(a_j)\|_2^2 + \|V\|_2^2) \right\} + \frac{2(4 \vee K)}{J^2} \varepsilon_{stat}^2 (\|V\|_2^2 + \|A\|_\infty^2) \\ &\leq \frac{16}{J^2} \sum_{j=1}^J \left\{ \|\nabla \ell_{N,j}(\Sigma_j) - \nabla \ell_{N,j}(\Sigma_j^*)\|_F^2 \right\} \|Z_j\|_2^2 + \frac{4(4 \vee K)}{J^2} \varepsilon_{stat}^2 \max_{j \in [J]} \|Z_j\|_2^2, \end{aligned} \quad (\text{B.28})$$

where the second inequality comes from $(\|\text{diag}(a_j)\|_2^2 \vee \|V\|_2^2) \leq \|Z_j\|_2^2$. \square

of Lemma B.5. We first upper bound $\|Z_j\|_2$ with $\|Z_j^*\|_2$ for every $j \in [J]$. We have

$$\begin{aligned}
\|Z_j\|_2 &= \left\| \begin{pmatrix} V \\ \text{diag}(a_j) \end{pmatrix} - \begin{pmatrix} V^*R \\ R^T \text{diag}(a_j^*)R \end{pmatrix} + \begin{pmatrix} V^*R \\ R^T \text{diag}(a_j^*)R \end{pmatrix} \right\|_2 \\
&\leq \left\| \begin{pmatrix} V \\ \text{diag}(a_j) \end{pmatrix} - \begin{pmatrix} V^*R \\ R^T \text{diag}(a_j^*)R \end{pmatrix} \right\|_2 + \|Z_j^*\|_2 \\
&\leq I_0 + \|Z_j^*\|_2 \\
&\leq \frac{\sigma_K(\Sigma_j^*)}{16} + \|Z_j^*\|_2 \\
&\leq \frac{17}{16} \|Z_j^*\|_2,
\end{aligned} \tag{B.29}$$

where the third inequality follows from (4.1), in particular that $I_0 \leq \sigma_K(\Sigma_j^*)/16$, and the last inequality follows because $\|Z_j^*\|_2 \geq \sigma_K(\Sigma_j^*)$.

Next, we lower bound $\|Z_j^0\|_2$ in terms of $\|Z_j^*\|_2$ for every $j \in [J]$. Similar to (B.29), we have

$$\begin{aligned}
\|Z_j^0\|_2 &= \left\| \begin{pmatrix} V^0 \\ \text{diag}(a_j^0) \end{pmatrix} - \begin{pmatrix} V^*R \\ R^T \text{diag}(a_j^*)R \end{pmatrix} + \begin{pmatrix} V^*R \\ R^T \text{diag}(a_j^*)R \end{pmatrix} \right\|_2 \\
&\geq - \left\| \begin{pmatrix} V^0 \\ \text{diag}(a_j^0) \end{pmatrix} - \begin{pmatrix} V^*R \\ R^T \text{diag}(a_j^*)R \end{pmatrix} \right\|_2 + \|Z_j^*\|_2 \\
&\geq -I_0 + \|Z_j^*\|_2 \\
&\geq -\frac{\sigma_K(\Sigma_j^*)}{16} + \|Z_j^*\|_2 \\
&\geq \frac{15}{16} \|Z_j^*\|_2.
\end{aligned} \tag{B.30}$$

Combining (B.29) and (B.30), we obtain $\|Z_j\|_2^2 \leq 2\|Z_j^0\|_2^2$. \square

B.5 Proofs of Auxiliary Lemmas

Lemma B.6. *Suppose V^* has orthonormal columns. Let*

$$R = \underset{Y \in \mathcal{O}(K)}{\text{argmin}} \|V - V^*Y\|_F^2, \quad R^+ = \underset{Y \in \mathcal{O}(K)}{\text{argmin}} \|V^+ - V^*Y\|_F^2.$$

Then

$$\|R^+ - R\|_F \leq 2\|V^+ - V^*R\|_F$$

and

$$\|R^T \text{diag}(a^*)R - R^{+T} \text{diag}(a^*)R^+\|_F \leq 4\|\text{diag}(a^*)\|_2 \|V^+ - V^*R\|_F.$$

Proof. Recall that V^* has orthonormal columns. This implies that for a matrix X , we have

$$\|V^*X\|_F^2 = \text{tr}(X^T V^{*T} V^* X) = \text{tr}(X^T X) = \|X\|_F^2.$$

Using the above property, we have

$$\begin{aligned}
\|R^+ - R\|_F &= \|V^*R^+ - V^*R\|_F = \|(V^+ - V^*R) + (V^*R^+ - V^+)\|_F \\
&\leq \|V^+ - V^*R\|_F + \|V^+ - V^*R^+\|_F \\
&\leq 2\|V^+ - V^*R\|_F,
\end{aligned} \tag{B.31}$$

where the last inequality follows as R^+ minimizes the distance $\|V^+ - V^*R\|_F$. This completes the proof for the first statement.

For the second statement, we have

$$\begin{aligned}
\|R^T \text{diag}(a^*)R - R^{+T} \text{diag}(a^*)R^+\|_F &= \|(R - R^+)^T \text{diag}(a^*)R + R^{+T} \text{diag}(a^*)(R - R^+)\|_F \\
&\leq \|\text{diag}(a^*)\|_2 (\|R\|_2 + \|R^+\|_2) \|R^+ - R\|_F \\
&\leq 4\|\text{diag}(a^*)\|_2 \|V^+ - V^*R\|_F,
\end{aligned}$$

where the last inequality follows from (B.31) and $\|R\|_2 = \|R^+\|_2 = 1$. \square

Lemma B.7. *Assume that V has orthonormal columns and*

$$\|V - V^*R\|_F \leq I_0^2/J, \quad \|\text{diag}(a_j) - R^T \text{diag}(a_j^*)R\|_F^2 \leq (J-1)I_0^2/J,$$

and $Z = (V^T, A)^T$. Under Assumption 4.1-4.3, we have

$$\frac{\eta}{J} \|\nabla_V f_N(Z)\|_{\mathcal{S}_U} \leq \frac{I_0}{6\sqrt{J}},$$

where I_0 is defined in (4.1).

of Lemma B.7. By (B.5), we have

$$\begin{aligned}
\frac{\eta}{J} \|\nabla_V f_N\|_{\mathcal{S}_U} &= \frac{2\eta}{J^2} \left\| \sum_{j=1}^J [\nabla \ell_{N,j}(\Sigma_j) V \text{diag}(a_j)]_{\mathcal{S}_U} \right\|_F \\
&\leq \frac{2\eta}{J^2} \left\{ \sum_{j=1}^J \left\| [\{\nabla \ell_{N,j}(\Sigma_j) - \nabla \ell_{N,j}(\Sigma_j^*)\} V \text{diag}(a_j)]_{\mathcal{S}_U} \right\|_F \right. \\
&\quad \left. + \left\| \sum_{j=1}^J [\nabla \ell_{N,j}(\Sigma_j^*) V \text{diag}(a_j)]_{\mathcal{S}_U} \right\|_F \right\}.
\end{aligned}$$

We can bound the second term of the above display using (B.25) and obtain

$$\begin{aligned}
&\leq \frac{2\eta}{J^2} \left\{ \|A\|_\infty \sum_{j=1}^J \|\nabla \ell_{N,j}(\Sigma_j) - \nabla \ell_{N,j}(\Sigma_j^*)\|_F + \varepsilon_{stat} J^{1/2} \|A\|_\infty \right\} \\
&= \frac{2\eta}{J^2} \left\{ \|A\|_\infty \sum_{j=1}^J \|\Sigma_j - \Sigma_j^*\|_F + \varepsilon_{stat} J^{1/2} \|A\|_\infty \right\}.
\end{aligned}$$

From (4.3), we have

$$\begin{aligned}\|\Sigma_j - \Sigma_j^*\|_F^2 &\leq 3 \{ (\|A\|_\infty^2 + \|A^*\|_\infty^2) \|V - V^*R\|_F^2 + \|\text{diag}(a_j) - R^T \text{diag}(a_j^*)R\|_F^2 \} \\ &\leq 3 \left(\max_{j \in [J]} \|Z_j\|_\infty^2 + \max_{j' \in [J]} \|Z_{j'}^*\|_\infty^2 \right) I_0^2,\end{aligned}$$

where the last inequality uses that $\|A\|_\infty \leq \max_{j \in [J]} \|Z_j\|_2$, $\|A^*\|_\infty \leq \max_{j \in [J]} \|Z_j^*\|_2$, and $1 = \|V\|_2 \leq \|Z_j\|_2$ for $j \in [J]$. Then

$$\frac{\eta}{J} \|\nabla_V f_N\|_{S_U} \leq \frac{2\eta}{J^2} \max_{j \in [J]} \left\{ 2JI_0 \|Z_j\|_2 (\|Z_j\|_2 + \max_{j' \in [J]} \|Z_{j'}^*\|_2) + \varepsilon_{stat} J^{1/2} \|Z_j\|_2 \right\}.$$

Applying (B.29), the above display can be bounded by

$$\begin{aligned}&\leq \frac{2\eta}{J^2} \max_{j \in [J]} \left\{ \frac{11}{5} JI_0 \|Z_j^*\|_2^2 + \frac{17}{16} \varepsilon_{stat} J^{1/2} \|Z_j^*\|_2 \right\} \\ &\leq \frac{9I_0\eta}{J} \max_{j \in [J]} \|Z_j^*\|_2^2 \\ &\leq \frac{32I_0\eta}{3J} \max_{j \in [J]} \|Z_j^0\|_2^2,\end{aligned}$$

where the second to last inequality follows by Assumption 4.3 and the last inequality follows by (B.30). Then, by Assumption 4.1, we have

$$\frac{\eta}{J} \|\nabla_V f_N\|_{S_U} \leq \frac{I_0}{6\sqrt{J}}, \quad (\text{B.32})$$

which completes the proof. \square

Lemma B.8. *Assume that V has orthonormal columns and let*

$$\bar{V}^+ = \Pi_{C_V} \{V - \eta/J [\nabla_V f_N(Z)]_{S_U}\}, \quad Z = (V^T, A)^T, \quad R = \underset{Y \in \mathcal{O}(K)}{\text{argmin}} \|V - V^*Y\|_F^2.$$

Assume that

$$\|V - V^*R\|_F \leq I_0^2/J, \quad \|\text{diag}(a_j) - R^T \text{diag}(a_j^*)R\|_F \leq (J-1)I_0^2/J,$$

then under Assumption 4.1, 4.2, and 4.3, we have

$$\|\bar{V}^+ - V^*R\|_2 \leq \frac{2I_0}{J^{1/2}} < 1.$$

of Lemma B.8. By definition, we have

$$\|\bar{V}^+ - V^*R\|_2 \leq \|\bar{V}^+ - V\|_2 + \|V - V^*R\|_2.$$

By Assumption 4.6, we have $\|V - V^*R\|_2 \leq I_0/J^{1/2}$. Then, it remains to show that

$$\|\bar{V}^+ - V\|_2 \leq \|\bar{V}^+ - V\|_F \leq I_0/J^{1/2}.$$

The first step is to apply Lemma A.4 on $\|\bar{V}^+ - V\|_F$. We first verify that the inner product of the k th column of $V - (\eta/J)[\nabla_V f_N]_{S_U}$ and v_k are nonnegative for $k \in [K]$. By Lemma B.7, we have

$$\left\langle v_k - \left(\frac{\eta}{J}[\nabla_V f_N]_{S_U}\right)_k, v_k \right\rangle \geq 1 - \left\| \left(\frac{\eta}{J}[\nabla_V f_N]_{S_U}\right)_k \right\|_2 \geq 1 - \frac{I_0}{6\sqrt{J}} > 0,$$

for every $k \in [K]$, which allows us to apply Lemma A.4. Note that the term $1 + 2\sqrt{s^*}/\sqrt{(s - s^*)}$ decreases as s increases. Under Assumption 4.2, $s \geq 2s^*$ and we have $1 + 2\sqrt{s^*}/\sqrt{(s - s^*)} \leq 3$. Therefore applying Lemma A.4 with $s = 2s^*$:

$$\|\bar{V}^+ - V\|_2 \leq \|\bar{V}^+ - V\|_F \leq 6 \left\| V - \frac{\eta}{J}[\nabla_V f_N]_{S_U} - V \right\|_F \leq \frac{I_0}{\sqrt{J}},$$

where the last inequality follows from Lemma B.7. □

C Quantification of Statistical Error

C.1 Proof of Proposition 4.8

Let $\Omega(s, P)$ be a collection of subsets of $[P]$, each with cardinality s . Let

$$\mathcal{S}_V = \mathcal{S}_V(K, s) = \{\mathcal{S}_{V_k} \in \Omega(s, P)\}_{k \in [K]},$$

be the set of the supports, where \mathcal{S}_{V_k} denotes the support of component k for $k \in [K]$. We first establish a bound on the statistical error for a fixed support \mathcal{S}_V and then take the union bound to establish a bound on the statistical error on the set $\Upsilon(2K, ms^*, 2m'\gamma^*, \delta_A)$, for some constant $m, m' > 0$. For some positive semi-definite matrix G , we define the sets

$$\begin{aligned} \mathcal{V}(\mathcal{S}_V, K) &= \{V \in \mathbb{R}^{P \times K} : \|v_k\|_2 = 1, \|V_{\mathcal{S}_V^c}\| = 0, k \in [K]\}; \\ \mathcal{T}(G, \gamma) &= \{\alpha = Gu : u^T \Lambda u \leq \gamma\}, \end{aligned}$$

where $G^\dagger = Q\Lambda Q^T$ is the eigendecomposition. For a positive semi-definite kernel matrix G and a positive scalar γ , we define the semi-norm $\|\cdot\|_{G, \gamma}$ as

$$\|x\|_{G, \gamma}^2 = \frac{1}{\gamma}(x^T G^\dagger x).$$

Therefore, the set $\mathcal{T}(G, \gamma)$ is a unit ball in $\|\cdot\|_{G, \gamma}$. We use $\mathcal{N}_{\mathcal{V}}(\epsilon_v)$ to denote the ϵ -net for $\mathcal{N}(\mathcal{V}(\mathcal{S}_V, 2K), \epsilon_v, \|\cdot\|_F)$ and $\mathcal{N}_{\mathcal{T}}(\epsilon_a)$ to denote the ϵ -net for $\mathcal{N}(\mathcal{T}(\tilde{G}, 2m'\gamma^*), \epsilon_a, \|\cdot\|_{\tilde{G}, 2m'\gamma^*})$. For a matrix $A \in \mathbb{R}^{K \times J}$, we use A_k to denote k th row of A and a_j to denote the j th column of A . We define the following set

$$\mathcal{U}(\mathcal{S}_V, 2m'\gamma^*) = \{\{U \text{diag}(a_j) V^T\}_{j \in [J]} : U, V \in \mathcal{V}(\mathcal{S}_V, 2K), A_k \in \mathcal{T}(\tilde{G}, 2m'\gamma^*), k \in [2K]\},$$

and let $\{\Delta_j = U \text{diag}(a_j) V^T\}_{j \in [J]} \in \mathcal{U}(\mathcal{S}_V, 2m'\gamma^*)$. Recall that $\nabla \ell_{N,j}(\Sigma_j^*) = \Sigma_j^* - S_{N,j}$ for $j \in [J]$. We have

$$\begin{aligned} & \sup_{\{\Delta_j\} \in \mathcal{U}(\mathcal{S}_V, 2m'\gamma^*)} \sum_{j=1}^J \langle \Sigma_j^* - S_{N,j}, \Delta_j \rangle \\ &= \sup_{\{\Delta_j\} \in \mathcal{U}(\mathcal{S}_V, 2m'\gamma^*)} \sum_{j=1}^J \langle S_{N,j} - \Sigma_j^* - E_j, \Delta_j \rangle + \sum_{j=1}^J \langle E_j, \Delta_j \rangle. \quad (\text{C.1}) \end{aligned}$$

For the second term in the above display, we have

$$\sum_{j=1}^J \langle E_j, \Delta_j \rangle = \frac{1}{2} \sum_{j=1}^J \langle E_j, \Delta_j + \Delta_j^T \rangle \leq \frac{1}{2} \sum_j \|E_j\|_2 \|\Delta_j + \Delta_j^T\|_F \leq \left(\max_j \|E_j\|_2 \right) \cdot \sum_j \|\Delta_j\|_F, \quad (\text{C.2})$$

where the first equality follows by the fact that E_j is symmetric.

Using Lemma C.2, we have

$$\begin{aligned} & \sup_{\{\Delta_j\} \in \mathcal{U}(S_V, 2m'\gamma^*)} \left| \sum_{j=1}^J \langle S_{N,j} - \Sigma_j^* - E_j, \Delta_j \rangle \right| \\ & \leq (1 - 2\epsilon_v - \epsilon_a)^{-1} \max_{\substack{U, V \in \mathcal{N}_V(\epsilon_v) \\ A_k \in \mathcal{N}_T(\epsilon_a), k \in [2K]}} \left| \frac{1}{2} \sum_{j=1}^J \langle S_{N,j} - \Sigma_j^* - E_j, \Delta_j + \Delta_j^T \rangle \right|. \quad (\text{C.3}) \end{aligned}$$

For a fixed set of $\{\Delta_j\}_{j=1}^J$ for $j \in [J]$, we let $Y_j^{(n)} = (1/2) \text{tr}\{(\Delta_j + \Delta_j^T)x_j^{(n)}x_j^{(n)T}\}$. Note that $E\{Y_j^{(n)}\} = (1/2) \text{tr}\{(\Delta_j + \Delta_j^T)(\Sigma_j^* + E_j)\}$. Consequently, we have

$$\begin{aligned} \frac{1}{4} \sum_{j=1}^J \text{tr}\{(\Sigma_j^* + E_j)(\Delta_j + \Delta_j^T)(\Sigma_j^* + E_j)(\Delta_j + \Delta_j^T)\} & \leq \frac{1}{4} \sum_{j=1}^J \|\Sigma_j^* + E_j\|_2^2 \text{tr}\{(\Delta_j + \Delta_j^T)^2\} \\ & = \frac{1}{4} \sum_{j=1}^J \|\Sigma_j^* + E_j\|_2^2 \|\Delta_j + \Delta_j^T\|_F^2 \\ & \leq \max_{j \in [J]} \|\Sigma_j^* + E_j\|_2^2 \sum_{j=1}^J \|\Delta_j\|_F^2 \\ & \leq 4\|A^*\|_\infty^2 \sum_{j=1}^J \|\Delta_j\|_F^2, \quad (\text{C.4}) \end{aligned}$$

where the last step follows from $\|\Sigma_j^* + E_j\|_2 \leq 2\|\Sigma_j^*\|_2 \leq \|A^*\|_\infty$ for all $j \in [J]$.

Then, using Lemma G.7,

$$\begin{aligned} & \text{pr} \left[\frac{1}{N} \left| \sum_{n=1}^N \sum_{j=1}^J Y_j^{(n)} - E\{Y_j^{(n)}\} \right| \geq \frac{\varepsilon}{4} \right] \\ & \leq 2 \exp \left\{ -N e_0 \left(\frac{\varepsilon^2}{16\|A^*\|_\infty^2 \sum_{j=1}^J \|\Delta_j\|_F^2} \wedge \frac{\varepsilon}{4\|A^*\|_\infty \max_{j \in [J]} \|\Delta_j\|_2} \right) \right\}, \end{aligned}$$

where e_0 are some absolute constant.

We choose $\epsilon_v = \epsilon_a = 1/4$. Taking the union bound over $\mathcal{N}_V(\epsilon_v)$, $\mathcal{N}_T(\epsilon_a)$ and the choice of

$\Omega(ms^*, P)$, we have

$$\begin{aligned} & \Pr \left[\max_{\mathcal{S}_V \in \{\Omega(ms^*, P)\}^{2K}} \max_{\substack{U, V \in \mathcal{N}_V(\epsilon_v) \\ A_k \in \mathcal{N}_T(\epsilon_a), k \in [2K]}} \frac{1}{N} \sum_{n=1}^N \left| \sum_{j=1}^J Y_j^{(n)} - E \{ Y_j^{(n)} \} \right| \geq \frac{\epsilon}{4} \right] \\ & \leq 2 \binom{P}{ms^*}^{4K} 9^{4Kms^* + 2Kr(\tilde{G})} \exp \left\{ -N e_0 \left(\frac{\epsilon^2}{16 \|A^*\|_\infty^2 \sum_{j=1}^J \|\Delta_j\|_F^2} \wedge \frac{\epsilon}{4 \|A^*\|_\infty \max_{j \in [J]} \|\Delta_j\|_2} \right) \right\}, \end{aligned} \quad (\text{C.5})$$

where we applied the metric entropy in Lemma C.1.

Given $0 < \delta < 1$, let

$$\nu \leq \frac{1}{e'_0} \left[\frac{1}{N} \left\{ \log \frac{1}{\delta} + Kr(\tilde{G}) + Ks^* + Ks^* \log \frac{Pe}{s^*} \right\} \right]^{1/2}$$

for some constant e'_0 . Combining (C.2) and (C.5) with (C.1), we have

$$\varepsilon_{stat} \left(\sum_{j=1}^J \|\Delta_j\|_F^2 \right)^{1/2} \leq \|A^*\|_\infty \left(\sum_{j=1}^J \|\Delta_j\|_F^2 \right)^{1/2} (\nu \vee \nu^2) + \left(\sum_{j=1}^J \|\Delta_j\|_F \right) \max_{j \in [J]} \|E_j\|_2, \quad (\text{C.6})$$

with probability at least $1 - \delta$. Using the Cauchy-Schwarz inequality,

$$\sum_{j=1}^J \|\Delta_j\|_F \leq J^{1/2} \left(\sum_{j=1}^J \|\Delta_j\|_F^2 \right)^{1/2}$$

and, therefore,

$$\varepsilon_{stat} \leq \|A^*\|_\infty (\nu \vee \nu^2) + J^{1/2} \max_{j \in [J]} \|E_j\|_2$$

with probability at least $1 - \delta$.

C.2 Metric Entropy of the Structured Set

We find the metric entropy of $\mathcal{N}(\mathcal{V}(\mathcal{S}_V, K), \epsilon_v, \|\cdot\|_F)$ and $\mathcal{N}(\mathcal{T}(G, \gamma), \epsilon_a, \|\cdot\|_{G, \gamma})$.

Lemma C.1. *Given a support set $\mathcal{S}_V(K, s) = \{\mathcal{S}_{V_k} \in \Omega(s, P)\}_{k \in [K]}$, let*

$$\mathcal{V}(\mathcal{S}_V, K) = \{V \in \mathbb{R}^{P \times K} : \|v_k\|_2 = 1, \|V_{\mathcal{S}_V^c}\| = 0, k \in [K]\}.$$

The metric entropy of $\mathcal{N}(\mathcal{V}(\mathcal{S}_V, K), \epsilon_v, \|\cdot\|_F)$ is

$$\log |\mathcal{N}(\mathcal{V}(\mathcal{S}_V, K), \epsilon_v, \|\cdot\|_F)| \leq Ks \log \left(1 + \frac{2}{\epsilon_v} \right).$$

Given G and γ , the metric entropy of $\mathcal{N}(\mathcal{T}(G, \gamma), \epsilon_a, \|\cdot\|_{G, \gamma})$ is

$$\log |\mathcal{N}(\mathcal{T}(G, \gamma), \epsilon_a, \|\cdot\|_{G, \gamma})| \leq r(G) \log \left(1 + \frac{2}{\epsilon_a} \right),$$

where $r(G)$ is the rank of G .

of Lemma C.1. The first result directly follows from Lemma 5.2 in Vershynin (2010). For the second results, we note that the set $\mathcal{T}(G, \gamma)$ is a $r(G)$ -dimensional unit ball in the semi-norm $\|\cdot\|_{G, \gamma}$. Therefore, we can again apply Lemma 5.2 in Vershynin (2010). \square

C.3 Inner Product on a ϵ -net

We define the following operator similar to the definition of $W^\star(V)$:

$$\widehat{W}^\star(U, V) = [\widehat{w}_{kj}^\star(u_k, v_k)] \in \mathbb{R}^{K \times J}, \quad \widehat{w}_{kj}^\star(u_k, v_k) = u_k^T \nabla_{N,j}(\Sigma_j^\star) v_k, \quad \nabla_{N,j}(\Sigma_j^\star) = \Sigma_j^\star - S_{N,j}.$$

Recall that $A = [a_1, \dots, a_j] \in \mathbb{R}^{K \times J}$. Then

$$\sum_{j=1}^J \langle \nabla_{N,j}(\Sigma_j^\star), U \text{diag}(a_j) V^T \rangle = \sum_{k=1}^K A_k^T \widehat{W}_k^\star(u_k, v_k),$$

where $A_k \in \mathbb{R}^J$ denote the k th row of A and $\widehat{W}_k^\star(u_k, v_k)$ denotes the k th row of $\widehat{W}^\star(U, V) \in \mathbb{R}^J$. Consequently, if every row $A_k \in \mathbb{R}^J$ lies in $\mathcal{T}(G, \gamma)$, we have

$$\sum_{j=1}^J \langle \nabla_{N,j}(\Sigma_j^\star), U \text{diag}(a_j) V^T \rangle = \sum_{k=1}^K A_k^T Q Q^T \widehat{W}_k^\star(u_k, v_k),$$

where Q is the matrix whose columns are eigenvectors of G . This is another representation of the statistical error and will help us to simplify the proof steps of the following lemma.

Lemma C.2 (Inner product on a net). *Given a support \mathcal{S}_V , a matrix G , and a positive scalar γ , we have*

$$\max_{\substack{U, V \in \mathcal{V}(\mathcal{S}_V, K) \\ A_k \in \mathcal{T}(G, \gamma), k \in [K]}} \sum_{k=1}^K A_k^T Q Q^T \widehat{W}_k^\star(u_k, v_k) \leq (1 - 2\epsilon_v - \epsilon_a)^{-1} \max_{\substack{U, V \in \mathcal{N}_{\mathcal{V}}(\epsilon_v) \\ A_k \in \mathcal{N}_{\mathcal{T}}(\epsilon_a), k \in [K]}} \sum_{k=1}^K A_k^T Q Q^T \widehat{W}_k^\star(u_k, v_k),$$

where Q denotes the matrix whose columns are eigenvectors of G .

Proof. Let \widehat{U} , \widehat{V} and \widehat{A} be the quantities that maximize

$$\widetilde{\epsilon} = \max_{\substack{U, V \in \mathcal{V}(\mathcal{S}_V, K) \\ A_k \in \mathcal{T}(G, \gamma), k \in [K]}} \sum_{k=1}^K A_k^T Q Q^T \widehat{W}_k^\star(u_k, v_k).$$

Then

$$\begin{aligned} \left| \sum_{k=1}^K A_k^T Q Q^T \widehat{W}_k^\star(u_k, v_k) \right| &= \left| \sum_{k=1}^K \widehat{A}_k^T Q Q^T \widehat{W}_k^\star(\widehat{u}_k, \widehat{v}_k) + \sum_{k=1}^K (A_k - \widehat{A}_k)^T Q Q^T \widehat{W}_k^\star(u_k, v_k) \right. \\ &\quad \left. + \sum_{k=1}^K \widehat{A}_k^T Q Q^T \{ \widehat{W}_k^\star(u_k, v_k) - \widehat{W}_k^\star(\widehat{u}_k, \widehat{v}_k) \} \right|. \end{aligned}$$

Using the triangle inequality, we have

$$\left| \sum_{k=1}^K A_k^T Q Q^T \widehat{W}_k^\star(u_k, v_k) \right| \geq \widetilde{\epsilon} - T_1 - T_2,$$

where

$$T_1 = \left| \sum_{k=1}^K (A_{k\cdot} - \widehat{A}_{k\cdot})^T Q Q^T \widehat{W}_{k\cdot}^*(u_k, v_k) \right|$$

and

$$T_2 = \left| \sum_{k=1}^K \widehat{A}_{k\cdot}^T Q Q^T \left\{ \widehat{W}_{k\cdot}^*(u_k, v_k) - \widehat{W}_{k\cdot}^*(\widehat{u}_k, \widehat{v}_k) \right\} \right|.$$

Let $\theta_k = (A_{k\cdot} - \widehat{A}_{k\cdot}) / \|A_{k\cdot} - \widehat{A}_{k\cdot}\|_{G,\gamma} \in \mathbb{R}^J$. Then $\|\theta_k\|_{G,\gamma} = 1$ for every $k \in [K]$ and $\theta_k \in \mathcal{T}(G, \gamma)$. Therefore, we have

$$\begin{aligned} T_1 &\leq \max_{k \in [K]} \|A_{k\cdot} - \widehat{A}_{k\cdot}\|_{G,\gamma} \left| \sum_{k=1}^K \theta_k^T Q Q^T \widehat{W}_{k\cdot}^*(u_k, v_k) \right| \\ &= \max_{k \in [K]} \|A_{k\cdot} - \widehat{A}_{k\cdot}\|_{G,\gamma} \left| \sum_{k=1}^K (Q Q^T \theta_k)^T Q Q^T \widehat{W}_{k\cdot}^*(u_k, v_k) \right| \leq \epsilon_a \widetilde{\epsilon}, \end{aligned}$$

where the inequality holds because $Q Q^T \theta_k \in \mathcal{T}(G, \gamma)$ for $k \in [K]$. For T_2 , we have

$$\begin{aligned} T_2 &= \left| \sum_{k=1}^K \widehat{A}_{k\cdot}^T Q Q^T \left\{ \widehat{W}_{k\cdot}^*(u_k, v_k) - \widehat{W}_{k\cdot}^*(\widehat{u}_k, \widehat{v}_k) \right\} \right| = \left| \sum_{j=1}^J \left\langle \nabla \ell_{N,j}(\Sigma_j^*), \sum_{k=1}^K \widehat{a}_{kj} (u_k v_k^T - \widehat{u}_k \widehat{v}_k^T) \right\rangle \right| \\ &\leq \widetilde{\epsilon} \max_{k \in [K]} \|u_k v_k^T - \widehat{u}_k \widehat{v}_k^T\|_F \\ &\leq \widetilde{\epsilon} \max_{k \in [K]} (\|v_k - \widehat{v}_k\|_2 + \|u_k - \widehat{u}_k\|_2) \leq 2\widetilde{\epsilon} \epsilon_v, \end{aligned}$$

where the second equality follows from $\widehat{A}_{k\cdot}^T Q Q^T = A_{k\cdot}$ for $k \in [K]$. \square

D Sample Complexity of Spectral Initialization

D.1 Proof of Theorem 4.9

Let $M_N = J^{-1} \sum_{j=1}^J S_{N,j}$, $M^* = E(M_N)$, and $R^0 = \operatorname{argmin}_{Y \in \mathcal{O}(K)} \|V^0 - V^* Y\|_F^2$. The proof proceeds in two steps. In the first step, we establish that

$$\operatorname{dist}^2(Z^0, Z^*) \leq e_1 \|M_N - M^*\|_2^2 + e_2 \sum_{j=1}^J \|S_{N,j} - \Sigma_j^*\|_2^2, \quad (\text{D.1})$$

where $e_1 = 5KJg^{-2}(1 + 16\varphi^2 \|A^*\|_\infty^2)$, $e_2 = 8K\varphi^2$, and $\varphi^2 = \max_{j \in [J]} \{1 + 4\sqrt{2} \|A^*\|_\infty / \sigma_K(\Sigma_j^*)\}$ with $g = \sigma_K(M^*) - \sigma_{K+1}(M^*) > 0$. In the second step, we bound $\|M_N - M^*\|_2$ and $\|S_{N,j} - \Sigma_j^*\|_2$ for $j \in [J]$ using Lemma G.5.

Step 1. We write

$$\operatorname{dist}^2(Z^0, Z^*) = T_1 + T_2,$$

where $T1 = \sum_{j=1}^J \|V^0 - V^* R^0\|_F^2$ and $T2 = \sum_{j=1}^J \|\text{diag}(a_j^0) - R^{0T} \text{diag}(a_j^*) R^0\|_F^2$. First, we find a bound on $\min_{Y \in \mathcal{O}(K)} \|V^0 - V^* Y\|_F^2$ that does not depend on R^0 . By Lemma G.3, we have

$$\min_{Y \in \mathcal{O}(K)} \|V^0 - V^* Y\|_F^2 \leq \frac{1}{2(\sqrt{2}-1)} \|V^0 V^{0T} - V^* V^{*T}\|_F^2. \quad (\text{D.2})$$

The following Lemma gives us a bound on $T2$ that does not depend on R^0 .

Lemma D.1. *Let $\varphi^2 = \max_{j \in [J]} \{1 + 4\sqrt{2}\|A^*\|_\infty / \sigma_K(\Sigma_j^*)\}$, we have*

$$T2 \leq 4K\varphi^2 \sum_{j=1}^J (5\|\Sigma_j^*\|_2^2 \|V^0 V^{0T} - V^* V^{*T}\|_2^2 + 2\|S_{N,j} - \Sigma_j^*\|_2^2). \quad (\text{D.3})$$

Putting (D.2) and Lemma D.1 together, we have

$$\begin{aligned} \text{dist}^2(Z^0, Z^*) &\leq \frac{J}{2(\sqrt{2}-1)} \|V^0 V^{0T} - V^* V^{*T}\|_F^2 \\ &\quad + 4K\varphi^2 \sum_{j=1}^J (2\|S_{N,j} - \Sigma_j^*\|_2^2 + 5\|\Sigma_j^*\|_2^2 \|V^0 V^{0T} - V^* V^{*T}\|_2^2). \end{aligned} \quad (\text{D.4})$$

Using Lemma G.2 to bound $\|V^0 V^{0T} - V^* V^{*T}\|_F$ and $\|V^0 V^{0T} - V^* V^{*T}\|_2$, and noting that $\|\Sigma_j^*\|_2 \leq \|A^*\|_\infty$, we obtain (D.1).

Step 2. We show that $\|M_N - M^*\|_2^2$ and $\|S_{N,j} - \Sigma_j^*\|_2^2$ are bounded with high probability when the eigengap g is bounded away from zero. We apply Lemma G.5 with $\|M^*\|_2 \leq \|A^*\|_\infty$ and obtain

$$\text{pr} \{ \|M_N - M^*\|_2 \geq h_M(\delta) \} \leq \frac{\delta}{J},$$

where

$$h_M(\delta) = \frac{2P\|A^*\|_\infty}{NJ} \log \frac{2PJ}{\delta} + \left(\frac{2P\|A^*\|_\infty^2}{NJ} \log \frac{2PJ}{\delta} \right)^{\frac{1}{2}}.$$

Similarly, for $J \geq 4$ and for every $j \in [J]$, we have

$$\text{pr} \{ \|S_{N,j} - \Sigma_j^*\|_2 \geq h_S(\delta) \} \leq \frac{J-1}{J} \frac{\delta}{J},$$

where

$$h_S(\delta) = \frac{2P\|A^*\|_\infty}{N} \log \frac{4PJ}{\delta} + \left(\frac{2P\|A^*\|_\infty^2}{N} \log \frac{4PJ}{\delta} \right)^{\frac{1}{2}}.$$

Then, collecting results and applying union bound, we have

$$\text{dist}^2(Z^0, Z^*) \leq \frac{5KJ}{g^2} (1 + 16\varphi^2 \|A^*\|_\infty^2) h_M^2(\delta) + 8KJ\varphi^2 h_S^2(\delta),$$

with probability at least $1 - \delta$. This implies that

$$\begin{aligned} \text{dist}^2(Z^0, Z^*) &\leq \phi(g, A^*) \left\{ \frac{KJP^2}{N^2} \left(\log \frac{4PJ}{\delta} \right)^2 + \frac{KJP}{N} \log \frac{4PJ}{\delta} \right\}; \\ \phi(g, A^*) &= 4\|A^*\|_\infty^2 \left\{ \frac{5(1 + 16\varphi^2 \|A^*\|_\infty^2)}{g^2 J} \vee 8\varphi^2 \right\}, \end{aligned} \quad (\text{D.5})$$

with probability at least $1 - \delta$ and $\phi(g, A^*)$ is a constant that depends on g and A^* . In particular, the bound holds only when the eigengap g is bounded away from zero.

D.2 Proof of Lemma D.1

We prove the result for $J = 1$ and drop the subscript j throughout the proof. The proof can be easily extended to the case where $J > 1$. Recall that $R^0 = \operatorname{argmin}_{Y \in \mathcal{O}(K)} \|V^0 - V^*Y\|_F^2$ and $\varphi^2 = \max_{j \in [J]} \{1 + 4\sqrt{2}\|A^*\|_\infty/\sigma_K(\Sigma_j^*)\}$. Similar to (B.3) in the proof of Lemma B.1, we have

$$\begin{aligned} \|\operatorname{diag}(a^0) - R^{0T} \operatorname{diag}(a^*) R^0\|_F^2 &\leq \varphi^2 \|V^0 \operatorname{diag}(a^0) V^{0T} - V^* \operatorname{diag}(a^*) V^{*T}\|_F^2 \\ &\leq 2K\varphi^2 \left\| \sum_{k=1}^K (v_k^{0T} S_N v_k^0) v_k^0 v_k^{0T} - \Sigma^* \right\|_2^2, \end{aligned} \quad (\text{D.6})$$

where we can write $V^0 \operatorname{diag}(a^0) V^{0T} = \sum_{k=1}^K (v_k^{0T} S_N v_k^0) v_k^0 v_k^{0T}$. Note that we can write $\Sigma^* = \sum_{k=1}^K (v_k^{*T} \Sigma^* v_k^*) v_k^* v_k^{*T}$. Applying the triangle inequality to the right hand side of (D.6), we have

$$\begin{aligned} \|\operatorname{diag}(a^0) - R^{0T} \operatorname{diag}(a^*) R^0\|_F^2 &\leq 4K\varphi^2 \left\{ \left\| \sum_{k=1}^K (v_k^{*T} \Sigma^* v_k^*) (v_k^0 v_k^{0T} - v_k^* v_k^{*T}) \right\|_2^2 \right. \\ &\quad \left. + \left\| \sum_{k=1}^K (v_k^{0T} S_N v_k^0 - v_k^{*T} \Sigma^* v_k^*) v_k^0 v_k^{0T} \right\|_2^2 \right\}. \end{aligned} \quad (\text{D.7})$$

Next, we bound the two terms on the right hand side of (D.7) separately. We have

$$\left\| \sum_{k=1}^K (v_k^{*T} \Sigma^* v_k^*) (v_k^0 v_k^{0T} - v_k^* v_k^{*T}) \right\|_2^2 \leq \|\Sigma^*\|_2^2 \left\| \sum_{k=1}^K v_k^0 v_k^{0T} - \sum_{k=1}^K v_k^* v_k^{*T} \right\|_2^2.$$

By the uniqueness of projection operators, the above display can be written as

$$= \|\Sigma^*\|_2^2 \|V^0 V^{0T} - V^* V^{*T}\|_2^2. \quad (\text{D.8})$$

Since v_1^0, \dots, v_K^0 are orthonormal to each other, we have

$$\begin{aligned} \left\| \sum_{k=1}^K \{v_k^{0T} S_N v_k^0 - v_k^{*T} \Sigma^* v_k^*\} v_k^0 v_k^{0T} \right\|_2^2 &\leq \max_{k \in [K]} |v_k^{0T} S_N v_k^0 - v_k^{*T} \Sigma^* v_k^*|^2 \\ &= \max_{k \in [K]} |v_k^{0T} S_N v_k^0 - v_k^{0T} \Sigma^* v_k^0 + v_k^{0T} \Sigma^* v_k^0 - v_k^{*T} \Sigma^* v_k^*|^2 \\ &\leq 2\|S_N - \Sigma^*\|_2^2 + 2 \max_{k \in [K]} |v_k^{0T} \Sigma^* v_k^0 - v_k^{*T} \Sigma^* v_k^*|^2 \\ &= 2\|S_N - \Sigma^*\|_2^2 + 2 \max_{k \in [K]} |\langle \Sigma^*, v_k^0 v_k^{0T} - v_k^* v_k^{*T} \rangle|^2. \end{aligned} \quad (\text{D.9})$$

Next, we upper bound the second term on the right hand side of (D.9). We have

$$\begin{aligned} \max_{k \in [K]} |\langle \Sigma^*, v_k^0 v_k^{0T} - v_k^* v_k^{*T} \rangle|^2 &\leq \|\Sigma^*\|_2^2 \max_{k \in [K]} \|v_k^0 v_k^{0T} - v_k^* v_k^{*T}\|_F^2 \\ &\leq 2\|\Sigma^*\|_2^2 \max_{k \in [K]} \|v_k^0 v_k^{0T} - v_k^* v_k^{*T}\|_2^2 \\ &\leq 2\|\Sigma^*\|_2^2 \|V^0 V^{0T} - V^* V^{*T}\|_2^2. \end{aligned} \quad (\text{D.10})$$

Plugging the result of (D.10) into (D.9), we have

$$\left\| \sum_{k=1}^K (v_k^{0T} S_N v_k^0 - v_k^{*T} \Sigma^* v_k^*) v_k^* v_k^{*T} \right\|_2^2 \leq 2 \|S_N - \Sigma^*\|_2^2 + 4 \|\Sigma^*\|_2^2 \|V^0 V^{0T} - V^* V^{*T}\|_2^2, \quad (\text{D.11})$$

where the last inequality follows by triangle inequality. Combining results from (D.8) and (D.11), we have

$$\|\text{diag}(a_j^0) - R^{0T} \text{diag}(a_j^*) R^0\|_F^2 \leq 4K\varphi^2 (5\|\Sigma_j^*\|_2^2 \|V^0 V^{0T} - V^* V^{*T}\|_2^2 + 2\|S_{N,j} - \Sigma_j^*\|_2^2),$$

for every $j \in [J]$. Hence, we complete the proof.

E Proof of Theorem 4.4

To proof Theorem 4.4, we need following lemma.

Lemma E.1 (Linear Convergence Rate). *Suppose that Assumptions 4.1–4.6 are satisfied. After I iterations of Algorithm 2, we have*

$$\sum_{j=1}^J \|\Sigma_j^I - \tilde{\Sigma}_j^*\|_F^2 \leq \beta^{I/2} (2\mu^2 \xi^2) \sum_{j=1}^J \|\Sigma_j^0 - \tilde{\Sigma}_j^*\|_F^2 + C_1 \varepsilon_{stat}^2, \quad C_1 = \frac{2\tau\mu^2\eta}{\beta^{1/2} - \beta}, \quad (\text{E.1})$$

where $\mu = \max_{j \in [J]} (17/8) \|Z_j^*\|_2$ and $\tau = J^{-1} \{9/2 + (1/2 \vee K/8)\}$.

Since $\|Z_j^*\|_2$ and μ are bounded, Lemma E.1 shows that Algorithm 2 achieves error smaller than $\delta + C_1 \varepsilon_{stat}^2$ after $I \gtrsim \log(1/\delta)$ iterations. The second term on the left hand side denotes the constant multiple of the statistical error, which depends on the distribution of the data and the sample size.

of Lemma E.1. Let $Z = (V^T, A)^T$ be an iterate obtained by Algorithm 2, $\Sigma_j = V \text{diag}(a_j) V^T$ for $j \in [J]$, and

$$R = \underset{Y \in \mathcal{O}(K)}{\text{argmin}} \|V - V^* Y\|_F^2.$$

We have the following decomposition

$$\begin{aligned} \Sigma_j - \tilde{\Sigma}_j^* &= (V - V^* R) R^T \text{diag}(\tilde{a}_j^*) R R^T V^{*T} \\ &\quad + V \{ \text{diag}(a_j) - R^T \text{diag}(\tilde{a}_j^*) R \} R^T V^{*T} + V \text{diag}(a_j) (V - V^* R)^T. \end{aligned}$$

Then

$$\|\Sigma_j - \tilde{\Sigma}_j^*\|_F \leq \{ \|\text{diag}(a_j)\|_2 + \|\text{diag}(\tilde{a}_j^*)\|_2 \} \|V - V^* R\|_F + \|\text{diag}(a_j) - R^T \text{diag}(\tilde{a}_j^*) R\|_F.$$

Since $\|\text{diag}(a_j)\|_2 \leq \|Z_j\|_2$ and $\|\tilde{Z}_j^*\|_2 \leq \|Z_j\|_2 + \|Z_j^*\|_2 \leq (17/8) \|Z_j^*\|_2$ from (B.29), we have

$$\|\Sigma_j - \tilde{\Sigma}_j^*\|_F \leq \mu \{ \|V - V^* R\|_F + \|\text{diag}(a_j) - R^T \text{diag}(\tilde{a}_j^*) R\|_F \}.$$

Combining Theorem 4.7 with Lemma B.1, in the I th iteration, we have

$$\begin{aligned}
\sum_{j=1}^J \|\Sigma_j^I - \tilde{\Sigma}_j^*\|_F^2 &\leq 2\mu^2 \text{dist}^2(Z^I, \tilde{Z}^*) \\
&\leq 2\mu^2 \left\{ \beta^{I/2} \text{dist}^2(Z^0, \tilde{Z}^*) + \frac{\tau\eta\varepsilon_{\text{stat}}^2}{\beta^{1/2}(1-\beta)^{1/2}} \right\} \\
&\leq 2\mu^2 \left\{ \beta^{I/2}\xi^2 \sum_{j=1}^J \|\Sigma_j^0 - \tilde{\Sigma}_j^*\|_F^2 + \frac{\tau\eta\varepsilon_{\text{stat}}^2}{\beta^{1/2}(1-\beta)^{1/2}} \right\},
\end{aligned}$$

which completes the proof. \square

of Theorem 4.4. We first note that under the assumptions, using Theorem 4.9, Assumption 4.6 is satisfied with probability at least $1 - \delta_0$. This allows us to use Lemma E.1 to bound $\sum_{j=1}^J \|\Sigma_j^I - \tilde{\Sigma}_j^*\|_F^2$. By triangle inequality, we have

$$\sum_{j=1}^J \|\Sigma_j^I - \Sigma_j^*\|_F^2 \leq 2 \underbrace{\sum_{j=1}^J \|\Sigma_j^I - \tilde{\Sigma}_j^*\|_F^2}_{\text{Estimation error}} + 2 \underbrace{\sum_{j=1}^J \|\tilde{\Sigma}_j^* - \Sigma_j^*\|_F^2}_{\text{Approximation error}}$$

and, therefore, it remains only to bound the approximation error. We have

$$\begin{aligned}
\sum_{j=1}^J \|\tilde{\Sigma}_j^* - \Sigma_j^*\|_F^2 &= \sum_{j=1}^J \|V^* \text{diag}(\tilde{a}_j^* - a_j^*) V^{*T}\|_F^2 \\
&= \sum_{j=1}^J \|\text{diag}(\tilde{a}_j^* - a_j^*)\|_F^2 \\
&= \|\tilde{A}^* - A^*\|_F^2.
\end{aligned}$$

Recall that each row of \tilde{A}^* is the projection of the corresponding row of A^* to the set $\tilde{\mathcal{C}}_A(c, \gamma)$, where $c \geq c^*$ and $\gamma \geq \gamma^*$. Recall that columns of $Q = (\tilde{Q}, Q_1)$ denote eigenvectors of G . For any $k \in [K]$, if $Q_1^T A_{k\cdot}^* = 0$, then we have no loss in projecting $A_{k\cdot}^*$ to $\tilde{\mathcal{C}}_A(c, \gamma)$. When $Q_1^T A_{k\cdot}^* \neq 0$, we want to quantify the loss of using truncated ellipsoid. Let $A_{k\cdot}^* = Q h_k^*$, $h_k^* \in \mathbb{R}^J$ for $k \in [K]$. Then $\tilde{A}_{k\cdot}^* = \tilde{Q} \tilde{h}_k^*$, where $\tilde{h}_{k_j}^* = h_{k_j}^*$ for $j \leq r(\tilde{G})$, $k \in [K]$. Therefore, for each row $k \in [K]$, we have

$$\|\tilde{A}_{k\cdot}^* - A_{k\cdot}^*\|_2^2 = \sum_{j=r(\tilde{G})+1}^J h_{k_j}^{*2} \leq \lambda_{r(\tilde{G})} \sum_{j=r(\tilde{G})+1}^J \frac{h_{k_j}^{*2}}{\lambda_j} \leq \lambda_{r(\tilde{G})} \gamma^* \leq \delta_A \gamma^*. \quad (\text{E.2})$$

Then $\|\tilde{A}^* - A^*\|_F^2 \leq K \delta_A \gamma^*$, which completes the proof. \square

F Proof of Proposition 4.5

The proof proceeds in three steps. First, we verify that the iterate Z^0 obtained by Algorithm 1 satisfies Assumption 4.6. In the second step, we bound the statistical and approximation errors. In the final step, we establish a bound on $\sum_{j=1}^J \|\Sigma_j^I - \Sigma_j^*\|_F^2$.

Step 1. The proof is similar to that of Theorem 4.9. Let $M_N = J^{-1} \sum_{j=1}^J S_{N,j}$ and $M^* = E(M_N)$. Since $\sigma_K(\Sigma_j^*) > E_j$ for every $j \in [J]$, the eigengap $g = \sigma_K(M^*) - \sigma_{K+1}(M^*) > 0$ is nonzero and we can apply Davis-Kahan “sin θ ” theorem, stated in Lemma G.2. From (D.1),

$$\text{dist}^2(Z^0, Z^*) \leq e_1 \|M_N - M^*\|_2^2 + e_2 \sum_{j=1}^J \|S_{N,j} - \Sigma_j^*\|_2^2.$$

From the definition of $\|\cdot\|_{\psi_2}$ in (G.1), for every $n \in [N]$ and $j \in [J]$, we have

$$\|x_j^{(n)}\|_{\psi_2}^2 \leq \max_{j \in [J]} \|\Sigma_j^* + E_j\|_2 \leq 2 \max_{j \in [J]} \|\Sigma_j^*\|_2 \leq 2 \|A^*\|_\infty.$$

Lemma G.6 then gives us

$$\|M_N - M^*\|_2 \lesssim \|A^*\|_\infty \left[\frac{1}{NJ} \left(2P + \log \frac{2J}{\delta_0} \right) + \left\{ \frac{1}{NJ} \left(2P + \log \frac{2J}{\delta_0} \right) \right\}^{\frac{1}{2}} \right], \quad (\text{F.1})$$

with probability at least $1 - \delta_0/J$. Similarly, for $J \geq 4$, we have for every $j \in [J]$,

$$\|S_{N,j} - \Sigma_j^*\|_2 \lesssim \|A^*\|_\infty \left[\frac{1}{N} \left(2P + \log \frac{4J}{\delta_0} \right) + \left\{ \frac{1}{N} \left(2P + \log \frac{4J}{\delta_0} \right) \right\}^{\frac{1}{2}} \right], \quad (\text{F.2})$$

with probability at least $1 - (J-1)\delta_0/J^2$. A union bound, together with (D.5), gives us

$$\text{dist}^2(Z^0, Z^*) \leq \phi(g, A^*) \left[\frac{KJ}{N^2} \left\{ 8P^2 + 2 \left(\log \frac{4J}{\delta_0} \right)^2 \right\} + \frac{KJ}{N} \left(4P + 2 \log \frac{4J}{\delta_0} \right) \right],$$

with probability at least $1 - \delta_0$.

This shows that $\text{dist}^2(Z^0, Z^*) \leq JI_0^2$ with probability at least $1 - \delta_0$ when $N \gtrsim K(P + \log J/\delta_0)$. From (D.2) and (D.4) we have that $\|V^0 - V^*R\|_F^2 \leq 5Kg^{-2} \|M_N - M^*\|_2^2$. From (F.1) we have that $\|V - V^*R\|_F^2 \leq I_0^2/J$ with high probability when $N \gtrsim K(P + \log J/\delta_0)$. Similarly, $\|\text{diag}(a_j) - R^T \text{diag}(a_j^*)R\|_F^2 \leq (J-1)I_0^2/J$ with high probability. This shows that Assumption 4.6 is satisfied..

Step 2. Let $r = r(\tilde{G})$. Recall that $G = Q\Lambda^\dagger Q^T$. Setting $\Lambda_{rr}^\dagger = \exp(-l^2 r^2) = \delta_A$, we have

$$r(\tilde{G}) = \left\{ \left(\frac{1}{l^2} \log \frac{1}{\delta_A} \right)^{\frac{1}{2}} \wedge J \right\}. \quad (\text{F.3})$$

Proposition 4.8 then yields

$$\varepsilon_{stat}^2 \leq 2(\nu_2 \vee \nu_2^2) + 2J \max_j \|E_j\|_2^2$$

where

$$\nu_2 \lesssim \frac{\|A^\star\|_\infty^2}{e_4 N} \left[\log \frac{1}{\delta_0} + \left\{ \left(\frac{1}{\alpha^2} \log \frac{1}{\delta_A} \right)^{\frac{1}{2}} \wedge J \right\} + K s^\star \log \frac{P}{s^\star} \right]$$

with probability at least $1 - \delta_0$.

If $s^\star \log P/s^\star < PJ$, then

$$\log \frac{1}{\delta_0} + Kr(\tilde{G}) + K s^\star \log \frac{P}{s^\star} \lesssim \left(\log \frac{1}{\delta_0} + KJP \right).$$

Therefore $(\nu_2 \vee \nu_2^2) \lesssim JI_0^2$. Combining with the assumption $\max_{j \in [J]} \|E_j\|_2 \lesssim I_0$, we establish that Assumption 4.3 holds with probability at least $1 - \delta_0$.

Step 3. Similar to the proof of Theorem 4.4, we combine results from Step 1 and 2 to obtain

$$\sum_{j=1}^J \|\Sigma_j^I - \Sigma_j^\star\|_F^2 \lesssim \delta_1 + \frac{Kr(\tilde{G}) + K s^\star \log(P/s^\star) + \log \delta_0^{-1}}{N} + J \max_{j \in [J]} \|E_j\|_2^2 + K\gamma^\star \delta_A \quad (\text{F.4})$$

after $I \gtrsim \log(1/\delta_1)$ iterations. We omit details for brevity.

In the final step, we choose a δ_A that satisfies $\delta_A \leq (16\gamma^\star)^{-1} \min_{j \in [J]} \sigma_K^2(\Sigma_j^\star)$ and obtains the optimal error of (F.4). Plugging (F.3) into (F.4), the optimal choice is $\delta_A^\star = (\gamma^\star lN)^{-1} (\log \gamma^\star lN)^{1/2}$. Note that δ_A^\star is smaller than $(16\gamma^\star)^{-1} \min_{j \in [J]} \sigma_K^2(\Sigma_j^\star)$, given that N is not too small. Then, plugging δ_A^\star into (F.4), we establish the result.

G Known Results

Lemma G.1 (Theorem 2.1.12 in Nesterov (2013)). *For a L -smooth and m -strongly convex function h , we have*

$$\langle \nabla h(X) - \nabla h(Y), X - Y \rangle \geq \frac{mL}{m+L} \|X - Y\|^2 + \frac{1}{m+L} \|\nabla h(X) - \nabla h(Y)\|^2.$$

Lemma G.2 (Davis-Kahan $\sin \theta$ theorem, adapted from Yu et al. (2015)).

Let $M_N = J^{-1} \sum_{j=1}^J S_{N,j}$ and $M^\star = E(M_N)$. V^\star is the matrix whose columns are top- K eigenvectors of M^\star , and V is the matrix whose columns are the top- K eigenvectors of M_N . Assume that the eigengap $g = \sigma_K(M^\star) - \sigma_{K+1}(M^\star) > 0$ is bounded away from zero. Then

$$\|VV^T - V^\star V^{\star T}\|_F \leq \frac{2\sqrt{K}}{g} \|M_N - M^\star\|_2, \quad \|VV^T - V^\star V^{\star T}\|_2 \leq \frac{2}{g} \|M_N - M^\star\|_2.$$

Moreover, we have

$$\min_{Y \in \mathcal{O}(K)} \|V - V^\star Y\|_F \leq \frac{2\sqrt{2}}{g} \|M_N - M^\star\|_F.$$

Lemma G.3 (Adapted from Lemma 5.4 in Tu et al. (2016)). *For any $X, U \in \mathbb{R}^{P \times K}$, we have*

$$\min_{Y \in \mathcal{O}(K)} \|U - XY\|_F^2 \leq \frac{1}{2(\sqrt{2}-1)\sigma_K^2(X)} \|UU^T - XX^T\|_F^2.$$

Lemma G.4 (Matrix Bernstein, adapted from Theorem 6.6.1 in [Tropp \(2015\)](#)). Consider a sequence of independent, random, Hermitian matrices X_1, \dots, X_N with dimension P . Moreover, assume that for $n \in [N]$, we have almost surely $\|X_n\|_2 \leq L$. Define

$$Y = \sum_{n=1}^N X_n - E(X_n), \quad \nu(Y) = \left\| \sum_{n=1}^N \text{var}(X_n) \right\|_2.$$

Then, for every $t \geq 0$, we have

$$\text{pr}(\|Y\|_2 \geq t) \leq 2P \exp \left\{ \frac{-t^2}{2(\nu(Y) + Lt)} \right\}.$$

Lemma G.5. Let x_1, \dots, x_N be independent centered random vectors in \mathbb{R}^P such that $\|x_n\|_2^2 \leq L$ almost surely and $S = E(N^{-1} \sum_{n=1}^N x_n x_n^T)$. Then

$$\text{pr} \left\{ \left\| \frac{1}{N} \sum_{n=1}^N x_n x_n^T - S \right\|_2 \geq t \right\} \leq 2P \exp \left\{ \frac{-Nt^2}{2L(\|S\|_2 + t)} \right\}.$$

Proof. For each sample, we have

$$\text{var}(x_n x_n^T) = E \left\{ (x_n x_n^T)^2 \right\} - E(x_n x_n^T)^2 \leq E \left\{ \|x_n\|_2^2 x_n x_n^T \right\} \leq L E(x_n x_n^T).$$

Consequently, we have

$$\left\| \frac{1}{N} \sum_{n=1}^N \text{var} \{x_n x_n^T\} \right\|_2 \leq L \|S\|_2.$$

The result follows from [Lemma G.4](#). □

Let Z be a sub-Gaussian random variable, and we define the sub-Gaussian norm as

$$\|Z\|_{\psi_2} = \sup_{p \geq 1} \frac{1}{\sqrt{p}} (E|Z|^p)^{\frac{1}{p}}.$$

Let Z be a P dimensional Gaussian random vector, then we define the sub-Gaussian norm as

$$\|Z\|_{\psi_2} = \sup_{x \in \mathcal{S}^{P-1}} \|\langle x, Z \rangle\|_{\psi_2}. \tag{G.1}$$

Lemma G.6 (Adapted from Corollary 5.50 in [Vershynin \(2010\)](#)). Let x_1, \dots, x_N be independent centered random vectors with sub-Gaussian distribution. Let $\|x_n\|_{\psi_2}^2 \leq L$ for every $n \in [N]$. Then, we have

$$\text{pr} \left\{ \left\| \frac{1}{N} \sum_{n=1}^N x_n x_n^T - S \right\|_2 \geq t \right\} \leq 2 \exp \left\{ 2P - e_0 N \left(\frac{t^2}{L^2} \wedge \frac{t}{L} \right) \right\},$$

for some absolute constant e_0 .

Lemma G.7 (Adapted from Proposition 1.1 in [Hsu et al. \(2012\)](#)). Let $A \in \mathbb{R}^{P \times P}$ be a matrix, and let $\Sigma = A^T A$. Let $x = (x_1, \dots, x_P)$ be an isotropic multivariate Gaussian random vector with zero mean. For all $t > 0$. We have

$$\text{pr} \left\{ \left| \|Ax\|_2^2 - E(\|Ax\|_2^2) \right| > t \right\} \leq 2 \exp \left[- \left\{ \frac{t^2}{4\|\Sigma\|_F^2} \wedge \frac{t}{2\|\Sigma\|_2} \right\} \right].$$

Moreover, consider K matrices A_1, \dots, A_K , with $\Sigma_k = A_k^T A_k$ for $k \in [K]$ and $x_k \in \mathbb{R}^P$ be isotropic multivariate random vectors. Then, for all $t > 0$, we have

$$\text{pr} \left\{ \left| \sum_{k=1}^K \|A_k x_k\|_2^2 - E(\|A_k x_k\|_2^2) \right| > t \right\} \leq 2 \exp \left\{ - \left(\frac{t^2}{4 \sum_{k=1}^K \|\Sigma_k\|_F^2} \wedge \frac{t}{2 \max_{k \in [K]} \|\Sigma_k\|_2} \right) \right\}.$$

of [Lemma G.7](#). The first part is shown in [Hsu et al. \(2012\)](#), we show the second result. Let $V_k \Lambda_k V_k^T$ be the eigendecomposition of Σ_k . define $z_k = V_k^T x_k$ which follows isotropic multivariate Gaussian distribution by the rotation invariance of Gaussian distribution. Then $\|A_k x_k\|_2^2 = \sum_{i=1}^P \lambda_{ki} z_{ki}^2$, where λ_{ki} is the i th diagonal entry of Λ_k . Then, we apply the chi-square tail inequality ([Laurent & Massart, 2000](#)) and obtain

$$\text{pr} \left\{ \sum_{k=1}^K \sum_{i=1}^P \lambda_{ki} z_{ki}^2 - \sum_{k=1}^K \text{tr}(\Sigma_k) > 2 \left(\varepsilon \sum_{k=1}^K \|\Sigma_k\|_F^2 \right)^{\frac{1}{2}} + 2\varepsilon \max_{k \in [K]} \|\Sigma_k\|_2 \right\} \leq e^{-\varepsilon}.$$

Consequently, for all $t > 0$, we have

$$\text{pr} \left(\left| \sum_{k=1}^K \|A_k x_k\|_2^2 - E(\|A_k x_k\|_2^2) \right| > t \right) \leq 2 \exp \left\{ - \left(\frac{t^2}{4 \sum_{k=1}^K \|\Sigma_k\|_F^2} \wedge \frac{t}{2 \max_{k \in [K]} \|\Sigma_k\|_2} \right) \right\}.$$

Here we complete the proof. □

H Additional Empirical Results

Table 1: Competing methods

Abbr.	Model	low-rank	smooth A	sparse V
M1	Sliding window principal component analysis	✓	✓	✗
M2	Hidden Markov model	✗	✗	✗
M3	Autoregressive hidden Markov model (Poritz, 1982)	✗	✓	✗
M4	Sparse dictionary learning (Mairal et al., 2010)	✓	✗	✓
M5	Bayesian structured learning (Andersen et al., 2018)	✓	✓	✓
M6	Sliding window shrunk covariance (Ledoit & Wolf, 2004)	✗	✓	✗
M*	Spectral initialization (Algorithm 1)	✓	✗	✗
M**	Proposed model (Algorithm 2)	✓	✓	✓
MQ**	Proposed model (Algorithm 2) with QR decomposition step	✓	✓	✓

Table 1 repeats the list of competing methods we use in the main text. We will use the same abbreviations in the following experiments.

H.1 More Simulations on Temporal Dynamics

In this section, we show additional simulation results with different temporal dynamics. Table 6 and Table 7 show the average log-Euclidean metric and the running time, respectively, where the data generation process is shown in Figure 1 in the main text. In the second part, we evaluate the model with discrete switching temporal dynamics as shown in Figure 4. This experiment is to evaluate the performance of the discrete switching case, analogous to the assumption of the hidden Markov model. The results are shown in Table 8.

Table 6: Average log-Euclidean metric of simulated data ($\sigma = 0.5$)

Methods	Mixing waveform			Sine waveform		
	$N = 1$	$N = 5$	$N = 10$	$N = 1$	$N = 5$	$N = 10$
M1 $W = 20$	0.45 ± 0.01	0.40 ± 0.01	0.38 ± 0.01	0.67 ± 0.03	0.63 ± 0.01	0.63 ± 0.01
M2	6.58 ± 0.31	0.68 ± 0.02	0.62 ± 0.01	6.22 ± 1.02	0.82 ± 0.01	0.80 ± 0.01
M3	6.91 ± 1.39	0.75 ± 0.02	0.65 ± 0.01	7.36 ± 0.24	0.87 ± 0.02	0.80 ± 0.01
M4	0.46 ± 0.01	0.43 ± 0.02	0.39 ± 0.02	0.64 ± 0.01	0.58 ± 0.03	0.54 ± 0.04
M5	0.41 ± 0.01	0.36 ± 0.01	0.34 ± 0.00	0.58 ± 0.01	0.54 ± 0.01	0.53 ± 0.01
M*	0.89 ± 0.05	0.41 ± 0.01	0.38 ± 0.01	0.94 ± 0.06	0.58 ± 0.02	0.57 ± 0.01
M**	0.41 ± 0.03	0.29 ± 0.03	0.30 ± 0.04	0.59 ± 0.02	0.51 ± 0.03	0.50 ± 0.02
MQ**	0.37 ± 0.02	0.31 ± 0.03	0.29 ± 0.03	0.58 ± 0.02	0.56 ± 0.02	0.56 ± 0.01

Table 7: Average running time of simulated data ($\sigma = 0.5$) ($\times 10^{-2}s$). ‡ denotes the scaling of $\times 10^2s$

Methods	Mixing waveform			Sine waveform		
	$N = 1$	$N = 5$	$N = 10$	$N = 1$	$N = 5$	$N = 10$
M1 $W = 20$	0.5 ± 0.1	0.4 ± 0.0	0.6 ± 0.0	0.5 ± 0.1	0.4 ± 0.0	0.5 ± 0.0
M2	$0.3^\ddagger \pm 4.0$	$7.9^\ddagger \pm 0.1^\ddagger$	$10.0^\ddagger \pm 0.4^\ddagger$	$0.3^\ddagger \pm 4.0$	$8.0^\ddagger \pm 0.1^\ddagger$	$8.3^\ddagger \pm 7.9$
M3	$1.9^\ddagger \pm 0.3^\ddagger$	$28.4^\ddagger \pm 0.1^\ddagger$	$24.5^\ddagger \pm 0.7^\ddagger$	$1.8^\ddagger \pm 0.2^\ddagger$	$28.4^\ddagger \pm 0.2^\ddagger$	$29.0^\ddagger \pm 4.1$
M4	$0.6^\ddagger \pm 0.3^\ddagger$	$5.2^\ddagger \pm 2.9^\ddagger$	$10.8^\ddagger \pm 5.1^\ddagger$	$0.7^\ddagger \pm 0.3^\ddagger$	$3.2^\ddagger \pm 1.5^\ddagger$	$7.8^\ddagger \pm 3.3^\ddagger$
M5	$3.5^\ddagger \pm 0.8^\ddagger$	$3.6^\ddagger \pm 1.3^\ddagger$	$3.8^\ddagger \pm 0.6^\ddagger$	$3.5^\ddagger \pm 0.8^\ddagger$	$3.6^\ddagger \pm 1.1^\ddagger$	$3.8^\ddagger \pm 0.9^\ddagger$
M*	0.1 ± 0.0	0.2 ± 0.0	0.2 ± 0.0	0.1 ± 0.0	0.2 ± 0.0	0.2 ± 0.0
M**	8.2 ± 1.6	4.5 ± 0.2	5.9 ± 0.6	6.7 ± 1.7	4.5 ± 0.8	4.3 ± 1.2
MQ**	18.1 ± 2.2	14.0 ± 0.6	13.4 ± 0.3	15.3 ± 2.4	12.9 ± 0.8	12.0 ± 0.6

Table 8: Simulation result of Figure 4

Methods	Average log-Euclidean metric			Running time ($\times 10^{-2}s$)		
	$N = 1$	$N = 5$	$N = 10$	$N = 1$	$N = 5$	$N = 10$
M1	0.58 ± 0.02	0.52 ± 0.01	0.50 ± 0.01	0.4 ± 0.1	0.4 ± 0.0	0.5 ± 0.1
M2	6.41 ± 0.42	0.70 ± 0.01	0.66 ± 0.01	31.4 ± 2.9	790.8 ± 6.3	829.7 ± 8.4
M3	8.90 ± 3.33	0.81 ± 0.04	0.68 ± 0.01	173.2 ± 21.0	2834.0 ± 7.3	2909.1 ± 16.6
M4	0.58 ± 0.01	0.50 ± 0.03	0.43 ± 0.03	44.8 ± 14.2	393.1 ± 225.4	961.6 ± 695.1
M5	0.50 ± 0.01	0.46 ± 0.01	0.43 ± 0.00	3521.0 ± 123.2	3596.6 ± 98.3	3800.6 ± 113.3
M*	0.94 ± 0.11	0.49 ± 0.01	0.46 ± 0.01	0.1 ± 0.0	0.3 ± 0.4	0.2 ± 0.0
M**	0.55 ± 0.03	0.42 ± 0.07	0.40 ± 0.09	6.8 ± 1.6	5.9 ± 1.0	5.7 ± 1.5
MQ**	0.54 ± 0.04	0.42 ± 0.04	0.38 ± 0.06	4.8 ± 0.1	3.8 ± 0.2	3.4 ± 0.3

H.2 More Experiments on High-Dimensional Data

For the data generation process, we randomly generate a sparse orthogonal matrix of $V^* \in \mathbb{R}^{P \times K}$. We first generate sparse orthogonal block diagonal matrices \tilde{V} with dimension $P \times P$ and then

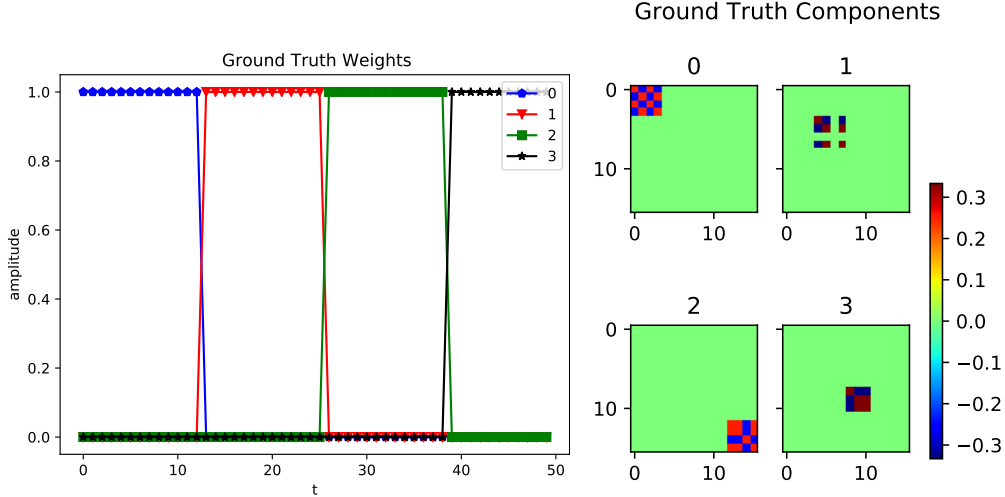


Figure 4: The left figure shows the ground truth of square temporal weights and the right figure shows the corresponding temporal components.

compute the QR decomposition of each block. We keep the orthogonal component of the QR decomposition in each block and then randomly permute the row of the matrix. Finally, we randomly pick K columns of \tilde{V} to compose V^* . For the temporal components A_k , for every $k \in [K]$, unless stated otherwise, we randomly select 6 knots and interpolate the knots with a cubic spline function. The location of each knot is uniformly distributed, with y -position drawn from $\text{unif}([0, 1])$ and x -position uniformly drawn from $\text{unif}([0, T])$.

Selections of kernel functions: In this experiment, we vary the number of knots to see how the choice of kernel length scale affects the estimations. Moreover, we choose different kernel functions to demonstrate the model generalization. We run the simulation with $N = 50$, $K = 10$, $P = 100$, and $J = 100$. The simulation results averaged by 20 trials are shown in Table 9. The result show that as the number of knots increases, indicating that the temporal signal fluctuates more intensively, the optimal choice of length scale decreases. We observe such behavior in all three kernel functions. As for selecting the kernel function, there is no clear distinction which function is the optimal choice for all cases but may require testing all combinations.

More experiments in high-dimensional setting: Table 10–11 show experimental results of $P = 100$, $J = 100$, $K = 10$ with different noise level $\{0.2, 0.1\}$. While most methods have improved results as the noise level decrease, M2 and M3 have downgraded results. This may be because M2 and M3 are already poor estimators.

H.3 Experiment on fMRI Data

In this section, we provide the remaining experiment result in Figure 5, the task correlation in Table 12, and the task activation map in Figure 6.

Table 9: $\text{dist}^2(Z, Z^*)/J$ of different kernel functions and kernel length scale

Methods	Number of knots in $J = 100$			
	5	10	15	20
Radial-basis function ($l = 5$)	0.16 ± 0.04	0.26 ± 0.05	0.52 ± 0.07	0.91 ± 0.17
Radial-basis function ($l = 10$)	0.12 ± 0.04	0.18 ± 0.05	0.33 ± 0.07	0.69 ± 0.18
Radial-basis function ($l = 50$)	0.09 ± 0.04	0.16 ± 0.05	0.76 ± 0.09	1.17 ± 0.11
Radial-basis function ($l = 200$)	0.08 ± 0.04	0.30 ± 0.05	0.84 ± 0.08	1.27 ± 0.16
Matérn five-half ($l = 5$)	0.15 ± 0.04	0.23 ± 0.05	0.44 ± 0.06	0.80 ± 0.18
Matérn five-half ($l = 10$)	0.13 ± 0.04	0.20 ± 0.05	0.36 ± 0.06	0.70 ± 0.18
Matérn five-half ($l = 50$)	0.10 ± 0.04	0.15 ± 0.05	0.31 ± 0.06	0.59 ± 0.12
Matérn five-half ($l = 200$)	0.09 ± 0.04	0.14 ± 0.05	0.31 ± 0.07	0.62 ± 0.19
Rational quadratic ($l = 5$)	0.14 ± 0.04	0.24 ± 0.05	0.51 ± 0.07	0.89 ± 0.18
Rational quadratic ($l = 10$)	0.17 ± 0.04	0.29 ± 0.05	0.61 ± 0.07	1.03 ± 0.18
Rational quadratic ($l = 50$)	0.10 ± 0.04	0.13 ± 0.05	0.43 ± 0.07	1.07 ± 0.18
Rational quadratic ($l = 200$)	0.08 ± 0.04	0.22 ± 0.05	0.81 ± 0.08	1.26 ± 0.16

Table 10: Average log-Euclidean metric of high dimensional low-rank data ($\sigma = 0.2$)

Methods	Number of training subjects				
	10	20	30	40	50
M1 $W = 20$	0.40 ± 0.01	0.37 ± 0.01	0.36 ± 0.01	0.36 ± 0.01	0.35 ± 0.01
M2	2.21 ± 0.01	2.07 ± 0.01	2.04 ± 0.01	2.02 ± 0.01	2.02 ± 0.01
M3	78.42 ± 7.46	1.66 ± 0.09	2.15 ± 0.01	2.20 ± 0.01	2.19 ± 0.01
M4	0.96 ± 0.02	0.43 ± 0.02	0.36 ± 0.04	0.36 ± 0.03	0.35 ± 0.03
M5	0.43 ± 0.01	0.39 ± 0.01	0.38 ± 0.01	0.37 ± 0.01	0.36 ± 0.01
M*	0.35 ± 0.01	0.31 ± 0.01	0.29 ± 0.01	0.29 ± 0.01	0.28 ± 0.01
M**	0.32 ± 0.02	0.29 ± 0.02	0.27 ± 0.01	0.27 ± 0.01	0.26 ± 0.01
MQ**	0.30 ± 0.02	0.28 ± 0.02	0.28 ± 0.02	0.28 ± 0.01	0.27 ± 0.01

Table 11: Average log-Euclidean metric of high dimensional low-rank data ($\sigma = 0.1$)

Methods	Number of training subjects				
	10	20	30	40	50
M1 $W = 20$	0.35 ± 0.00	0.33 ± 0.00	0.33 ± 0.00	0.32 ± 0.00	0.32 ± 0.00
M2	3.03 ± 0.01	2.90 ± 0.00	2.87 ± 0.00	2.85 ± 0.00	2.85 ± 0.00
M3	73.62 ± 9.48	2.25 ± 0.15	2.98 ± 0.01	3.03 ± 0.01	3.01 ± 0.00
M4	1.00 ± 0.05	0.48 ± 0.05	0.41 ± 0.05	0.37 ± 0.05	0.39 ± 0.03
M5	0.39 ± 0.01	0.36 ± 0.01	0.35 ± 0.01	0.34 ± 0.01	0.33 ± 0.01
M*	0.31 ± 0.01	0.27 ± 0.02	0.25 ± 0.01	0.24 ± 0.01	0.24 ± 0.01
M**	0.28 ± 0.02	0.26 ± 0.02	0.24 ± 0.01	0.23 ± 0.01	0.23 ± 0.01
MQ**	0.29 ± 0.02	0.26 ± 0.02	0.25 ± 0.01	0.24 ± 0.01	0.23 ± 0.01

Table 12: The correlation of the components with task activation.

Task	Rank of the correlation, order from largest to smallest (component index)														
Right Hand Tapping	9	0	6	5	3	2	14	13	12	11	10	7	1	4	8
Left Foot Tapping	9	4	6	2	14	13	12	11	10	3	1	0	5	7	8
Tongue Wagging	4	1	2	7	14	13	12	11	10	3	9	8	0	5	6
Right Foot Tapping	8	7	6	14	13	12	11	10	3	2	4	1	5	0	9
Left Hand Tapping	8	7	5	3	1	2	6	14	13	12	11	10	0	4	9

References

- ANDERSEN, M. R., WINTHER, O., HANSEN, L. K., POLDRACK, R. & KOYEJO, O. (2018). Bayesian structure learning for dynamic brain connectivity. In *21st International Conference on Artificial Intelligence and Statistics, AISTATS 2018*.

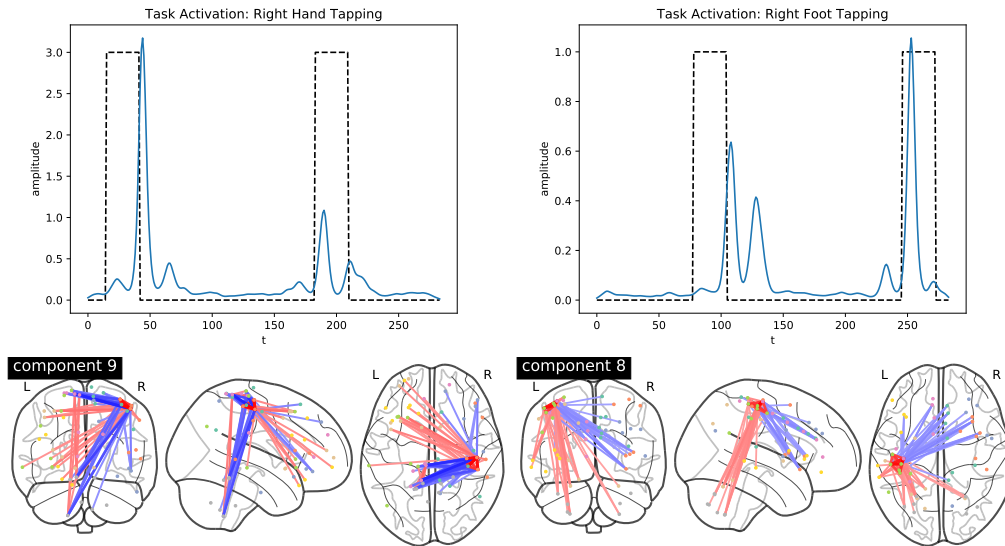


Figure 5: The top row shows the estimated temporal components (blue solid line) whose correlations are the largest with respect to the task activations (black dotted line). The bottom row shows the corresponding spatial component of the above task.

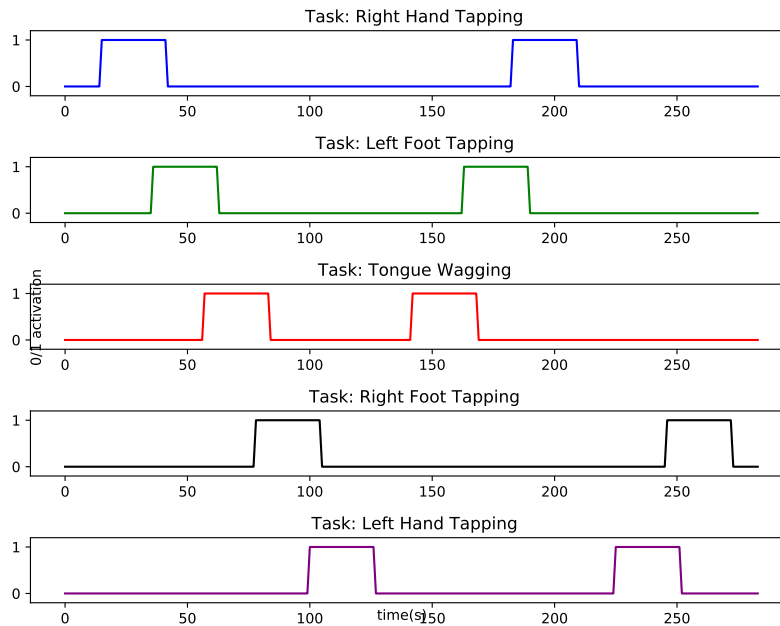


Figure 6: The activation map of the Human Connectome Project motor dataset (Van Essen et al., 2013). For each task, the activation time is partially overlapping with the other tasks.

HSU, D., KAKADE, S., ZHANG, T. et al. (2012). A tail inequality for quadratic forms of subgaussian random vectors. *Electronic Communications in Probability* **17**.

- LAURENT, B. & MASSART, P. (2000). Adaptive estimation of a quadratic functional by model selection. *Annals of Statistics* , 1302–1338.
- LEDOIT, O. & WOLF, M. (2004). A well-conditioned estimator for large-dimensional covariance matrices. *Journal of multivariate analysis* **88**, 365–411.
- LI, X., ZHAO, T., ARORA, R., LIU, H. & HAUPT, J. (2016). Stochastic variance reduced optimization for nonconvex sparse learning. In *International Conference on Machine Learning*.
- MAIRAL, J., BACH, F., PONCE, J. & SAPIRO, G. (2010). Online learning for matrix factorization and sparse coding. *Journal of Machine Learning Research* **11**, 19–60.
- NESTEROV, Y. (2013). *Introductory Lectures on Convex Optimization: A Basic Course*, vol. 87. Springer Science & Business Media.
- PORITZ, A. (1982). Linear predictive hidden markov models and the speech signal. In *ICASSP'82. IEEE International Conference on Acoustics, Speech, and Signal Processing*, vol. 7. IEEE.
- STEWART, G. (1977). Perturbation bounds for the qr factorization of a matrix. *SIAM Journal on Numerical Analysis* **14**, 509–518.
- TROPP, J. A. (2015). An introduction to matrix concentration inequalities. *Foundations and Trends® in Machine Learning* **8**, 1–230.
- TU, S., BOCZAR, R., SIMCHOWITZ, M., SOLTANOLKOTABI, M. & RECHT, B. (2016). Low-rank solutions of linear matrix equations via procrustes flow. In *International Conference on Machine Learning*. PMLR.
- VAN ESSEN, D. C., SMITH, S. M., BARCH, D. M., BEHRENS, T. E., YACOB, E., UGURBIL, K., CONSORTIUM, W.-M. H. et al. (2013). The WU-Minn human connectome project: An overview. *Neuroimage* **80**, 62–79.
- VERSHYNIN, R. (2010). Introduction to the non-asymptotic analysis of random matrices. *arXiv preprint arXiv:1011.3027* .
- YU, Y., WANG, T. & SAMWORTH, R. J. (2015). A useful variant of the Davis–Kahan theorem for statisticians. *Biometrika* **102**, 315–323.